Global Clinical Engineering Journal

Vol.7 Issue 4

Publisher International Medical Sciences Group, LLC

GlobalCE

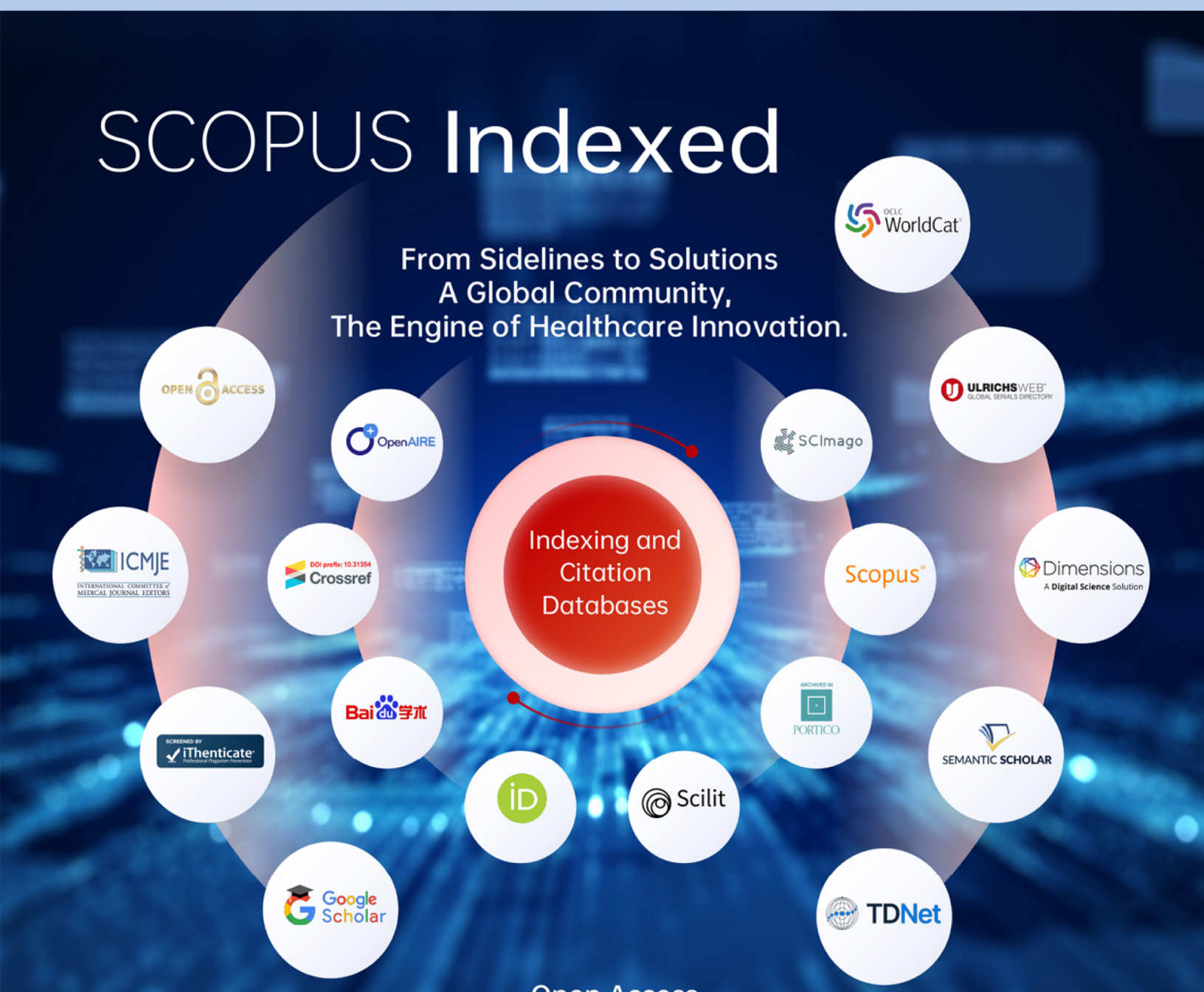

www.GlobalCE.org

ISSN: 2578-2762

Editor's Corner

No Sidelines in Clinical Engineering

The Momentum of a Global Milestone

The Global Clinical Engineering Alliance (GCEA) has just concluded an extraordinary milestone event — the 6th International Clinical Engineering and Health Technology Management Congress (ICEHTMC) — held in Shenzhen, China, often called the Silicon Valley of China.

This Congress redefined expectations for professional gatherings in our field: over 400 abstracts, six daily parallel conference rooms, 100+ posters, and a vibrant program of workshops, panels, and roundtables. The venue became a true magnet for innovation, hosting eight additional conferences on related topics, transforming Shenzhen into the global capital of clinical engineering for one remarkable week.

During the same Congress, GCEA conducted its Annual Members' Meeting, held officer elections, and released its comprehensive Annual Report – "The State of the Alliance."

Participants joined both in person and virtually from nearly 100 countries, reflecting a truly global community. The event achieved an unprecedented 3,000,000 online touches through its live streaming broadcast — a testament to the reach and relevance of clinical engineering worldwide.

"On the clinical engineering playing field, everyone is a player — not a watcher, not a fan."

— ***Dr. Yadin David,*** *Opening Ceremony Keynote*

Celebrating Progress and Setting New Directions

At the Opening Ceremony, several key announcements underscored the dynamism of our profession:

- Expansion of the GCEA Awards Program — adding new categories for innovation, leadership, service, and education.
- Launch of the Global MedTech Alliance — connecting inventors, manufacturers, distributors, users, and patients to accelerate equitable access to technology.
- Publication of a new book *The Essence of Intelligent Systems* by Dr. Ricardo Silva, Chair of the Awards Committee, showcasing the scholarship and creativity of our field.

The Global Clinical Engineering Journal was proud to support the Congress by publishing the Congress Proceedings and inviting presenters to further contribute to a Special Issue. Together, these initiatives mark the coming of age of the clinical engineering discipline — a recognition that our collective expertise shapes modern healthcare.

A Living Global Community

Today, GCEA embraces more than 50,000 members worldwide, representing every continent and every healthcare system model. We are not a static organization but a living network of professionals advancing healthcare, safety and innovation together.

Our initiatives demonstrate this vitality:

Program	Purpose / Impact
Healthcare Technology Foundation (HTF)	The world's only global foundation dedicated to create evidence for better patient safety through technology.
GCEA Awards Program	Promotes excellence, collaboration, service, and visibility of past for future CE professionals.
Professional Development & Education Committee	Delivers multilingual webinars, books, guides, and structured training opportunities.
Global Clinical Engineering Accreditation Program (GCEAP)	Establishes measurable standards of excellence for CE departments worldwide.
Global Clinical Engineering Journal (GCEJ)	Provides a platform for scholarly sharing knowledge, innovation, and the voice of the profession.

Together, these programs show that GCEA is not a static organization — it is a **movement**, connecting expertise with purpose and passion.

Is This Our Inflection Point?

After such success, one question remains:

Was the 6th ICEHTMC Congress an isolated triumph — or an inflection point for our discipline?

While our membership surpasses 50,000, fewer than **1%** submitted abstracts to the Congress. Many remain **on the sidelines** — perhaps due to time, low confidence, or competing priorities. Yet clinical engineering is like a team sport that only succeeds when everyone participates.

"Our achievements should not be measured by numbers alone but by how deeply each of us engages."

We must move from spectatorship to stewardship. Every professional voice adds dimension to the dialogue — every contribution advances global healthcare.

Volunteerism: The Power Behind Progress

GCEA and this Journal exist because of volunteers. Every webinar, guideline, award, and publication represents someone's dedication. These acts of service — often invisible — are the lifeblood of our profession.

Now is the time for each of us to ask:

What can I give back? How can I make an impact?

You can:

- Join a committee or working group.
- Submit a manuscript or share a case study.
- Mentor a young professional.
- Organize an event for Global CE Day.
- Contribute ideas to strengthen GCEA's mission.

Every act of engagement brings us closer to our vision: a world where healthcare technology is safe, effective, and accessible for all.

Erasing the Sidelines Forever

The 6th ICEHTMC proved what is possible when we unite. Our challenge now is to sustain the momentum — to

ensure that every clinical engineer, from every region, feels ownership in this global effort.

I invite you to join this movement. Write to me. Share your ideas. Let's make it easier for every professional to participate, contribute, and lead.

Together, **we will erase the sidelines forever** — transforming this Congress from a moment of pride into a lasting turning point for the discipline of clinical engineering.

From the bottom of my heart, thank you for your commitment, your service, and your belief in the power of collaboration.

Let's continue, **together we can build a better future for Global Clinical Engineering.**

Yadin David

EdD, PE, CCE, FAIMBE, FACCE, FIUPESM

Editor-in-Chief

Global Clinical Engineering Journal

CONTENTS

Received April 29, 2025, accepted June 30, 2025, publication date for online-first November 12, 2025.

Original Research Article

Evaluating Hybrid Deep Learning and Traditional Methods for PET Image Reconstruction

Asma Benyelles* and Amel Korti

Biomedical Engineering Laboratory, Faculty of Technology, University of Abou Bekr Belkaid, Tlemcen, Algeria.

* Corresponding Author Email: asma.benyelles@univ-tlemcen.dz

ABSTRACT

Background and Objective: Positron Emission Tomography (PET) images typically exhibit high noise levels and limited spatial resolution. This paper presents a comparative investigation of traditional PET image reconstruction methods, including Filtered Back Projection (FBP), Algebraic Reconstruction Technique (ART), and Ordered Subset Expectation Maximization (OSEM), alongside hybrid approaches that incorporate deep learning techniques.

Methods: The deep learning approach employed in this work is based on Generative Adversarial Networks (GANs), a powerful framework well suited for inverse problems and image generation tasks such as PET reconstruction. This approach is tested on a publicly available dataset consisting of PET images stored in DICOM format. Performance is evaluated using two standard metrics: the Peak Signal-to-Noise Ratio (PSNR) and the Mean Squared Error (MSE).

Results: The results demonstrate that our proposed methods outperform existing approaches in terms of performance while requiring less reconstruction time. Quantitatively, the Peak Signal-to-Noise Ratio (PSNR) of the reconstructed images is approximately 50 dB. Qualitatively, the observed high image quality supports these quantitative findings.

Conclusion: Our proposed hybrid method is highly effective for noisy PET images, enabling accurate reconstruction and preserving pertinent information and regions of interest, thereby facilitating medical diagnosis.

Keywords—*Positron emission tomography, Deep learning, Generative adversarial networks, Image reconstruction, Evaluation.*

INTRODUCTION

A key field in contemporary medical imaging, nuclear medicine visualizes and examines physiological and pathological processes at the molecular level using low dosages of radioactive tracers—radiopharmaceuticals. Injected, ingested, or inhaled radiopharmaceuticals enter the body and emit gamma rays, detected by imaging tools such as gamma

cameras and positron emission tomography (PET) scanners. The obtained raw data provides vital information for diagnosing and tracking certain diseases through the spatial distribution of the radiotracer within tissues. However, converting this data into high-quality images suitable for clinical interpretation requires sophisticated reconstruction methods that minimize artefacts, reduce noise, and maintain anatomical accuracy. PET images are degraded and have a low signal-to-noise ratio due to short scan durations and low-dose radiotracers.[1,2]

Analytical and iterative techniques have traditionally dominated image reconstruction in nuclear medicine. One of the earliest and most frequently used methods, Filtered Back Projection (FBP), is quite sensitive to noise and experiences resolution loss despite employing mathematical filtering on projection data. Iterative reconstruction methods, such as the Algebraic Reconstruction Technique (ART) and Ordered Subsets Expectation Maximization (OSEM), were introduced to address these limitations by refining the reconstruction through multiple iterations. Although these techniques improve image quality and noise suppression, they remain computationally expensive and require careful parameter tuning to balance resolution and noise reduction.[3]

By introducing data-driven approaches capable of understanding complex visual patterns, Artificial Intelligence (AI), especially deep learning, has transformed medical image reconstruction by reducing noise, recovering fine structural features, and accelerating the reconstruction process. Convolutional Neural Networks (CNNs) and Generative Adversarial Networks (GANs), as examples of deep learning models, have demonstrated exceptional ability in improving image quality. Unlike conventional methods that rely on explicit mathematical models, deep learning–based solutions use vast datasets to derive optimal representations of medical images, making them highly adaptable to variations in data acquisition protocols and scanner characteristics.[4]

Apart from purely deep learning–based reconstruction techniques, hybrid approaches that combine artificial intelligence with traditional methodologies have emerged as promising alternatives. These hybrid methods deliver superior image fidelity, enhanced noise suppression, and reduced computational demands by leveraging the strengths of conventional algorithms—such as the robustness of iterative reconstruction—alongside the learning capabilities of neural networks. By integrating deep learning models into existing reconstruction systems, hybrid approaches offer a balanced solution that improves image quality while maintaining the interpretability and reliability of traditional methods.[5,6]

Ida Häggström et al. developed a deep learning network to address major challenges in Positron Emission Tomography (PET) image reconstruction.[7] Their approach, DeepPET, directly and rapidly reconstructs high-quality, quantitative PET images from sinograms using a deep convolutional encoder-decoder network. They created a large dataset of over 291,000 reference images by randomly selecting parameters derived from a whole-body digital phantom and simulating actual PET scans, thereby producing noisy sinogram data to train, validate, and test DeepPET. The findings showed that DeepPET generates higher-quality images than traditional methods. Requiring significantly less time than conventional reconstruction techniques, the study concludes that the end-to-end encoder-decoder network architecture can effectively produce high-quality PET images.

This research compares hybrid reconstruction methods with conventional and deep learning–based algorithms for scintigraphy imaging. We evaluate the effectiveness of hybrid approaches that integrate deep learning with traditional methods, compared to single deep learning models and analytical or iterative techniques. Key parameters such as noise suppression, resolution retention, computational efficiency, and clinical interpretability will guide the assessment of model performance. The objective is to determine whether hybrid methodologies can bridge the gap between traditional techniques and AI-driven reconstruction, thereby yielding more precise and reliable medical imaging solutions. The concluding section of this study will present our findings, highlighting the advantages and disadvantages of each strategy while exploring prospective avenues for AI-assisted reconstruction in nuclear medicine.

MATERIALS AND METHODS

This section details the database, hardware, software, and methods employed in this study.

Database

The database used in this study consists of 80,000 PET images in DICOM format, with a resolution of 128 × 128 pixels, sourced from the Parkinson's Progression Markers Initiative website.[8] For training, validation, and testing purposes, the dataset was divided into proportions of 70%, 15%, and 15%, respectively.

The database was converted into sinograms. We applied our GAN model to 70% of the training sinograms to capture sinogram characteristics, and then used the remaining data to validate and test the model.

Hardware Reconstruction

Reconstructions were performed on a high-performance workstation equipped with an Intel Core i9-13900K processor clocked at 5.8 GHz, providing 24 cores for maximum computational parallelism. Graphical processing power was supplied by an NVIDIA GeForce RTX 4090 graphics card with 24 GB of GDDR6X memory, which was essential for accelerating intensive deep learning operations and complex reconstructions. The workstation also included 128 GB of DDR5 RAM at 6,000 MHz, ensuring smooth handling of large datasets. Storage was managed by a 2 TB PCIe Gen4 NVMe SSD, enabling extremely fast data loading and writing times. This advanced hardware configuration was critical for minimizing reconstruction times and supporting the use of sophisticated deep learning models.

Software Implementation

Our reconstruction framework was developed using Python 3.8, leveraging a comprehensive set of libraries for deep learning and image processing. The core of the deep learning model, a Generative Adversarial Network (GAN), was built with PyTorch 1.x, enabling efficient training and deployment on GPU hardware. Data handling and numerical operations were managed using NumPy, while performance evaluation utilized torchmetrics. Image loading, preprocessing, and traditional reconstruction methods, such as the Radon transform and ART (Algebraic Reconstruction Technique), were implemented using scikit-image (skimage) and OpenCV (cv2). Visualization of results was performed with Matplotlib, and the training process was monitored using tqdm for progress bar visualization. This robust software stack enabled seamless integration of advanced deep learning techniques with established classical reconstruction algorithms[9].

Generative Adversarial Networks (GANs)

Generative Adversarial Networks (GANs), introduced in the early 2010s, are a class of machine learning models comprising two opposing convolutional neural networks: the generator and the discriminator. The generator aims to synthesize sinograms from the input database, striving to produce outputs that closely resemble authentic sinograms. The discriminator evaluates input sinograms to determine their authenticity, distinguishing between real and generated data. The GANs equation is presented in Equation (1).

$$Min_G Max_D f(D,G) = E_x\left[\log\left(D(x)\right)\right] + E_z\left[\log\left(1 - D\left(G(z)\right)\right)\right] \quad (1)$$

In this context, E_x denotes the expected value across all real sinograms; $D_{(x)}$ represents the Discriminator's probability estimate that input x is real; $G_{(z)}$ represents the output of the Generator for noise z; $D(G_{(z)})$ represents the Discriminator's probability estimate for the authenticity of the generated sinograms; and E_z indicates the expected value across the Generator's entire random input space.

The architecture consists of two main components: a generator *(G)*, designed to create images intended to fool the discriminator, and a discriminator *(D)*, designed to distinguish between real and synthetically generated images. The generator G defines a probability distribution representing the distribution of its produced samples $G_{(z)}$ given a latent variable distribution z–pz. The primary goal of a GAN is to train the generator's distribution to closely approximate the actual data distribution. A shared loss function for both *D* and *G* enables a GAN to be optimized through simultaneous minimization and maximization.[10]

After applying our GAN model, we obtain enhanced sinograms, which are then reconstructed into images using traditional reconstruction methods such as Filtered Back Projection (FBP), Algebraic Reconstruction Technique

(ART), and Ordered Subset Expectation Maximization (OSEM), as presented in the following sections.

Filtered Back Projection (FBP)

Filtered Back Projection (FBP) is a fundamental and computationally straightforward analytical technique for tomographic image reconstruction. The method typically involves applying a ramp filter and windowing to attenuate noise, correcting for blurring by filtering the projection data (sinogram) in the frequency domain. The reconstructed image is then generated by back-projecting these filtered projections onto the image grid.[11]

$$f(x,y)=\int_0^{\pi}[P(\theta,r)*h(r)]_{r=xcos(\theta)+ysin(\theta)}d\theta \quad (2)$$

The FBP equation reconstructs the image value *f(x-,y)* at each point from the projection data *P(θ,r)*, also known as the sinogram. This process involves filtering each projection with a kernel *h(r)* (or |ω| in the frequency domain) and then summing these filtered contributions over all angles (integrating over *θ*).

Algebraic Reconstruction Technique (ART)

The Algebraic Reconstruction Technique (ART) is an early iterative method for image reconstruction. Starting with an initial image estimate, ART iteratively updates pixel values along projection rays to minimize the difference between the observed and projected data.[12]

$$p_i=\sum_{j=1}^{N}w_{ij}f_j for i=1,\ldots M \quad (3)$$

In the linear system used by ART for reconstruction, *pi* represents the i^{th} projection measurement, f_j denotes the value of the j^{th} pixel, and w_{ij} is a weight indicating the contribution of the j^{th} pixel to the i^{th} measurement, such as the extent of intersection between projection ray *i* and pixel *j*.

Ordered Subset Expectation Maximization (OSEM)

Primarily used in Positron Emission Tomography (PET) and Single-Photon Emission Computed Tomography (SPECT) emission tomography (PET, SPECT), Ordered Subsets Expectation Maximization (OSEM) is an accelerated iterative statistical reconstruction method. OSEM, a faster variant of the Expectation Maximization (EM) algorithm, processes ordered subsets of projection data in each iteration to improve convergence speed, updating the image estimate based on these subsets.[13]

$$f_j^{(k+1)}=\frac{f_j^{(k)}}{\sum_{i\in S_m}aij}\sum_{i\in S_m}aij\frac{g_i}{\sum_l ailf_l^{(k)}} \quad (4)$$

This equation shows how the current estimate $f_j^{(k)}$ is adjusted based on the ratio of measured projections g_i to estimated projections, weighted by the system matrix a_{ij} for the current subset S_m.

The quality of final images was evaluated using Mean Squared Error (MSE) and Peak Signal to Noise Ratio (PSNR).

Mean Squared Error (MSE)

The Mean Squared Error (MSE) is a commonly used and straightforward metric that quantifies the difference between the test image and the reconstructed image. It is defined by the following equation:[14]

$$MSE=\frac{1}{N\cdot M}\sum_{i=1}^{M}\sum_{j=1}^{N}\left(f(i,j)-f'(i,j)\right)^2 \quad (5)$$

where *f(i,j)* is the original image; *f'(i,j)* is the degraded image; *M* and *N* refer to the number of rows and columns, respectively.

Peak Signal to Noise Ratio (PSNR)

The performance of the proposed method is evaluated using the Peak Signal-to-Noise Ratio (PSNR) and the Mean Squared Error (MSE). The perceptual quality metric, PSNR, is calculated by comparing the reconstructed image with the original image.[15] The equations used to assess these performance measures are:

$$PSNR=\frac{10\log_{10}\left(I(i,j)\right)^2_{max}}{MSE} \quad (6)$$

where *I(i,j)* is the original image; $I(i,j)_{max}$ is the highest intensity value, *I* is the original image; and *MSE* is the mean squared error.

The next section details and shows a schematic illustration of our proposed method.

Proposed Method

A key obstacle in applying supervised learning to PET imaging is the difficulty of acquiring a large collection of high-quality scans in clinical practice, which is why the process begins with an input sinogram derived from an image.

The training dataset, representing 70% of the total database, was first converted into sinograms using the Radon transform. A GAN architecture, based on a deep convolutional structure, was applied to these sinograms for enhancement. This architecture consists of a Generator and a Discriminator. The Discriminator processes the sinograms to distinguish between real and generated data, outputting a probability score through a Sigmoid activation function in its final layer. The training of both networks involved optimizing their parameters using the Adam algorithm, a widely used adaptive method known for its efficiency and robustness. Training was conducted for 100 epochs, allowing the networks to learn and converge over the entire dataset multiple times.

The Generator consists of six two-dimensional convolutional layers with a fixed kernel size and padding to preserve the spatial dimensions of the input throughout the network. The input to the Generator is a tensor of dimension (N, 1, H, W). This input is processed by the first convolutional layer (conv1), followed by Instance Normalization and a Parametric Rectified Linear Unit (PReLU) activation function, which provides greater flexibility compared to the standard Rectified Linear Unit (ReLU). The subsequent layers follow a similar structure up to the residual connection, where the output of the last convolution is added to the original input of the Generator. This residual connection facilitates training and can enhance the quality of generated sinograms by preserving low-level information.

After completing the training phase, the performance of the trained GAN model was evaluated on a separate test dataset. The test images were first converted into sinograms and then enhanced using the GAN to achieve improved quality and reduced noise.

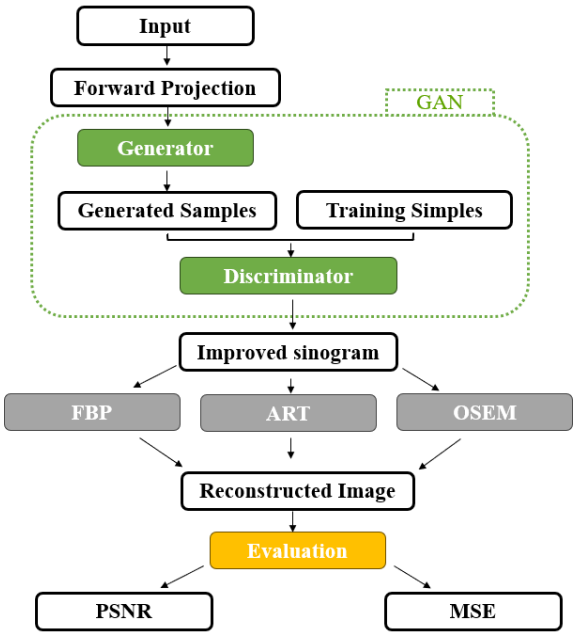

FIGURE 1. Schematic illustration of the hybrid deep learning method for PET data: They are separated into three sections; denoising of sinogram using GAN, reconstruction methods (FBP, ART, and OSEM), and evaluation with MSE and PSNR.

The enhanced sinogram is then input into traditional reconstruction algorithms: Filtered Back Projection (FBP), Algebraic Reconstruction Technique (ART), and Ordered Subsets Expectation Maximization (OSEM). The resulting reconstructed images are quantitatively evaluated using Peak Signal-to-Noise Ratio (PSNR) and Mean Squared Error (MSE) metrics to assess the effectiveness of GAN-based sinogram enhancement in improving reconstruction quality across different algorithms. Figure 1 illustrates the proposed method.

The next section details both the numerical and descriptive findings obtained using the methods mentioned previously.

RESULTS

This section presents the quantitative and qualitative results obtained from our proposed GAN model prior to reconstruction using the three traditional methods.

Three sinograms were selected to evaluate the proposed GAN model. Figures 2 and 3 show the reconstructed

images, and Table 1 presents the comparison results obtained using the evaluation metrics.

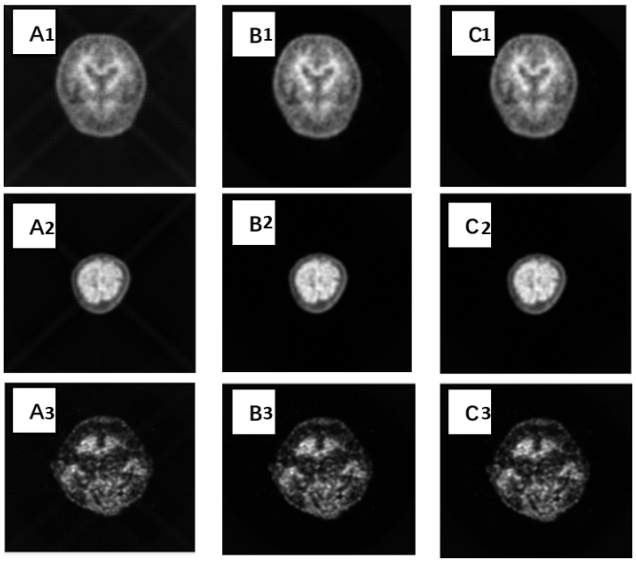

FIGURE 2. Schematic illustration of the hybrid deep learning method for PET data. The process is divided into three sections: denoising of the sinogram using GAN, reconstruction methods (FBP: column A, ART: column B, and OSEM: column C), and evaluation with MSE and PSNR.

TABLE 1. Values of PSNR, MSE, and reconstruction time for the proposed GAN model and the DeepPET model.

	EVALUATION		
	PSNR	**MSE**	**TIME(S)**
GAN-FBP	53.1906 54.2026 53.1381	$1.82e^{-5}$ $1.77e^{-5}$ $1.85e^{-5}$	3.45 3.48 3.44
GAN-ART	52.1756 51.5336 52.9978	$1.43e^{-5}$ $1.47e^{-5}$ $1.52e^{-5}$	5.56 5.76 5.88
GAN-OSEM	55.4581 55.7497 55.8165	$1.44e^{-5}$ $1.31e^{-5}$ $1.49e^{-5}$	9.69 9.89 9.08
DeepPET-FBP	51.7503 53.9884 54.5005	$1.53e^{-5}$ $1.49e^{-5}$ $1.52e^{-5}$	10.08 9.75 10.1
DeepPET-ART	52.2001 54.62 54.3875	$1.52e^{-5}$ $1.48e^{-5}$ $1.49e^{-5}$	11 11.5 11.31
DeepPET-OSEM	53.3665 54.004 55.1297	$1.51e^{-5}$ $1.5e^{-5}$ $1.47e^{-5}$	11.33 12.5 12.2

Figure 2 shows the datasets reconstructed using the three proposed hybrid methods. The GAN was applied to the sinogram of each image to enhance quality and reduce artifacts. These enhanced sinograms were then reconstructed using traditional methods and evaluated using PSNR and MSE metrics. Three distinct objects, differing in size, shape, and density, were selected to assess the range of results achievable with our proposed methodology. The statistical results are presented in Table 1.

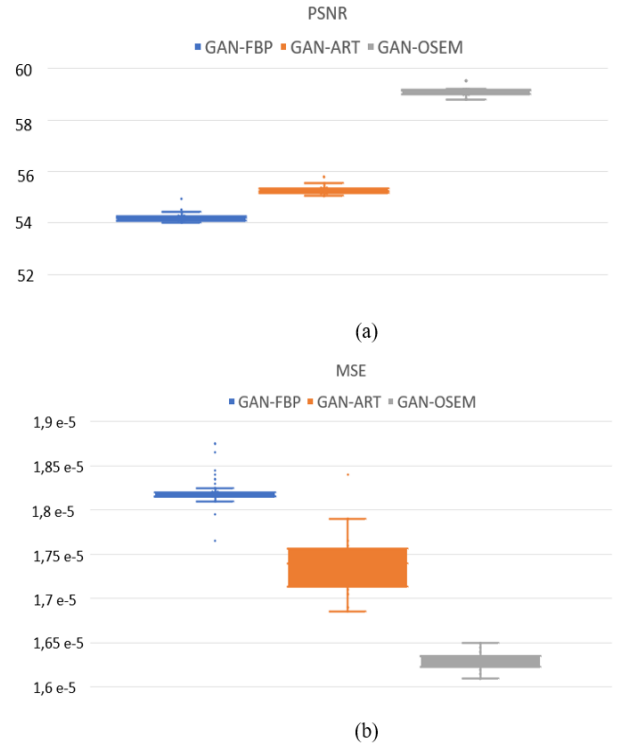

FIGURE 3. The variation of PSNR (a) and MSE (b) across 12,000 test images for GAN-FBP, GAN-ART, and GAN-OSEM.

Table 1 presents the PSNR and MSE values, along with the reconstruction time for each approach. The selection of these metrics is motivated by several factors. In PET imaging, accurate measurement of tracer uptake is crucial; MSE allows assessment of how well the reconstruction method preserves quantitative information within the images. Considering the inherently noisy nature of PET images, PSNR evaluates the effectiveness of the reconstruction technique in suppressing noise while maintaining the radiotracer distribution signal.

Figure 3 illustrates the variation of PSNR (a) and MSE (b) across 12,000 test images in our database for GAN-FBP, GAN-ART, and GAN-OSEM.

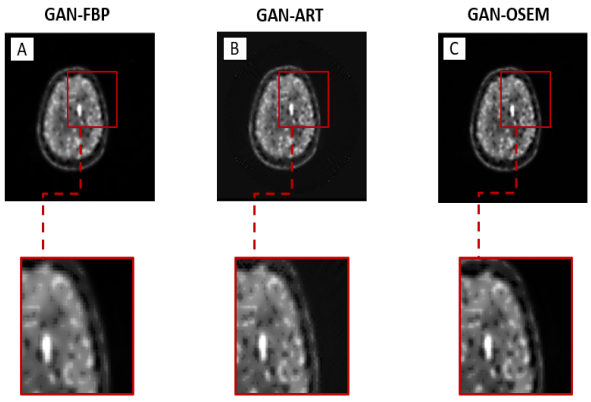

FIGURE 4. Examples of denoised PET images using emerging methods. Each column (A) to (C) shows the same PET slice. From left to right, the reconstructed results are from GAN-FBP, GAN-ART, and GAN-OSEM.

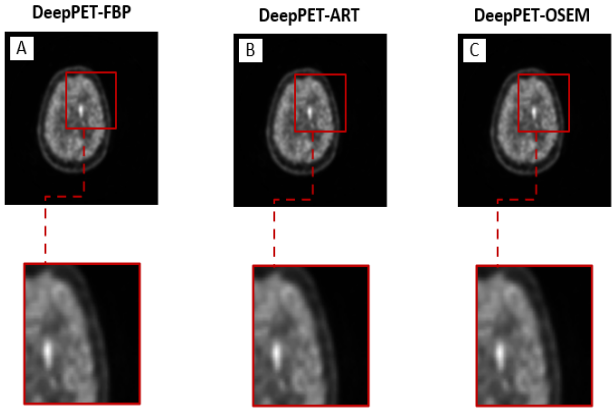

FIGURE 5. Examples of denoised PET images using the DeepPET method. Each column (A) to (C) shows the same PET slice. From left to right, the reconstructed results are from DeepPET-FBP, DeepPET-ART, and DeepPET-OSEM.

To validate our proposed GAN model, we compare it with the DeepPET model and obtain the results in Figure 4.

Figures 4 and 5 display the same brain scan reconstructions using different methods: FBP, ART, and OSEM. Each method presents both a full image and a zoomed-in view of a specific region, allowing for visual comparison of reconstruction quality. The results highlight the differences between DeepPET and the proposed method in terms of reconstructed image quality.

DISCUSSION

The performance of the proposed deep learning–enhanced reconstruction methods—GAN-OSEM, GAN-FBP, and GAN-ART—was comprehensively evaluated on a dataset of 12,000 images using PSNR and MSE as the primary metrics.

For the GAN-OSEM approach, PSNR values remained consistently high, ranging from approximately 54.2 dB to 55.8 dB, with most values clustered around 55.0 dB, indicating excellent overall image quality. Correspondingly, MSE values for GAN-OSEM were notably low, generally fluctuating between 1.25×10^{-5} and 1.55×10^{-5}. The relatively narrow spread for both metrics suggests robust and stable performance across the entire dataset, with minimal extreme variations.

For GAN-FBP, PSNR values were generally lower than those observed with GAN-OSEM, ranging from approximately 53.5 dB to 55.25 dB, with a mean around 54.0 dB. MSE values for GAN-FBP were higher, typically between 1.65×10^{-5} and 1.95×10^{-5}, indicating a greater average reconstruction error compared to GAN-OSEM. While performance remained strong, the slightly wider spread of data points suggests a marginally less consistent output quality.

For the GAN-ART method, PSNR values showed the lowest range among the three approaches, varying approximately between 52.0 dB and 55.0 dB, with most values concentrated around 53.0–53.5 dB. MSE values for GAN-ART were also the highest, typically ranging from 1.2×10^{-5} (with this lower bound appearing as an outlier, as most values exceeded 1.3×10^{-5}) to 2.0×10^{-5}, indicating the largest reconstruction errors. Despite having the lowest mean PSNR and highest mean MSE, the visual distribution for GAN-ART appeared relatively stable, although at a lower performance level compared to the other two methods.

Overall, the visual analysis of these 12,000 data points demonstrates that GAN-OSEM consistently achieves the highest PSNR and lowest MSE, indicating superior image reconstruction quality and precision. GAN-FBP follows, offering good performance but with slightly higher errors, while GAN-ART, although still effective, consistently produces the lowest PSNR and highest MSE among the

three hybrid approaches. The observed fluctuations across all 12,000 images for each method underscore the importance of evaluating performance over large datasets to capture the full range of metric variation.

The GAN-FBP method we propose is computationally efficient compared to iterative techniques. It offers a quick reconstruction process, is easy to implement, and tends to be robust and stable. Our technique provides satisfactory results even with noisy data, making it suitable for situations where noise is not a major concern. In situations where rapid image reconstruction is crucial, GAN-FBP is often the preferred choice.

The distinguishing characteristic of the GAN-ART algorithm lies in its adaptability, as it is capable of processing several forms of tomographic data. Our approach incrementally enhances the solution with each iteration, resulting in improved convergence. GAN-ART can generate scenarios to fill in missing projections or views in the data, allowing for more accurate reconstructions. Additionally, this method is flexible and can be applied to various imaging system geometries and configurations, resulting in faster reconstructions, particularly for large datasets.

The GAN-OSEM technique we employ utilizes code to implement the OSEM denoising algorithm for PET image reconstruction based on deep learning enhancement. This process is carried out iteratively over subsets, with the image being updated based on the ratio of measured and estimated sinograms.

The DeepPET model by Ida Häggström et al.,[7] applied to the sinogram and then reconstructed using traditional techniques, shows remarkable results in terms of noise and blur reduction but remains limited by the data in our database, which are voluminous, as it takes longer to reconstruct compared to our proposed methods. Figures 4 and 5 illustrate the differences between the four methods studied in this article and perceptually validate our results.

The evaluation of the reconstruction quality is performed using PSNR and MSE metrics. This method yields superior outcomes due to its iterative nature, which facilitates incremental enhancement of image quality and results in more precise reconstruction, especially in situations with low data counts. GAN-OSEM is proficient in addressing diverse systematic errors and artifacts encountered in PET imaging, including attenuation, scatter, and random events. The GAN-OSEM algorithm iteratively rectifies these effects, thereby enhancing image quality.

Traditional direct methods are unable to recover all pertinent information during the transformation of the sinogram into images, consequently leading to a loss of object details, contour definition, and regions of interest. This results in a significantly reduced signal-to-noise ratio. In contrast, these hybrid methods incorporating deep learning enable the generation of missing information, thereby ensuring good quality in the reconstructed images. The obtained results confirm that the hybrid approach is more effective than traditional methods, demonstrating a higher signal-to-noise ratio across all three proposed methods. Notably, GAN-OSEM clearly outperforms the other two. It is important to acknowledge that our proposed algorithm possesses limitations, such as the necessity for very large quantities of training data to effectively distinguish between generated and real sinograms. Despite its adaptability to various object types and shapes and its robustness, our method still requires further improvement to accommodate images from other modalities, aiming toward a more generalized algorithm. Another limitation of this study is that the validation only used an online database. In future studies, we plan to validate the results using a regional real-data database. We will also work on generalizing our algorithm to other modalities, such as MRI and CT, to better adapt the denoising and reconstruction method for large amounts of data.[16]

CONCLUSION

We conducted a comparative study for PET image denoising and reconstruction using deep learning with traditional methods, which demonstrates that the hybrid GAN-OSEM method yields qualitatively and quantitatively promising results, exhibiting reduced reconstruction time compared to traditional approaches and minimal noise and blurring in the reconstructed images. This methodology proves efficacious in the context of voluminous and noisy DICOM images, enabling effective reconstruction and the preservation of pertinent information and regions of interest, thereby facilitating medical diagnosis. The use

of deep learning is expected to be crucial in enhancing the performance of PET imaging as well as image processing.[17]

While our evaluation has demonstrated the robustness of the algorithm on a large set of clinical data, a more in-depth characterization of its intrinsic performance in terms of spatial resolution and contrast could be obtained through complementary studies. In this regard, the use of phantom images, such as the Jaszczak phantom, would be relevant for a controlled analysis of reconstruction capabilities. Furthermore, the evaluation of the Modulation Transfer Function (MTF) is envisioned to objectively quantify the resolution of the reconstructed image and will constitute a key direction for our future work.

AUTHOR CONTRIBUTIONS

Conceptualization, A.B. and A.K.; Methodology, A.B.; Software, A.B.; Hardware, A.B., Validation, A.K.; Formal Analysis, A.B.; Investigation, A.B.; Resources, A.B.; Data Curation, A.B.; Writing–Original Draft Preparation, A.B.; Writing–Review & Editing, A.B.; Visualization, A.B.; Supervision, A.K.; Project Administration, A.K.

ACKNOWLEDGMENTS

Not applicable.

FUNDING

This research received no external funding.

DATA AVAILABILITY STATEMENT

Not applicable.

CONFLICTS OF INTEREST

The authors declare they have no competing interests.

ETHICS APPROVAL AND CONSENT TO PARTICIPATE

Not applicable.

CONSENT FOR PUBLICATION

Not applicable.

FURTHER DISCLOSURE

Not applicable.

REFERENCES

1. Wang, Y., Li, E., Cherry, S.R., et al. Total-body PET kinetic modeling and potential opportunities using deep learning. *PET Clin*. 2021;16(4):613–625. https://doi.org/10.1016/j.cpet.2021.06.009.
2. Hashimoto, F., Ote, K., Onishi, Y. PET image reconstruction incorporating deep image prior and a forward projection model. *IEEE Trans Radiat*. 2022;6(8):841–846. https://doi.org/10.1109/TRPMS.2022.3161569.
3. Gong, K., Guan, J., Kim, K., et al. Iterative PET image reconstruction using convolutional neural network representation. *IEEE Trans Med Imaging*. 2019;38(3):675–685. https://doi.org/10.1109/TMI.2018.2869871.
4. Yi, X., Walia, E., Babyn, P.S. Generative adversarial network in medical imaging: a review. *Med Image Anal*. 2019;58(2):101552. https://doi.org/10.1016/j.media.2019.101552.
5. Andersen, A.H. and Kak, A.C. Simultaneous algebraic reconstruction technique (SART): a superior implementation of the ART algorithm. *Ultrason Imaging*. 1984;6(1):81–94. https://doi.org/10.1016/0161-7346(84)90008-7.
6. Long, Y., Huo, X., Liu, H., et al. An extended simultaneous algebraic reconstruction technique for imaging the ionosphere using GNSS data and its preliminary results. *Remote Sens*. 2023;15(11):2939. https://doi.org/10.3390/rs15112939.
7. Häggström, I., Schmidtlein, C.R., Campanella, G., et al. DeepPET: a deep encoder-decoder network for directly solving the PET image reconstruction inverse problem. *Med Image Anal*. 2019;54:253–262. https://doi.org/10.1016/j.media.2019.03.013.
8. Parkinson's Progression Markers Initiative (PPMI). Available online: https://www.ppmi-info.org/.
9. ARAMIS Project-Team. Algorithms, models and methods for images and signals of the human brain. Inria Paris Centre, CNRS, INSERM, Sorbonne Université, France, 2023. Available online: https://radar.inria.fr/rapportsactivite/RA2023/aramis/ARAMIS-RA-2023.pdf.
10. Wang, Z., She, Q., Ward, T.E. Generative adversarial networks in computer vision: a survey and taxonomy. Preprint. 2019, arXiv:1906.01529. Available online: https://arxiv.org/abs/1906.01529.
11. Beckmann, M. and Nickel, J. Optimized filter functions for filtered back projection reconstructions. https://doi.org/10.3934/ipi.2025003.

12. Hartling, K., Mahoney, F., Rand, E.T., et al. A comparison of algebraic reconstruction techniques for a single-detector muon computed tomography system. *Nucl Instrum Methods Phys Res A*. 2021;987:164834. https://doi.org/10.1016/j.nima.2020.164834.

13. Zeng, T., Gao, J., Gao, D. A GPU-accelerated fully 3D OSEM image reconstruction for a high-resolution small animal PET scanner using dual-ended readout detectors. *Phys Med Biol*. 2020;65(24). https://doi.org/10.1088/1361-6560/aba6f9.

14. Anaya-Sánchez, H., Altamirano Robles L., Díaz Hernández, R., et al. WGAN-GP for synthetic retinal image generation: enhancing sensor-based medical imaging for classification models. *Sensors*. 2024;25(1):167. https://doi.org/10.3390/s25010167.

15. Al-Najjar, Y. Comparative analysis of image quality assessment metrics: MSE, PSNR, SSIM and FSIM. *Int J Sci Res*. 2024;13(3):110–114. https://doi.org/10.21275/SR24302013533.

16. Hashimoto, F., Onishi, Y., Ote, K., et al. Deep learning-based PET image denoising and reconstruction: a review. *Radiol Phys Technol*. 2024;17:24–46. https://doi.org/10.1007/s12194-024-00780-3.

17. He, W., Zhao, Y., Zhao, X., et al. A CNN-based four-layer DOI encoding detector using LYSO and BGO scintillators for small animal PET imaging. *Phys Med Biol*. 2023;68(9). https://doi.org/10.1088/1361-6560/accc07.

Received October 12, 2024, accepted June 9, 2025, publication date for online-first November 17, 2025.

Engineering Report

Healthcare Technology Management in Ethiopia

Mulugeta Mideksa Amene*

Consultant Biomedical Engineering, Addis Ababa, Ethiopia.

* Corresponding Author Email: mulugetamideksa@gmail.com

ABSTRACT

This document provides an in-depth analysis of healthcare technology management (HTM) in Ethiopia, identifying significant deficiencies and challenges in the management of medical devices (MDs) within the healthcare system. The primary objective of this study is to identify gaps in the lifecycle management of MDs in Ethiopia and to provide recommendations for improvement. The findings reveal a conspicuous absence of a dedicated MD policy and health technology assessment (HTA) institutes, leading to inefficiencies, as MDs are managed under drug policies. Biomedical engineers (BMEs) play a crucial role in managing the entire lifecycle of MDs, which can mitigate risks and corruption associated with these devices. However, the healthcare system faces several challenges, including a lack of quality control measures, inadequate training for BMEs, and poor integration between universities and health facilities, all of which impact the effectiveness of HTM. The document recommends the establishment of a national HTA institute, the formulation of a dedicated MD policy, and the enhancement of links between educational institutions and healthcare facilities to improve the management of MDs. Strengthening the role of BMEs and implementing robust systems for HTM are essential for improving healthcare quality and patient safety in Ethiopia.

Keywords—*Healthcare technology management (HTM), Health technology assessment (HTA), Health technology regulation (HTR), Biomedical engineer (BME), Biomedical technicians (BMT), Regional health bureaus (RHB).*

INTRODUCTION

Health Technology Management in Ethiopia

Health technology management (HTM)—particularly in the realm of medical devices (MDs)[1]—is underdeveloped and underrecognized in Ethiopia's healthcare system. While some progress has been made, current efforts remain narrowly focused on maintenance, failing to establish a comprehensive and system-wide HTM framework. The risk level of medical devices is shown in Figure 1.

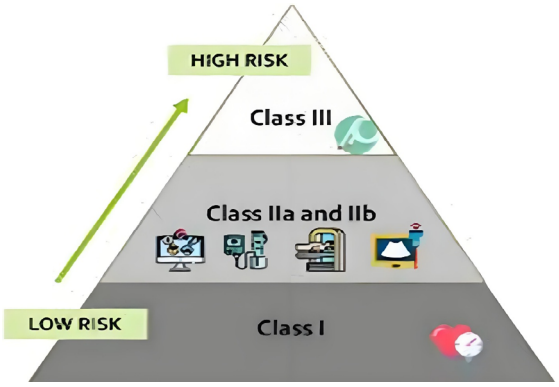

FIGURE 1. Risk level of medical devices.

Systemic Gaps in HTM Implementation

• Ethiopia lacks a full-fledged HTM system. Existing mechanisms do not account for internal and external influencing factors (Figure 2).

• HTM activities are fragmented and often fall under pharmaceutical policies and institutions, resulting in blurred responsibilities.

Marginalization of Biomedical Engineering (BME)

• According to the WHO's role of BME in HTM guidance (Figure 3), BME involvement across the full life cycle of MDs in Ethiopia is invisible or sidelined.

• Most notably, BME professionals are excluded from key processes such as procurement, where pharmacists have assumed authority.

• This is institutionalized through the job description (JD) of pharmacists at all levels of the health system, including in the Ministry of Health-Human Resources (MoH-HR).[2]

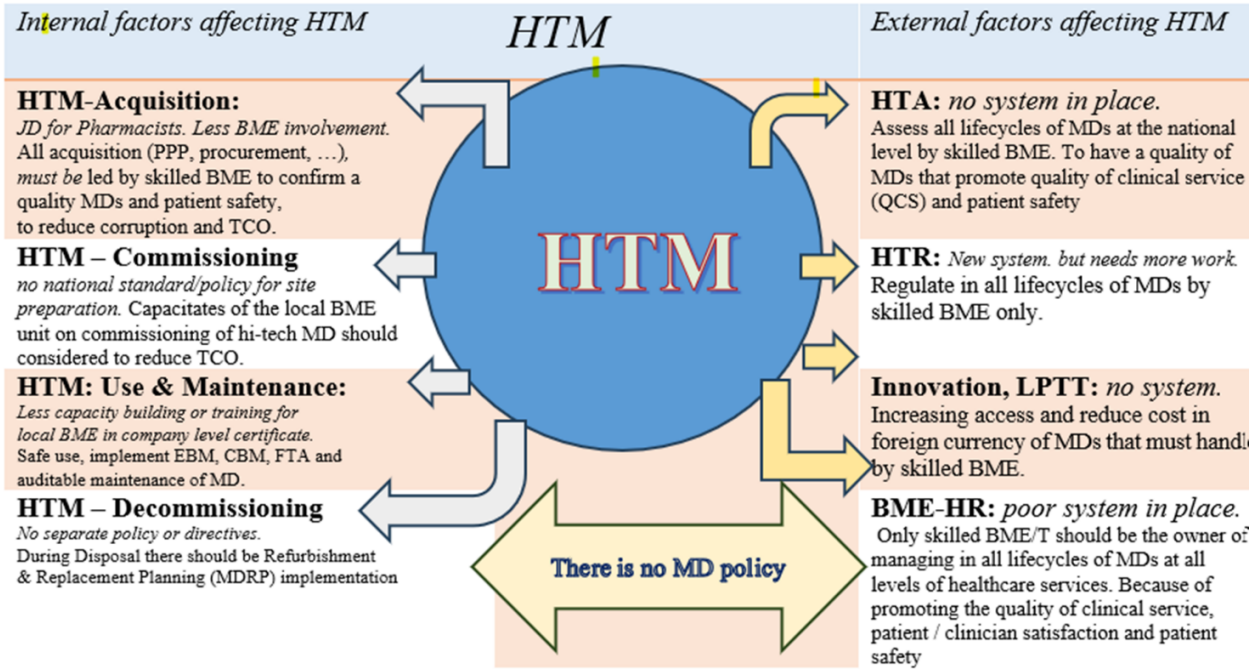

FIGURE 2. HTM determinant factors in the Ethiopian MOH situation.

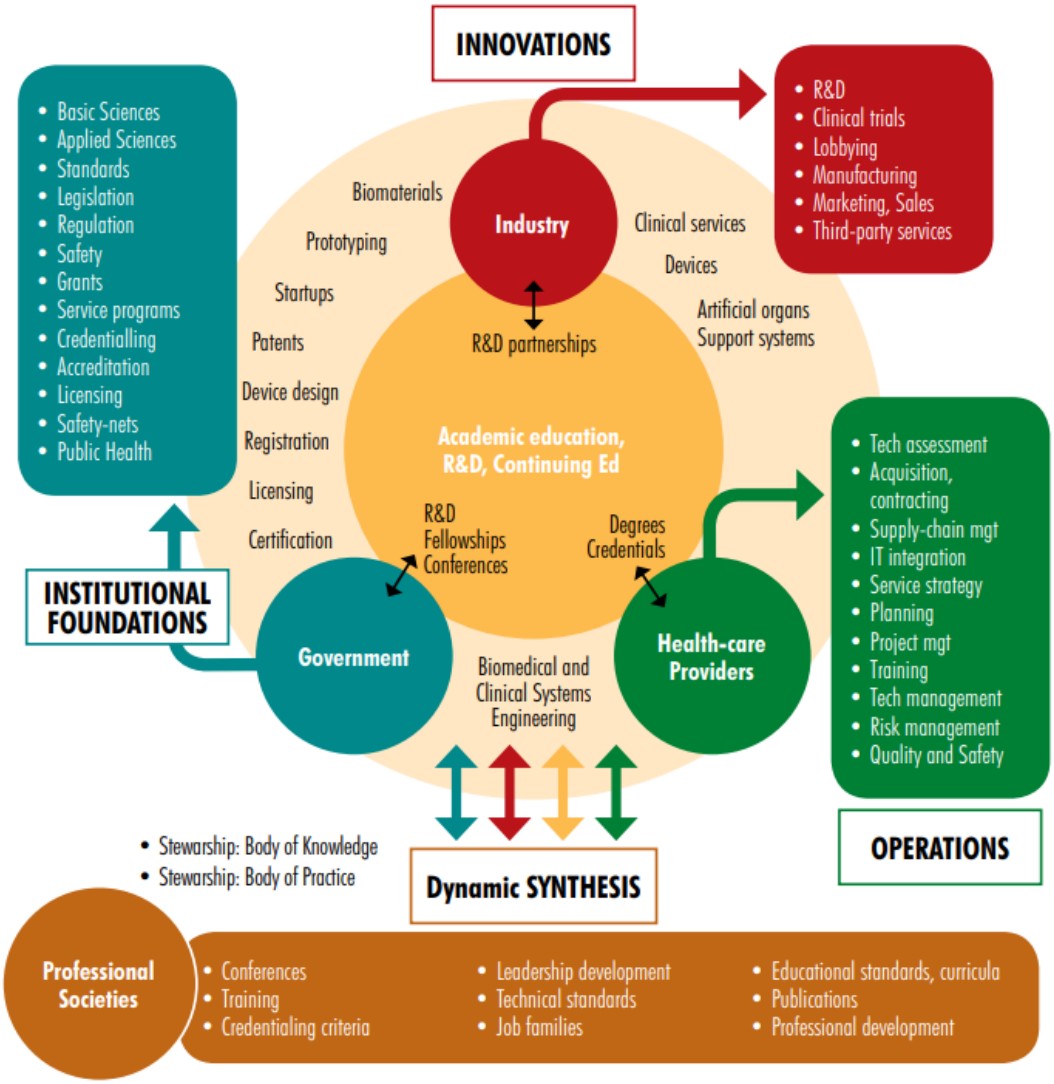

FIGURE 3. Role of BME in healthcare sectors (WHO).

Workforce and Equity Issues

• There exists a salary disparity: A 4-year pharmacy graduate earns significantly more than a 5-year BME graduate, reflecting the undervaluation of BME roles.

• Pharmacists currently lead HTM functions across:

o Regional health bureaus (RHBs)

o Some health facilities

o MoH and its agencies (e.g, Ethiopian Pharmaceutical Supply Service 'EPSS')

Historical Context and Policy Misalignment

• The 1993 drug policy has been the de facto framework for managing MDs, grouping them under medicinal products. Currently, an ongoing revision process is underway.

• The formerly effective techno-center that managed HTM at the national level was disbanded because of decentralization, leaving BME out of leadership roles.

• While the Ethiopian Food and Drug Administration and Control Authority (EFMHACA). Now, the Ethiopian Food and Drug Authority (EFDA) and EPSS were formed

to fill this gap, and pharmacists continue to dominate HTM leadership, sidelining technical experts.

• A new medical and medicine policy (MMP) and roadmap have been drafted, but they conflate medicines and MDs, risking continued mismanagement.

The ACCE leaders are presented in Figure 4, and the chronological order of the gradual growth of the CE/BME field in Ethiopia is shown in Figure 5.

FIGURE 4. From right to left: Jennifer Jackson (Former Chair of ACCE), Mulugeta (Former S&T Commissioner), Dr. Tedros Ghebreyeesus (Former Minister of MoH, now Director-General of WHO), Dr. Ismael Cardero (Former Orbis Eye Foundation engineer), Peter Heiman (Former WHO technical advisor, head of Health Mission in Laos), Andrei Issakov (Former head of Medical Devices Unit at WHO), last person on the left Gebru (Former ESEC-Director). Photo taken during the 6th ACEW in Addis Ababa, Ethiopia, in 2006.[6]

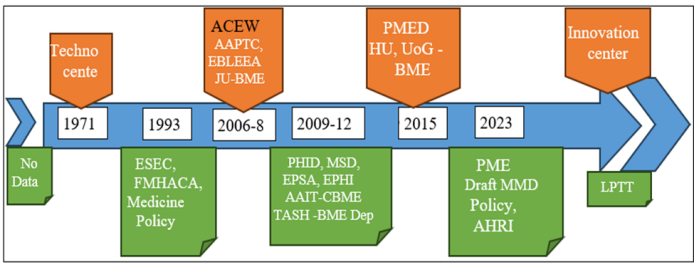

FIGURE 5. The chronological order of the gradual growth of the CE/BME field in Ethiopia.

Historical Evolution and Institutionalization of BME in Ethiopia

The Role of the Ministry of Science & Technology (MoST)

In the absence of a centralized techno-center, the MoST played a pivotal role in sustaining and promoting the field of biomedical engineering (BME) in Ethiopia.

A key turning point was the Sixth American Clinical Engineering Workshop (ACEW) held in 2006 in Addis Ababa, in collaboration with the MoH. This event significantly:

• Raised awareness about the importance of BME.

• Stimulated interest and recognition from the MoH.

• Triggered national-level action to establish BME training and professional development programs.

Institutional Milestones in BME Education & Professionalization

Following the ACEW:

• Addis Ababa Polytechnique College (AAPT) initiated the first formal Biomedical Technicians (BMT) program.

• The Ethiopian Biomedical and Laboratory Equipment Engineering Association (EBLEEA) was established (2007–2009), creating a professional platform for engineers.

Between 2008 and 2015, the BME field expanded to:

• Five universities: Jimma University (JU), Addis Ababa University (AAU), Hawassa University (HU), University of Gondar (UOG), and Bahir Dar University (BU).

• Five polytechnic colleges: Adama, Nekemte, Debre Tabor, Jimma, and Dessie.

Organizational Restructuring at the MoH

In 2008, the MoH was reformed, and **eight directorates** were created. Among these:

• The Public Health Infrastructure Directorate was given the responsibility for MDs and infrastructure, including Information and Communication Technology (ICT) support.

• Simultaneously, BME responsibilities were included within the Clinical Services Directorate, resulting in mandate overlaps and confusion.

To resolve this, the MoH:

• Created a dedicated directorate: the Pharmacy and Medical Equipment Directorate (PMED) under the General Directorate of Clinical Services.

• BME (HTM) has now been downgraded to a desk under the PMED Chief Executive, though it deserves elevation to the level of a parallel chief executive to reflect its importance.

Future Challenges and Opportunities

One emerging mandate overlap is between the PMED and the ICT Chief Executive Office, particularly in medical software, which, according to WHO, is classified as a subset of MDs. This signals the need for:

• Clear role delineation between PMED (MD disk) and ICT leadership.

• Enhanced integration of BME with digital health strategies.

• Greater support for BME, HTM, HTA, and Health Technology Regulation (HTR) in the national health agenda.

The BME sector in Ethiopia has overcome significant challenges and is poised for further growth. With the establishment of training programs, professional associations, and specialized directorates, the foundation is set. The continued recognition of BME as an essential technical and clinical field—alongside medicines, ICT, and infrastructure—will determine its success in supporting safe, effective, and equitable health service delivery.

Statement of the Problem: HTM in Ethiopia

HTM, HTA, and HTR in Ethiopia remain critically underdeveloped. Despite the essential role of MDs in modern healthcare delivery, their governance, evaluation, and lifecycle management are significantly lacking. According to a WHO survey, corroborated by national observations, the following major issues persist:

Key Problems Identified:

• No National HTM Policy

o Ethiopia lacks a dedicated MD policy to guide planning, regulation, acquisition, and lifecycle management of MDs.

• No HTA Institution

There is no national HTA body, limiting evidence-based decision-making in the adoption of technology.

• Weak HTM Structures

The HTM directorates at national, regional, and facility levels are either weak or nonfunctional, leading to fragmented implementation.

• Low Availability of High-Tech MDs

Ethiopia has significantly fewer high-tech MDs per capita than comparable low- and middle-income countries (LMICs), contributing to diagnostic and treatment gaps.

• Disjointed Regulation and Support

While EFDA regulates MDs, technical support is provided by MOH, creating role confusion and inefficiencies.

• Lack of Evidence-Based BME Deployment

No scientific evidence or policy guidance supports the structured deployment of Biomedical Engineers/Technicians (BME/BMT) in health institutions.

• Procurement Gaps

MD procurement focuses almost exclusively on initial (purchase) costs, with no consideration of hidden costs (e.g., maintenance, training, calibration, disposal).

Patient Safety Risks

The lack of a robust HTM system severely compromises patient safety and the quality of care. According to the U.S. FDA, over the past decade:[6,7]

• Seven thousand to nine thousand deaths occur per year because of medical errors.

• Over 80,000 deaths and 1.7 million injuries were linked to MDs.

Given Ethiopia's weak regulatory oversight and near-total absence of calibration, quality audits, and decommissioning systems, the risk of harm is likely even higher.

Systemic Maintenance & Training Deficiencies

• Maintenance practices are limited to corrective maintenance (CM) and planned preventive maintenance (PPM). There is no reverse engineering or reengineering.

• No systematic decommissioning process exists, resulting in unsafe or obsolete devices remaining in use. Patient safety is compromised.

• The lack of ongoing training and regulatory frameworks for BME professionals further weakens patient safety and clinical quality services.

The current state of HTM in Ethiopia presents a critical threat to patient safety, resource efficiency, and health system sustainability. Urgent actions are required to establish a scientific HTA body and empower and properly position BME professionals.

UNICEF reported an average global rate of 17 deaths per 1,000 live births in 2022. Globally, 2.3 million children died in the first month (28 days) of life in 2022—approximately 6,300 neonatal deaths every day. In Ethiopia, there were 27.1 deaths per 1,000 live births. It is above the global average.

UNICEF reported in 2017 that 320,000 babies are born too soon each year, and 23,100 children under five die due to direct preterm complications. Not including stillbirth (> 20 weeks' baby dies in the womb). Because of obstetric complications, 10,000 mothers' deaths occur per year.

General Objective

To assess the gap and recommend the whole life cycle of MD (healthcare technology) management in Ethiopia. The medical device life cycle phases are shown in Figure 6, and the medical devices interconnection phase is presented in Table 1.

• Need for the study: Almost no research has been conducted on HTM and HTA.

• Delimitation of the study: Covers all life cycles of MDs from 1971 to 2024.

• Limitation of the study: Not including pharmaceuticals (Medicines/drugs).

• Operational definitions: HTM, HTA, HTR, MD, BME, BMT.

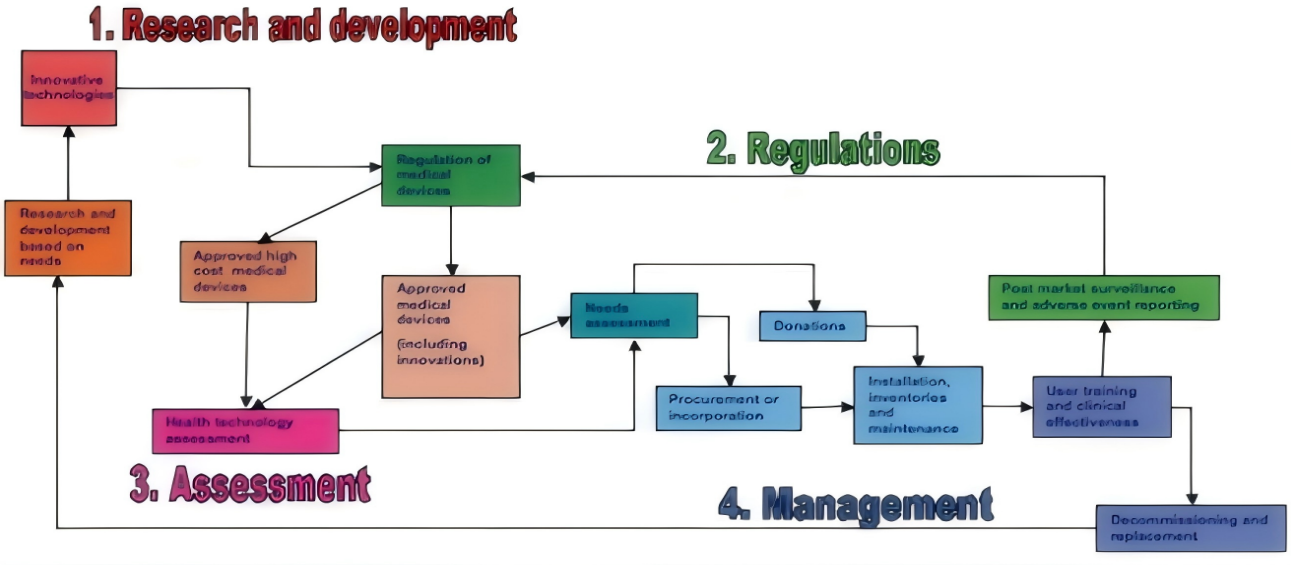

FIGURE 6. The medical device life cycle phases of R and D, HTR, HTA, and HTM (WHO).

METHOD

Sample Size and Sampling Techniques

Research Sampling and Technique

A. For quantitative total population sampling:

• **Total population sampling** is a type of nonprobability sampling—a purposive sampling technique that involves examining the entire population.

Select almost all that is the total population sampling: (five BME Universities, six BMT colleges, six federal Hospitals, thirteen RHB, one MoH, and its three agencies).

B. For a qualitative nonprobability consecutive sampling method:

• **Nonprobability sampling** is a more conducive and practical method for my research to deploy surveys in the real world.

Because of its speed, cost-effectiveness, and ease of availability of the sample.

o To fine-tune my results from a selected group of samples, conduct research over a period, analyze the results, and then move on to another group through a questionnaire, Key Informant interview (KII), Focal Group Discussion (FGD), and site observation.

C. Data analysis or interpretation

The Excel sheets and Google Forms were utilized. The thematic content analysis method was used to analyze the results of the interviews, identifying, analyzing, and reporting on patterns or themes detected in the data. Data obtained from the KII were summarized per category or thematic area.

• Coding: Organizing quantitative data about HTM.

• Editing: Correcting grammatical errors, removing any contradictory information that doesn't have proof, and refining my work into a polished, clear, and impactful document.

• Tabulating: A systematic and logical representation of numeric data in a table format.

TABLE 1. Medical devices interconnection phase of R and D, HTR, HTA, and HTM (WHO).

	R & D	Regulations	HTA	HTM
Perspective	Innovative knowledge, application and tools for health services	Safety & efficacy	Population served	Health services provider
Orientation	Personal health services	Population safety	Population health	Community health services
Requirement (Output)	Improve and/or new tools and services	Mandatory compliance	Recommendation on highly complex technologies	Community health services
Method	Innovation and improvement	Performance testing, safety assessment, and post-market reporting	Systematic analysis, critical review	Operational management of the technology life cycle
Criteria	Market adoption	Safety and quality standards	Epidemiology data, statistics, analysis of efficacy, effectiveness, and appropriateness	Needs analysis, specifications, and reliable device availability for clinical use
Output	Enhanced health service	Risk mitigation and prevention of harm	Responsiveness and maximization of clinical outcome and cost-effectiveness	Improved health delivery; sustainable availability of high-quality and safe devices

FINDINGS, ANALYSIS, AND INTERPRETATION

MD Sector in Ethiopia

Policy & Regulatory Gaps

- **Absence of a Dedicated MD Policy:**

Ethiopia is one of 38 countries globally lacking a standalone MD policy.

The existing drug policy subsumes MDs, treating them as medicinal products, which leads to regulatory ambiguity.

- **Lack of HTA and LPTT Systems:**

No formal HTA institutions.

No structured framework to support MD innovation, and local production and technology transfer (LPTT).

Institutional and Organizational Issues

- **Weak BME Unit Structures:**

No clearly defined BME organizational structure across all government levels (except EFDA).

Lack of mandate clarity for BME functions in the MoH, Regional Health Bureau (RHBs), Zonal Health Bureau (ZHB), Armauer Hansen Research Institute (AHRI), and Ethiopian Pharmaceutical Supply Services (EPSS).

- **Pharmacists' Overreach:**

Pharmacists are authorized under their JDs to engage in MD procurement—a role outside their professional scope and ethically questionable.

- **Workforce Imbalance:**

Approximately 50% of Biomedical engineers and technicians work in public health facilities, indicating a potential human resource bottleneck in rural or underserved regions.

Systemic & Academic Disconnect

- **University—Health Facility Disconnect:**

Minimal collaboration between academic institutions and health facilities, affecting research, innovation, and capacity-building in the MD sector.

Positive Developments

The MD Structure of The Ethiopian Food and Drug Authority (EFDA) is a Benchmark (Figure 7).[8]

The EFDA has a well-established and independent MD regulatory unit.

The new organogram of the EFDA is exemplary and should be benchmarked by other institutions (e.g., MoH, RHBs, ZHBs, and EPSS).

SUMMARY

BMEs graduated from five Universities in BSc = 1,775, MSc = 155, and PhD = 2; BMT completed the Level 4 program from six Polytechnic Colleges, 2,085 BMT in diploma, and Technologist in BSc = 0. Out of them, 147 BMEs are employed in the education sector. 451 BMEs and 571 BMTs are deployed in the health sector. In the next 5 years, Ethiopia will likely get 1,115 BMEs in BSc,

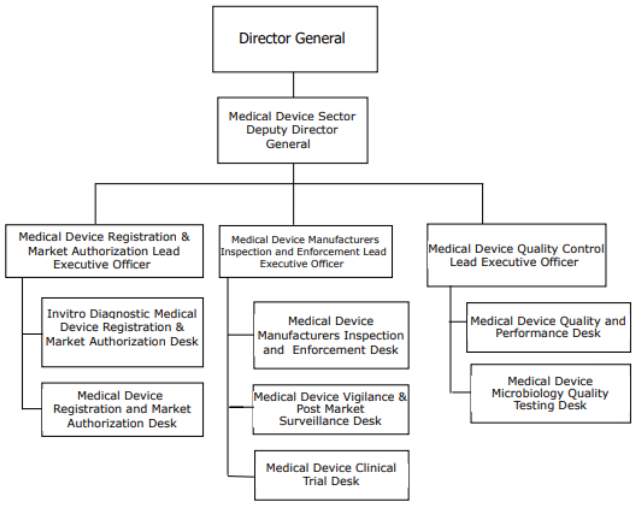

FIGURE 7. The new Ethiopian Food and Drug Authority (EFDA) BME-Director organizational structure.[8]

MSc, and PhD degrees, and 400 BMTs in the Level 4 program. Need a BM-Technologist program to upgrade the Biomedical Technician program and fill the gap between the BMEs and BMTs.

CONCLUSION AND RECOMMENDATION

Conclusion of Strategic Pillars of Effective MD Management

1. HTM (MD Acquisition till Decommissioning)

• Must be handled by Biomedical Engineering (BME) professionals to ensure transparency, reduce corruption, and mitigate risks.

• Multiple acquisition modalities should be utilized:

o Leasing

o Public–private partnerships (PPP)

o Rental

o Loans, etc.

2. HTA, Innovation, LPTT, and Refurbishment

• These are the keys to increasing access to MDs, especially in resource-limited settings (LMIS like Ethiopia).

• Should be supported by a robust national reliability system.

o HTA for informed decision-making.

o Innovation and LPTT to enhance self-reliance.

o Refurbishment programs to extend the life of usable MDs.

3. HTR Ensures the Quality and Safety of MDs

• Encourages clinical trials, particularly in innovation and LPTT phases.

4. BME-HR Development

• Bridging Academic Research and Clinical Practice in the CE/BME field.

• Just as clinicians are embedded in the realities of patient care, biomedical engineers, public health professionals, and health technology experts thrive when academic research and hands-on applications go hand in hand. Here's why that collaboration is so vital:

• Real-World Relevance: Working with health facilities grounds academic training in real needs — whether it's maintaining oxygen systems or implementing HTM strategies.

• Innovation Pipeline: University research can feed directly into practical innovations in medical devices, diagnostics, and system design.

• Capacity Building: Embedding students and faculty in clinical environments trains a workforce that is not only technically skilled but systems aware.

• Co-Development of Solutions: Partnerships foster co-creation of tools and policies that are feasible, scalable, and context-appropriate, especially in LMIS (Like Ethiopia).

• Senior HTM Leaders With their deep expertise in HTM and their commitment to capacity-building, they are uniquely positioned to advocate for and help design these kinds of collaborations, especially where university-based biomedical engineering programs can serve national healthcare goals.

• Would you be interested in sketching out what an ideal university–health facility partnership could look like for Ethiopia or the broader African context? We could co-develop a framework together.

• Critical for managing the entire life cycle of MDs—from planning and acquisition up to decommissioning. Need specialty-focused training.

Without a distinct HTM policy, dedicated BME leadership, and clear delineation of roles, Ethiopia risks continued

inefficiencies, safety issues, and underutilization of medical technologies. Urgent reform is needed to establish a structured, inclusive, and technically led HTM system.

RECOMMENDATION

• **Standardization of MDs**: Implementing standardization through long-term agreement (LTA) holders or other modalities such as leasing, PPP, rental, government procurement, innovation, and refurbishing of MDs is essential.

• **Open System for in vitro Diagnostics (IVD)**: IVD systems should be open and use universal standard reagents and consumables.

• **The Universities should effectively partner with health facilities in practice.**

Here's a structured approach that could turn that vision into an operational reality:

1. Embed Joint Training Programs

• **Clinical Internships**: Embed biomedical engineering, public health, and health economics students in hospitals and clinics for hands-on experience.

• **Residency-Like Models**: Like medical residencies, develop structured rotations where students assist with equipment maintenance, data collection, or health technology assessments.

• **Shared Curriculum Development**: Design modules co-taught by academic faculty and health facility staff that cover both theory and on-the-ground realities.

2. Establish Innovation Hubs and Living Labs

• **Health Tech Incubators**: Set up joint university–hospital innovation centers to develop, test, and iterate context-appropriate technologies (e.g., oxygen delivery systems, remote diagnostics).

• **Real-Time Problem Solving**: Let students and researchers work alongside hospital staff to co-develop low-cost, locally sourced solutions.

• **Device Piloting and Feedback Loops**: Health facilities can act as early adopters, offering feedback to university researchers and developers.

3. Co-Design Research and Policy Initiatives

• **Operational Research**: Tackle system-level challenges like HTM system strengthening, supply chain bottlenecks, or equipment uptime tracking.

• **Joint Grant Writing**: Collaborate on securing funding from donors or ministries for research that serves national health priorities.

• **Policy Advisory Councils**: Include both academic researchers and hospital leaders in national or regional policy formulation.

4. Build Institutional Partnerships and Incentives

• **Memorandums of Understanding (MoUs)**: Formalize collaborations with clear roles, timelines, and outcomes.

• **Dual Appointments**: Encourage shared positions so experts can teach in universities and serve in clinical roles (especially in biomedical engineering and HTM management).

• **Metrics for Impact**: Define joint KPIs such as equipment improvements, reduced turnaround time on diagnostics, or innovations deployed.

5. Anchor the Partnership in Public Health Equity

• Ensure these partnerships prioritize **low-resource settings**, rural hospitals, and marginalized populations.

• Use the collaboration to **decentralize innovation** and build capacity where it's most needed — a mission you've already championed through your global work.

6. Establish the Biomedical Technologist (BMT) Programs:

Establishing Biomedical Technologist (BMT) programs involves several key steps to transition existing Biomedical Technicians into Technologists, enhancing their skills and

qualifications. Here's a structured approach to developing these programs:

• Needs Assessment

Evaluate Current Workforce: Assess the skills, qualifications, and experience of the existing Biomedical Technicians (500–2,000).

Identify Gaps: Determine the knowledge and skills required for Biomedical Technologists that are currently lacking in the technician workforce.

• Curriculum Development

Core Competencies: Develop a curriculum that covers essential topics such as advanced biomedical equipment technology, regulatory compliance, quality assurance, and healthcare informatics.

Hands-On Training: Incorporate practical training sessions with advanced medical devices and technologies.

Interdisciplinary Learning: Include courses on collaboration with healthcare professionals, ethics, and patient safety.

• Accreditation and Standards

Accreditation: Seek accreditation from relevant educational bodies to ensure the program meets industry standards.

Certification Preparation: Align the curriculum with certification requirements for Biomedical Technologists.

• Program Structure

Duration: Determine the length of the program (e.g., 2-3 years) based on the depth of training needed.

Delivery Mode: Offer flexible learning options, including online, hybrid, and in-person classes to accommodate working technicians.

• Partnerships

Healthcare Institutions: Collaborate with hospitals and clinics for internships and real-world training opportunities.

Industry Experts: Engage industry professionals to provide guest lectures and mentorship.

• Funding and Resources

Budgeting: Develop a budget that includes costs for faculty, materials, and facilities.

Grants and Scholarships: Explore funding opportunities to support students transitioning from technician to technologist roles.

• Recruitment and Enrollment

Awareness Campaigns: Promote the program through workshops, webinars, and informational sessions to attract current technicians.

Application Process: Create a streamlined application process for interested candidates.

• Support Services

Advising and Counseling: Provide academic advising and career counseling services to help students navigate their educational journey.

Alumni Network: Establish an alumni network for ongoing support and professional development.

• Evaluation and Feedback

Program Assessment: Regularly evaluate the program's effectiveness through student feedback, job placement rates, and employer satisfaction.

Continuous Improvement: Use assessment data to make necessary adjustments to the curriculum and training methods.

• Certification and Career Advancement

Certification Preparation: Ensure students are prepared for national certification exams upon program completion.

Career Pathways: A Guide to Career Advancement Opportunities within the Biomedical Field.

By following these steps, BMT programs can effectively transition Biomedical Technicians into more advanced roles as Biomedical Technologists, ultimately enhancing the quality of healthcare technology management.

• **Establishing a separate structure for the specialization of the BME directorates**.

Based on clinical services: Imaging, Laboratory, Life support system/devices, Ophthalmic, and Orthopedics/rehabilitation (including assistive technologies)

• **Innovation and Reengineering**:

There should be a system in place for innovation, Local Production and Technology Transfer (LPTT), reengineering, and research and development.

• **HTA Institute**: An HTA institute should be established at the national level.

• **Recruitment of BMEs**: Facilitating and promoting the export of skilled Biomedical Engineering personnel to foreign or neighboring countries can help address the job creation of skilled BME professionals in Ethiopia.

AUTHOR CONTRIBUTIONS

Dr Mulugeta Mideksa Amene is the sole author of this work and is responsible for all aspects of the research and writing.

ACKNOWLEDGMENTS

I am also grateful to the Ethiopian Biomedical Engineering Association, MOH BME team, Tikur Anbessa Specialized Hospital's Biomedical Engineering teams, the university BME staff (AAU, UoG, JU, and AAPTC), for their unwavering support and collaboration throughout the project lifecycle.

Lastly, I want to express my gratitude to our stakeholders and sponsors for their trust and investment in this project. Their support has been crucial in realizing our objectives and delivering a high-quality engineering report.

In conclusion, I am honored to have been part of this project and am proud of what we have accomplished together. I look forward to the opportunity to collaborate again in the future.

FUNDING

This research received no external funding.

DATA AVAILABILITY STATEMENT

Not applicable.

CONFLICTS OF INTEREST

I declared that I did not have any (potential) conflicts or competing interests with any institutes, organizations, or agencies that might influence the integrity of results or the objective interpretation of their submitted works.

ETHICS APPROVAL AND CONSENT TO PARTICIPATE

Not applicable.

CONSENT FOR PUBLICATION

Not applicable.

FURTHER DISCLOSURE

Not applicable.

REFERENCES

1. WHO. Global atlas of medical devices. 2022. Available online: https://www.who.int/publications/i/item/9789240062207.
2. WHO. Human resources for medical devices, the role of biomedical engineers. 2017. Available online: https://www.who.int/publications/i/item/9789241565479.
3. The International Consortium of Investigative Journalists. Medical devices harm patients worldwide as governments fail to ensure safety. Available online: https://www.icij.org/investigations/implant-files/medical-devices-harm-patients-worldwide-as-governments-fail-on-safety/.

4. WHO. National drug policy of the transitional government of Ethiopia. 1993. Available online: https://extranet.who.int/mindbank/item/723.
5. Jackson, J.L. Advanced Clinical Engineering Workshop: Ethiopia. *J Clin Eng*. 2006;31(3):137. Available online: https://journals.lww.com/jcejournal/citation/2006/07000/advanced_clinical_engineering_workshop__ethiopia.18.aspx.
6. FDA. Errors in health care: A leading cause of death and injury. Available online: https://www.ncbi.nlm.nih.gov/books/NBK225187/.
7. Amoore, J. and Ingram, P. Quality improvement report: Learning from adverse incidents involving medical devices. *BMJ*. 2002;325(7358):272–275. https://doi.org/10.1136/bmj.325.7358.272.
8. EFDA. Organizational structure description with roles and responsibilities. 2023. Available online: https://www.scribd.com/document/791615251/EFDA-organizational-Structure-description-with-roles-and-responsibilities-ed
9. WHO. Human resources for medical devices, the role of biomedical engineers. 2017. Available online: https://www.who.int/publications/i/item/9789241565479.
10. Healthcare technology assessment international (HTAi). Shaping the future of HTA. Available online: http://www.htai.org/index.php?id=428.
11. Ethiopia's health strategies and policies. Available online: https://www.afro.who.int/countries/ethiopia/news/ethiopian-ministry-health-launches-five-year-national-health-equity-strategy-high-level-advocacy.
12. UNICEF, Neonatal mortality, March 2024. Available online: https://data.unicef.org/topic/child-survival/neonatal-mortality/.

Received January 25, 2024, accepted July 15, 2025, publication date for online-first December 12, 2025.

Original Research Article

Comparison of the Performance Test of Reusable Patient Circuit and Disposable Patient Circuit of Ventilator

Li Bao, Yunming Shen, Siwei Xiang and Kun Zheng*

The Children's Hospital, Zhejiang University School of Medicine, Hangzhou, China.

* Corresponding Author Email: zhengkun@zju.edu.cn

ABSTRACT

Two kinds of ventilator patient circuits are used widely in clinical routine, namely, reusable patient circuits and disposable patient circuits. Is their performance the same in clinical application? Comparison of the performance test of these two kinds of ventilator circuits with a ventilator gas flow analyzer is given in this paper. Thirty ventilators were randomly selected to test their performance with these two types of circuits. Then, the paired t-test method was used to analyze whether the difference in performance test between the two circuits was significant. For respiratory rate, tidal volume, and end airway pressure, there were no significant differences between these two circuits ($p > 0.05$). For the airway peak pressure, the reusable patient circuit was significantly higher than the disposable patient circuit ($p < 0.05$), but the actual value of the difference was very small, only about 0.2 mbar, which did not have any significant clinical meaning. Therefore, in the experimental environment, there is no difference in performance test results between disposable circuits and reusable circuits.

Keywords—*Ventilator, Reusable patient circuit, Disposable patient circuit, Performance test.*

INTRODUCTION

Medical ventilator is the most common clinical first aid and life support equipment that can replace, control, or change human respiration, increase lung ventilation, improve respiratory function, and reduce the consumption of respiratory function. It can provide respiratory support for patients with respiratory failure and play an important role in clinical treatment. Medical ventilator is also a clinical high-risk medical equipment. According to years of monitoring and analysis by the State Food and Drug Administration and the US FDA, ventilators belong to the high-risk category of medical equipment.[1] So it is necessary to arrange at least one ventilator quality control test every year.

The complete ventilator system includes five parts: air source, air oxygen mixer, main engine, humidifier, and respiratory circuit.[2] For respiratory circuits, two kinds of patient circuits are used widely in clinical routine, namely, reusable patient circuits and disposable patient circuits. The reusable patient circuit is a reusable silicone thread pipe, and the disposable patient circuit is a PVC material thread pipe. The reusable silicone circuit, after a long time of repeated disinfection, will be subjected to aging, air leakage, damage, and other problems; also, repeated use is more likely to cause cross-infection among patients. The disposable patient circuit features lightweight, sufficient length, a transparent tube body, resistance to kinking, and a well-sealed cup. Therefore, clinical preference is to use the disposable patient circuit. Although the disposable patient circuit has advantages in economy, safety, health, and other aspects, its material is inferior to the reusable patient circuit, including thickness, elasticity, etc. Thus, is it feasible to apply it in clinical settings for evaluating whether two circuits provide consistent ventilator performance and comparable clinical therapeutic outcomes. At present, there is a lot of research literature on the influence of the disposable patient circuit on clinical therapeutic effect, while there is almost no research literature on the influence of ventilator performance. This paper evaluates whether reusable patient circuit and disposable patient circuit provide the same ventilator performance.

MATERIALS AND METHODS

Quality Control Tools and Contents

The air flow analyzer (VT 650, Fluke Biomedical, America) is used in our hospital for ventilator quality control, which can detect a variety of airflow parameters, including tidal volume, respiratory rate, oxygen absorption concentration, airway peak pressure, end airway pressure, and other indicators. The analyzer itself is qualified and within the validity period.

Thirty ventilators were randomly selected, including Evita 4 (Draegerwerk AG & Co. KGaA, Germany) and Maquet Servo-i (Getinge, Sweden). For quality control of the 30 pediatric ventilators (configured for children weighing 15–30 kg), a new reusable patient circuit and a disposable patient circuit (both suitable for this weight range) were used, respectively, with quality control data recorded.[3–7] The quality control of a ventilator refers to Calibration Specification for Ventilator (JJF 1234-2018)[8], including tidal volume, respiratory rate, airway peak pressure, airway end pressure, oxygen concentration, and various alarms.

Paired *t*-test

The t-test includes single-sample, independent-sample, and paired-sample. Single-sample refers to one sample, independent-sample refers to two groups of samples that have no correlation, and paired-sample refers to two samples that are associated according to a certain parameter. In this paper, the reusable patient circuit and disposable patient circuit of the same ventilator were compared, that is, they were paired according to the ventilator and belonged to the paired sample.[9–11]

The paired *t*-test is essentially a single-sample *t*-test. First, the difference is calculated according to the pairing, and then the difference is *t*-tested. That is, for each ventilator, quality control results of the reusable patient circuit are subtracted from quality control results of the disposable patient circuit to obtain the pairing difference X_n, as shown in Formula (1), where $n = 1, 2, 3\ldots$ represents ventilator number, R represents quality control parameters, including tidal volume, peak airway pressure, end airway pressure, respiratory rate, etc.

$$X_n = R_{reusable\ circuti} - R_{disposable\ circuit} \quad (1)$$

Then, calculate the mean value $\bar{X}$ and the sample standard deviation s of the paired difference, as shown in Formulas (2) and (3). Formulas (2) and (3) are substituted into Formula (4) to construct the *t* statistic. $\bar{X}$ refers to mean of paired differences, *s* refers to the sample standard deviation of paired differences, *t* refers to the t-statistic, and *n* refers to the number of paired samples.

$$\bar{X} = \frac{1}{n}\sum_{i=1}^{n} X_i \quad (2)$$

$$S^2 = \frac{1}{n-1}\sum_{i=1}^{n}(X_i - \bar{X})^2 \quad (3)$$

$$t = \frac{\bar{X} - 0}{\frac{s}{\sqrt{n}}} \sim t(n-1) \quad (4)$$

Finally, look up the table to obtain the P-value and calculate the confidence interval NCI of the pairing difference, as shown in Formula (5). $p < 0.05$ indicates a significant difference, and the confidence interval of paired difference is above or below the 0 scale line, where above the 0 scale line indicates that the reusable patient circuit is significantly higher than the disposable patient circuit, whereas below the 0 scale line indicates that it is significantly lower. $p > 0.05$ means that the difference is not significant, that is, there is no difference between the reusable patient circuit and the disposable circuit, and the confidence interval of the paired difference crosses the 0 scale line and has no significant positive or negative direction.

$$N_{CI} = \bar{X} \pm 2.12\frac{s}{\sqrt{n}} \quad (5)$$

Research on Quality Control Results

Thirty ventilators were randomly selected, and quality control tests were conducted on each ventilator using the reusable patient circuit and the disposable patient circuit, respectively, and quality control data were recorded. The alarms in the quality control data are qualitative indicators, and their performance is basically consistent between the two circuits. Thus, they will not be discussed in detail below. The respiratory rate is exactly the same as the ventilator setting, which will not be discussed in detail. Oxygen concentration is not discussed in detail, considering the failure of oxygen batteries in some ventilators. The remaining tidal volume, peak airway pressure, and end airway pressure are analyzed in detail below.

Tidal Volume

Under the conditions of VCV (Volume-Controlled Ventilation) mode and *f* = 30 times/min, *I:E* = 1:1.5, PEEP = 2 mbar (Positive End-Expiratory Pressure), and FiO_2 = 40% (oxygen concentration), two kinds of circuits were used to test the calibration points of tidal volume such as 50 mL, 100 mL, 150 mL, 200 mL, and 300 mL, respectively. The *t*-test results are shown in Figure 1. For tidal volume ranging from 200 mL to 300 mL, the confidence interval of the paired difference all cross the 0 scale line, indicating that the use of the reusable patient circuit and the disposable patient circuit has no difference. For the tidal volume = 50 mL, 100 mL, and 150 mL, the confidence interval of paired difference is above the 0 scale line, that is, the test value of the reusable patient circuit is significantly 1–2 mL higher than that of the disposable patient circuit, accounting for 2%–3%, which is within the required range of the tidal volume error. In other words, although there is a significant difference between the two circuits, the difference is very small and does not affect the quality control conclusion.

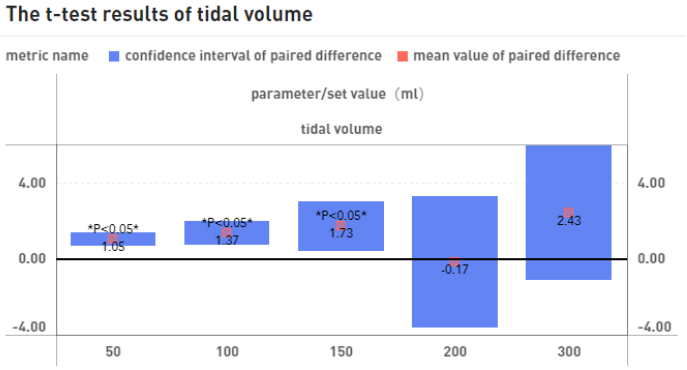

FIGURE1. The t-test results of tidal volume (mL).

Peak Airway Pressure

Under the conditions of PCV mode and *f* = 15 times/min, *I:E* = 1:2, PEEP = 0 mbar, and FiO_2 = 40%, two kinds of circuits were used to test the calibration points of airway peak pressure such as 10 mbar, 15 mbar, 20 mbar, 25 mbar, and 30 mbar, respectively. The *t*-test results are shown in Figure 2. The confidence interval of the paired difference

is above the 0 scale line, that is, the airway peak pressure of the reusable patient circuit is significantly higher than that of the disposable patient circuit, which indicates that the sealing performance of the reusable patient circuit is better than that of the disposable patient circuit. Zheng Kun's paper also has a similar research description.[12] They found that the reusable silicone threaded circuit is made of silicone, featuring a thick tube wall, slow heat dissipation, excellent thermal insulation performance, and good compliance. The material of the disposable PVC circuit is PVC, which has a thin pipe wall, fast heat dissipation, poor thermal insulation performance, and poor compliance. The peak airway pressure measured by the reusable patient circuit is about 0.2 mbar higher on average than that of the disposable patient circuit, accounting for 1%–2%. The difference is very small, that is, although there is a significant difference between the two kinds of circuits, the difference is small and does not affect the quality control dimension.

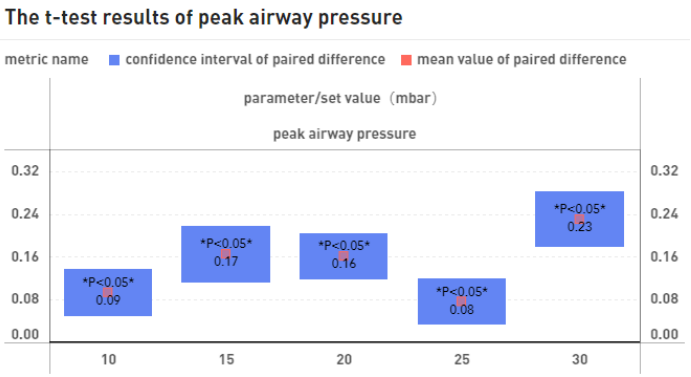

FIGURE 2. The *t*-test results of peak airway pressure (mbar).

End Airway Pressure

Under the conditions of the VCV mode and VT = 400 mL, f = 15 times/min, $I:E$ = 1:2, and FiO_2 = 40%, two kinds of circuits were used to test the end airway pressure calibration points, such as 2 mbar, 5 mbar, 10 mbar, 15 mbar, and 20 mbar, respectively. The *t*-test results are shown in Figure 3. The confidence interval of the paired difference is across the 0 scale line, that is, there is no statistically significant difference in the end airway pressure measured by the reusable patient circuit and the disposable circuit. And, the average difference in the measured end-airway pressure between the two circuits is about 0.02 mbar, which is very small.

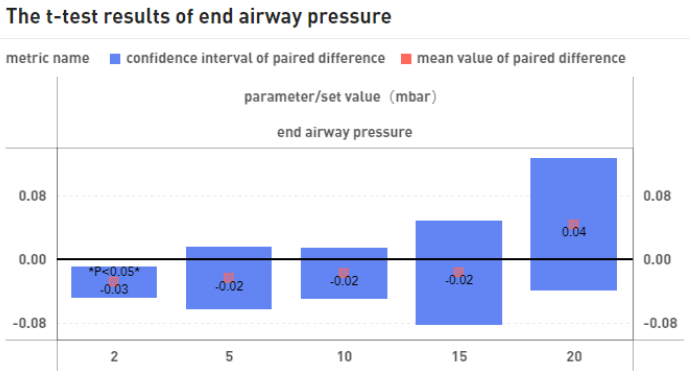

FIGURE 3. The *t*-test results of the end airway pressure (mbar).

DISCUSSION

This study found that the reusable patient circuit and the disposable patient circuit do not affect the quality control results. For respiratory rate, tidal volume, and end airway pressure, there were no statistically significant differences between the two kinds of circuits ($p > 0.05$). For airway peak pressure, the reusable patient circuit was significantly higher than the disposable patient circuit ($p < 0.05$), but the difference was very small, only about 0.2 mbar, accounting for 1%–2%, within the error range, which did not affect the quality control results.

Yang Qiuyue et al.[13] found that the treatment effect of the disposable patient circuit of a noninvasive ventilator was significantly better than that of the reusable patient circuit and could significantly reduce the nursing workload, which was reflected in the number of calls to the nursing staff, the amount of humidification fluid used, and the number of suction times of the disposable patient circuit group being significantly lower than that of the reusable patient circuit group. Xiao Chunlian et al.[14] found that the disposable circuit system could reduce the workload of the ventilator circuit care, reduce the viscosity of airway sputum, and reduce the incidence of ventilator-related pneumonia, which is worthy of widespread clinical application.

The disposable circuit has fine heating wires built inside, which communicate with the temperature control module of the humidifier through a dedicated interface to

achieve real-time temperature compensation. Reusable circuits have no built-in heating wires, or their interfaces are not compatible with the temperature control systems of mainstream humidifiers. Repeated disinfection may damage the electronic components. Therefore, they cannot participate in the dynamic regulation of humidity. The heaters utilize disposable heated wire circuits to provide 100% humidity and rainout prevention. Rainout in a circuit can be a major cause of desaturation in a patient when the excess water in a circuit is inadvertently dumped down the ET tube (Endotracheal Tube) and aspirated by the patient. This can cause adverse effects to the patient.

According to our studies and those of our peers, the disposable circuit provides the same ventilator performance as the reusable patient circuit, with advantages in the clinical treatment effect. These results show that the disposable circuit can be used in clinical practice. Obviously, we simulate the response of the membrane lung to two kinds of circuits, which has some limitations. In complex cases, especially in young infants, further evaluation is needed to better realize the compliance of the circuits to the function of the relevant ventilation pattern, especially the tidal volume compensation. The advantages of the disposable circuit in clinical treatment effect also need to be verified by subsequent multidimensional analysis, especially for the study of the clinical treatment effect in children.

SUMMARY

This study found that the reusable patient circuit and the disposable patient circuit do not affect ventilator quality control results, that is, two kinds of ventilator patient circuits provide the same ventilator performance. Combined with the peer's research on the therapeutic effect of two kinds of ventilator patient circuits, the disposable circuit can be used in clinical practice.

AUTHOR CONTRIBUTIONS

Conceptualization, L.B. and S.W.X.; Methodology, L.B and S.W. X; Software, L.B. and S.W.X.; Hardware, L.B. and S.W.X.; Validation, L.B.; Formal Analysis, L. B.; Investigation, L.B.; Resources, Y.M.S and K.Z.; Data Curation, L.B.; Writing–Original Draft Preparation, L. B.; Writing–Review & Editing, L.B.; Visualization, L.B.; Supervision, Y.M.S. and K. Z.; Project Administration, L.B.; Funding Acquisition, Y.M.S and K.Z.

ACKNOWLEDGMENTS

Not applicable.

FUNDING

This research received no external funding.

DATA AVAILABILITY STATEMENT

Not applicable.

CONFLICTS OF INTEREST

The authors declare they have no competing interests.

ETHICS APPROVAL AND CONSENT TO PARTICIPATE

Not applicable.

CONSENT FOR PUBLICATION

Not applicable.

FURTHER DISCLOSURE

Not applicable.

REFERENCES

1. Wu, M. Research of reducing the failure rate of ventilator in our hospital. *China Med Dev*. 2017;32(7):94–96. https://doi.org/10.3969/j.issn.1674-1633.2017.07.026.
2. Sun, Z. Basic structure and maintenance of ventilator. *Equip. Manag. Maint*. 2022;(12):10–12. https://doi.org/10.16621/j.cnki.issn1001-0599.2022.06D.05.
3. Xu, S.N., Dong, C., Li, W.Z., et al. Research on rapid detection technology for quality control of emergency ventilator. *Chin. J. Med. Instrum*. 2022;46(3):336–341.https://doi.org/10.3969/j.issn.1671-7104.2022.03.021.

4. Wang, W.J. and Li, X.H. Quality control and effect analysis of medical ventilator. *J Anhui Med Coll*. 2022;21(3):16–18. https://doi.org/10.3969/j.issn.1671-7104.2022.03.021.
5. Gómez-Alzate, D., Pérez-Buitrago, S., Córdova, M., et al. Quality characteristics of the Masi Peruvian mechanical ventilator manufacturing process. In *2021 43rd Annual International Conference of the IEEE Engineering in Medicine & Biology Society (EMBC)*, Mexico, 2021, pp. 1557–1561. https://doi.org/10.1109/EMBC46164.2021.9630439.
6. Farre, R., Artigas, A., Torres, A., et al. A simple procedure to measure the tidal volume delivered by mechanical ventilators: a tool for bedside verification and quality control. *Arch Bronconeumol*. 2023,59(1):61–62. https://doi.org/10.1016/j.arbres.2022.07.008.
7. Alvarado, A.E.L., de Oliveira Rosa, D.A., Mello, S. G., et al. Quality Assessment of Emergency Corrective Maintenance of Critical Care Ventilators within the Context of COVID-19 in Sao Paulo, Brazil. *Glob Clin Eng J*. 2021;4(1):27–36. https://doi.org/10.31354/globalce.v4i1.108.
8. General Administration of Quality Supervision, Inspection and Quarantine of the People's Republic of China. Ventilator calibration specifications. National Metrological Technical Specifications Public System; 2018. Available online: https://jjg.spc.org.cn/resmea/standard/JJF%25201234-2018/.
9. Xu, M.F., Fralick, D., Zheng, Z., et al. The differences and similarities between two-sample t-test and paired t-test. *Shanghai Arch Psychiatry.* 2017,29(3):184–188. https://doi.org/10.11919/j.issn.1002-0829.217070.
10. Gao, F., Liu, Y.Y., Li, C.P., et al. How to use t test correctly—the basic concepts and preconditions of t test. *Sichuan Ment. Health*. 2020;33(3):211–216. https://doi.org/10.11886/scjsws20200526003.
11. Daya, S. The t-test for comparing means of two groups of equal size. *Evid Based Obstet Gynecol*. 2003;5(1):4–5. https://doi.org/10.1016/S1361-259X(03)00054-0.
12. Zheng, K. Effect of different ventilator circuits on airway humidification in patients with invasive mechanical ventilation. *Chin J Pharm Econ*. 2014(12):67–68. https://doi.org/CNKI:SUN:ZYWA.0.2014-12-038.
13. Yang, Q.Y., Wang, F.Y., Xu, L.L. Clinical study on the difference of treatment effect and nursing between noninvasive ventilator disposable circuit and routine circuit. *Zhejiang Med. J*. 2021; 43(13):1465–1466, 1474. https://doi.org/10.12056/j.issn.1006-2785.2021.43.13.2020-3583.
14. Xiao, C.L., Fang, M., Feng, L.Q., et al. Analysis of applied value of the constant temperature and humidification disposable breath circuit system for patient treated by ventilator. *Nurs. Res. Pract*. 2011;8(7):67–68. https://doi.org/10.3969/j.issn.1672-9676.2011.07.035.

This paper is part of the Special Issue on Design and Manufacturing in Biomedical Engineering.
Guest Editor: Dr. Jashanpreet Singh, University Center for Research and Development, Chandigarh University, Punjab, India.
Prof. Dr. Chander Prakash, University Center for Research and Development, Chandigarh University, Punjab, India.

Received January 6, 2025, accepted July 12, 2025, publication date for online-first December 10, 2025.

Review

A Critical Review of 3D Printing in Bioimplants' Applications

Vikas Sharma[1], Jashanpreet Singh[1,*] and Amanpreet Singh[2]

[1] University Center for Research and Development, Chandigarh University, Mohali, Punjab, India.
[2] Centre for Research Impact and Outcome, Chitkara University Institute of Engineering and Technology, Chitkara University, Rajpura, Punjab, India.

[*] Corresponding Author Email: jashanpreet.e17331@cumail.in

ABSTRACT

3D printing is rapidly revolutionizing the field of biomedical engineering, particularly in the production of customized implants. This manuscript explores the diverse applications of AM for the fabrication of implants in various medical disciplines such as orthopaedics, dentistry, and craniofacial surgery. Selective laser melting (SLM), fused deposition modelling (FDM), and stereolithography (SLA) are examined as the main additive fabrication techniques in terms of bioimplant manufacturing. It also includes a variety of biomaterials applied in 3D printing with emphasis on their mechanical capabilities, compatibility, and applicability in various procedures. With the help of digital design files and advanced printing techniques, healthcare providers can supply implants with respect to a patient's exact anatomy, resulting in better fit, high performance, and more comfort than conventional mass-produced options.

The paper also highlights the advantages of AM, such as reduced surgical period and enhanced patient outcomes because of the precise customization of implant geometries. The use of 3D printing in practice has disadvantages and major obstacles, such as production limitations, cost of production, strict regulations, and long-term clinical evidence. This review discusses the future possibilities and potential of 3D printing to enhance personalized medicine and the need for interdisciplinary cooperation to address existing barriers.

Keywords—*Additive manufacturing, 3D printing, Orthopaedics, Customized implants, Regenerative medicine, Personalized medicine.*

INTRODUCTION

Additive manufacturing (AM) or three-dimensional (3D) printing is a transformative technology used in the development of 3D objects using layer-by-layer material deposition based on 3D models.[1] The 3D printing technology has created a transformational change in medical implantology (i.e., design, placement, and management of medical implants), especially in the designing and manufacturing of orthopaedic implants.[2] The AM technology allows the production of patient-specific implants (PSIs) according to individual anatomic needs. Thus, it overcomes the shortcomings of the conventional implant manufacturing processes. AM directly creates a complex part from a computer-aided design (CAD), not possible with the conventional manufacturing processes based on subtractive subtraction of a material. 3D printing enables the fabrication of implants with complex geometry and improved functional characteristics based on high-resolution imaging, CAD, and layer-by-layer material deposition to provide unprecedented possibilities in medical applications with customization and precision.

The 3D printing or AM also has a profound effect on the biomedical industry, with the capability to produce complex, customized medical devices, vaccines, and tissues.[3] 3D printing reduced the burden of material production, truncated the pattern of preparation, and offered a wider domain to treat diseases.[4] In orthopaedics, 3D printing is utilized for a wide range of applications, including joint replacements, fixation devices, and spinal fusion systems. The notion of designing complex surface structures and customization of implants to the specific needs of patients has transformed the way surgical operations are planned and implemented.[5] These customized implants not only improve surgical outcomes but also reduce complications associated with misalignment and suboptimal fit. Furthermore, the technology is rapidly evolving to address challenges, such as regulatory compliance, material biocompatibility, and scalability, making it an integral component of modern orthopaedic practices.

3D printing is an emerging technology with a lot of potential to be translational in biology and medicine.[6] Lately, 3D living and non-living materials are under extensive scrutiny for a possible alternative to the traditionally used and proffered solutions to testing and combating antimicrobial resistance (AMR). To be able to control the cell and micro-environment accurately with the complex presence and activities of the cell, AM has a good chance to promote medical treatment. The technology used in 3D bioprinting has made cell-laden scaffolds more applicable and functional.[7] One of the prerequisites for the evolution of 3D printing in tissue engineering is the research of innovative compatible biomaterials for use in bioprinting with fast crosslinking properties. The developers should consider the key aspects of making the technology printable so that it can enhance the coding of the fabrication process, as well as cell encapsulation. 3D printing methods could help in many medical and pharmaceutical areas, including tissue regeneration, printing organs, and drug delivery.[8] The technology has presented itself as a game-changer in the biomedical sector, with 3D printing presenting a wide range of applications and advantages.[9] It is very important in facilitating the increase and reconstruction of destroyed tissues. It is able to build structures (resembling the native tissue) and regenerate the tissue by precisely depositing cells, biomaterials, and growth factors. It will facilitate the production of complex cellular structures and even working organs in the future. This is when multi-type cells and biomaterials are combined in three-dimension (3D) to produce functional structures. In medical engineering, 3D printing has taken the form of a more potent production stage.[9] These techniques are very helpful to produce a variety of complex and specialized biomedical products of high precision, layer by layer of materials, biomolecules, and living cells.

The selection and manufacturing process of the tissue engineering materials is an important factor in the context of compatibility, sensitivity, and interaction with other organs in case of a failed organ replacement.[10] A versatile range of biomaterials, such as polymers, hydrogels, ceramics, composites, and metals, can be achieved by 3D printing.[11] It makes possible the construction of complex structures with high resolution and accuracy. Implants and prostheses are manufactured using 3D printing, which

means that they are exact to the anatomy of the patient.[9] This has the potential to result in more compatibility with the surrounding tissues and enhances long-term performance. Customized prosthetics and orthotics are also developed using this technology; this offers a superior fit, additional comfort, and enhanced functionality. 3D printing provides the opportunity of rapid prototyping prosthetic and orthotic design, in which designers and clinicians are able to test and update the design instantly by following the patient input, so that the resulting devices are superior and more humane in use. 3D printing has its prospects in the perspective of mechanical engineering through the finite element analysis of implants, that is, a computational technique of modelling how implants respond to different loads to optimize their design and functionality.[12] Furthermore, the implants are now done through 3D printing, thus enabling a unique implant with intricate geometries to suit patient's specific requirements.

This paper explores the diverse applications and benefits of 3D printing in orthopaedic implants, with a focus on its role in enhancing surgical precision, improving patient outcomes, and advancing sustainable manufacturing practices. Additionally, this paper highlights the challenges facing the widespread adoption of this technology and the future directions that hold promise for overcoming these barriers. Through a comprehensive analysis, this review paper elaborates the pivotal role of 3D printing in the development of personalized medicine and the practice of high-quality orthopaedic surgery through a broader analysis.

3D PRINTING TECHNIQUES FOR BIOMEDICAL IMPLANTS

The integration of the concept of 3D printing or AM in biomedical implants has transformed the development and fabrication of medical equipment.[13] Different methods of 3D printing have been developed, which are characterized by their own inimitable benefits. These methods increase the efficiency and placement of bioimplants into the human body.[14] It discusses five major 3D printing methods applicable in the designing of biomedical implants: powder bed fusion (PBF), binder jetting, material extrusion (M/E), directed energy deposition (DED), and stereolithography (SLA). Table 1 demonstrates the 3D printing methods and materials applied to bioimplants.

TABLE 1. 3D printing techniques and materials for bioimplants.

S. No.	Technique	Materials	Application	Benefits	Drawbacks	References
1.	Selective laser sintering (SLS)	Polycarbonate (PC), polyurethane (PU), etc.	Customized implants, surgical tools, prosthetics, etc.	High strength, durability, and complex geometries	Expensive, limited resolution, and rough surface finish	15–17
2.	Stereolithography (SLA)	Photopolymerizable resins such as acrylates, epoxies, and polyurethanes	Dental models, prosthetics, surgical guides, etc.	High-resolution, smooth surface finish, and accuracy	Expensive, limited material selection, and potentially toxic photo initiators	18
3.	Fused deposition modelling (FDM)	Polylactic acid (PLA), polyethylene terephthalate (PET), polyethylene oxide (PEO), etc.	Customized implants, surgical guides, prosthetics, etc.	Low-cost, versatile, and easy to use	Limited strength and stiffness, poor resolution, and rough surface finish	19–21
4.	Electrospinning (ESP)	Polycaprolactone (PCL), poly (vinyl alcohol) (PVA), collagen, etc.	Tissue engineering, wound healing, and drug delivery	High porosity, biocompatibility, and fiber diameter control	Limited mechanical strength and complex 3D structures	22–24
5.	Inkjet printing (IJP)	Hydrogels, synthetic polymers, bioinks, etc.	Tissue engineering, drug delivery, and regenerative medicine	High flexibility, scalability, and control over composition	Limited mechanical properties, resolution, and stability	25,26
6.	Digital light processing (DLP)	Poly (ethylene glycol) diacrylate (PEGDA), GelMA, Polyurethane (PU)	Tissue engineering, drug delivery, and surgical planning	High resolution, accuracy, and speed	Limited material selection, biocompatibility, and mechanical properties	27,28

Powder Bed Fusion

One of the most common 3D printing techniques is power bed fusion, which involves the process of melting or sintering powdered materials through layer-by-layer selectivity into solid objects.[29] Figure 1 presents a schematic diagram of PBF. It works particularly well in applications involving biomedical implants for producing complex geometries that closely mimic natural bone structures. The technique commonly utilizes titanium (Ti) and cobalt–chromium (Co-Cr) alloys that are considered biocompatible metals because of their strong, durable, and biocompatible nature with human tissues. A major advantage of PBF is its ability to allow the development of porous structures, leading to facilitated osseointegration. In the osseointegration, an implant properly connects with the surrounding bone, which reduces the complications related to stress shielding. Therefore, the surrounding bone is resorbed.[29] For example, PBF can be used to create implants in a trabecular lattice structure that allows oriented in-growth of bones, enhancing the effective life and functionality of orthopaedic implants. Also, the PBF can create complex internal architectures and allows manipulating implants to be more suitable to fit biological functions; this has made it gain popularity in orthopaedic and dental surgery.

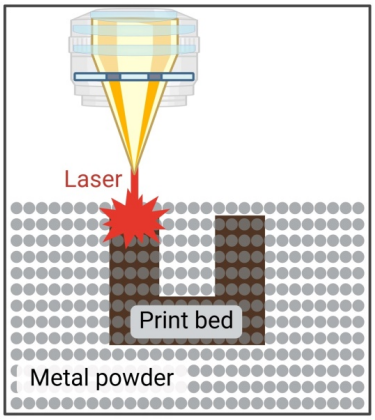

FIGURE 1. Schematic diagram of powder bed fusion (PBF) technique.

Binder Jetting Technique

Another 3D printing method is binder jetting technology (BJT), in which powders are fused with the help of a liquid agent,[30] as schematically shown in Figure 2. The technique offers high accuracy in producing intricate forms and has little waste of materials. BJT can specifically be applied in biomedical engineering to make ceramic and metal implants. Multi-material constructs can also be produced by BJT. Thus, it allows dissimilar properties within the same implant to be combined together, for example, using bioactive ceramics with metals to facilitate improved bone healing.[31] For instance, a dental implant made by combining Ti, providing good mechanical strength, with bioactive glass, offering osteoconductivity, using BJT integrates more favourably with the tissue of the jawbone. In addition, BJT has the ability to scale to mass production, so it provides an inexpensive solution in manufacturing patient-specific implants in larger volumes with high fidelity to patient anatomy.[32]

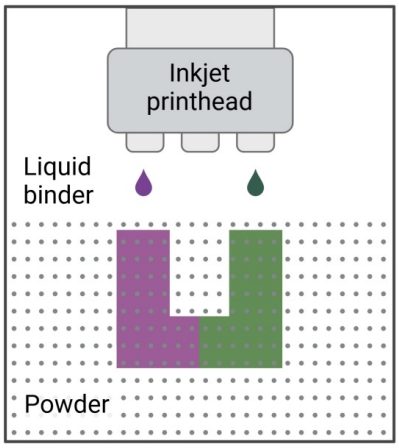

FIGURE 2. Schematic diagram of the binder jetting technique.

Material Extrusion Technique

In biomedical applications, one of the most accessible and widely adopted procedures of 3D printing is the material extrusion technique (MET).[33] It consists of extrusion of a thermoplastic or bioink material through a nozzle to stack the layers side by side, as exemplified in Figure 3. MET (in bioimplants) is especially successful in creating polymer-based implants that require flexibility and biocompatibility. MET is customized easily depending on the information of the patient through medical imaging techniques, such as computed axial tomography (CAT) scan and magnetic resonance imaging (MRI). The mechanical properties and tissue integration of composite filament applications, which are constituted of polymers

and bioactive fillers, are increased with the use of MET. Polymer scaffolds, 3D-printed and impregnated with hydroxyapatite (HA), had the ability to imitate natural bone structure and ensured a good ambience in terms of proliferation and regeneration of cells.[34]

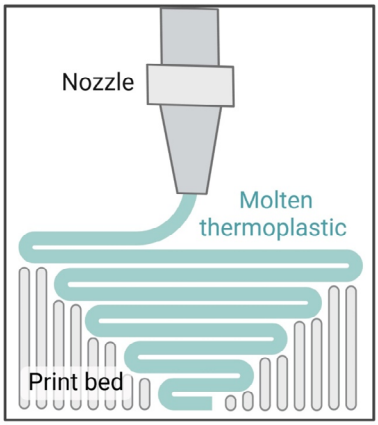

FIGURE 3. Schematic diagram of the material extrusion technique (MET).

Directed Energy Deposition

Directed energy deposition (DED) involves focused energy sources, such as lasers or electron beams, to melt deposited materials on the substrate, as shown in Figure 4.[35,36] DED is advantageous in repairing the existing implant or in post-processing the implant after formation. In biomedical applications, DED is used to make large-scale implants of tailored properties by varying the composition of materials throughout the deposition sequence. This ability has led to the production of functionally graded materials in which properties vary gradually throughout the implant. This allows these materials to adapt more effectively to physiological loads and perform better with time.[37] Furthermore, DED has the potential to manufacture patient-specific osteotomy instruments and orthopaedic implants that can fit the anatomical demands of the patient.[38]

Stereolithography

Stereolithography (SLA) involves the use of ultraviolet (UV) light in curing photopolymer resins progressively into solid objects.[18] SLA is acknowledged due to its high-resolution printing and smooth finish of the surface, as presented in Figure 5. Thus, it has been used for

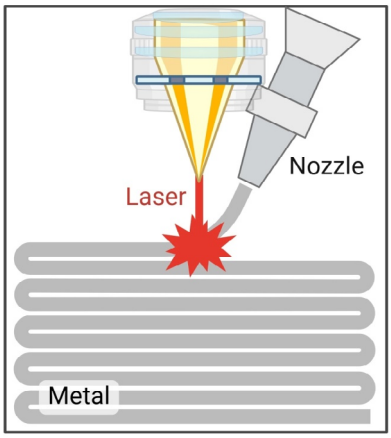

FIGURE 4. Schematic presentation of the directed energy deposition (DED) technique.

creating highly complex models required in bioimplants, particularly in the fields of dentistry and craniofacial surgery. Moreover, new developments in biocompatible resins have increased the scope of SLA to be used in manufacturing temporary implants or tissue-supportive scaffolds. For instance, with the help of SLA technology, it is possible to make cranial plates that are perfect to be shaped on defects and traumas in the skull as a result of trauma or surgical operations. It decreases the period of recovery and increases patient satisfaction.

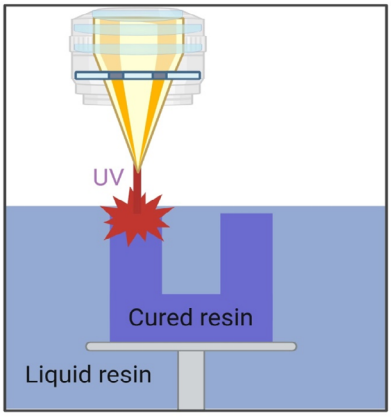

FIGURE 5. Schematic presentation of stereolithography (SLA) technology.

One new way to make one-of-a-kind products is using 3D printing. In the biomedical industry, the most common 3D printing methods include extrusion printing/bioprinting, SLA, powder deposition printing (such as FDM), laser-assisted printing (such as selective laser

sintering [SLS] or selective laser melting [SLM]), and direct ink writing (DIW)/inkjet bioprinting.[39,40] The first method of creating 3D objects was SLA. This method often makes use of thermoset photopolymers. The process of solidifying liquid resins allows the generation of object models. The area of 3D printed ceramic biomedical devices has reported extensive use of these approaches.[41] Composites made of SLA have potential applications in the fields of dentistry and cardiovascular medicine. Another 3D printing technology is digital light processing (DLP), which largely uses the same light source as SLA but with a different printing approach.[27] The DLP manufacturing really shines for developing conductive products for the electrical industry. That means conductive polymer systems are a viable option for the method's first components.

MATERIALS FOR 3D PRINTING OF BIOMEDICAL IMPLANTS

Metallic Materials

Various types of 3D printing metallic materials (Figure 6) are as follows.

Titanium and Its Alloys

Owing to their high specific strength, good corrosion resistance, and excellent biocompatibility, Ti and its alloys have been utilized extensively in biomedical implants since the 1970s.[42] Ti exhibits an α-phase (hexagonal), close-packed lattice structure at ambient temperature, and if heated to 883 °C, the β-phase with body-centered cubic structure appears. An increase in β/α transus temperature is one way that alloying elements, such as aluminium (Al), carbon (C), and oxygen (O), prolong the α-phase, and a decrease in the transus temperature is another way that molybdenum (Mo), tantalum (Ta), and niobium (Nb) employ.[42] Thus, α, near-α, (α + β), and β type alloys are the four primary categories into which Ti alloys accrue. Ti alloys can have their grain size changed by plastic deformation, and osseointegration is enhanced in alloys with smaller grains, because there are fewer atoms per grain and a higher surface energy. Specifically, as contrasted with traditional Ti-64 (with a high strength-to-weight ratio) variations—ultrafine-grained commercially pure titanium (CP-Ti) and Ti-64 alloys (with a grain structure in the submicrometer to nanometre range)—exhibit far superior vascular and bone cell adhesion.[43] The formation of a passive TiO_2 coating by CP-Ti and Ti-64 occurs naturally. This film contains OH^- ions, which interact with the mineral components of the bones and enhance osteointegration. Ti-64 is used by half of all biomedical implants, but it's not without its fears. It contains cytotoxic Al and vanadium (V); thus, new alloys without these elements have been developed specifically for implant applications.[44]

Gallium Alloys

In contrast to solid metals, gallium (Ga) alloys have a wide range of medicinal uses, such as nerve reconnection, vascular embolization, tumor therapy, and flexible interconnects.[45] Metal thiolate complex functionalization of Ga alloy nanoparticles has opened new avenues for drug delivery.[46] Antennas and electrodes used in biological applications benefit from Ga alloys' self-healing properties. For instance, when a Ga alloy-filled channel is cut, the alloy forms a protective oxide that stops liquid metal from escaping or dripping out. When the two pieces are rejoined, the liquid metal eventually combines, and electrical conduction is normalised. Additionally, the channel is able to mechanically mend itself if it is composed of a self-healing polymer.

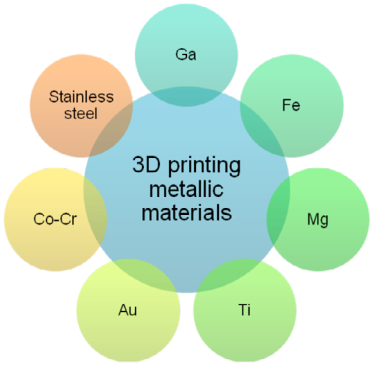

FIGURE 6. Various types of 3D printing metallic materials.

Iron

Proteins in hemoglobin and myoglobin are responsible for carrying oxygen to the tissues. Other proteins and

enzymes involved in metabolism contain iron (Fe), an important trace element for nearly all living things.[47] It is known that the elevated Fe concentrations are poisonous. The outstanding mechanical properties of Fe-based materials make them an attractive option for biodegradable implants.[48]

Magnesium and ITS ALLOYS

In addition to its role in energy metabolism and protein synthesis, magnesium (Mg aids in the regulation of blood sugar and maintenance of bone strength. The kidneys filter out excess Mg after its absorption in the digestive tract.[49] Infection and formation of hydrogen bubbles are two issues when using Mg alloys as implants. The solution to this is to nucleate Mg alloy as metallic glass, an amorphous, one-phase structure, which eliminates hydrogen bubbles. Because of its flammability, 3D printing of Mg scaffolds requires an inert or vacuum environment.[43]

Gold

The many desirable properties of gold (Au) include its high infrared reflectance, ductility, electrical conductivity, and thermal conductivity, which make it an ideal material for use in engineering.[50] Owing to the high cost of Au, only electroplated objects are used. Ocular prosthetics, especially for the surgery of the upper eyelids, endovascular stents, soluble injectable compounds to treat or prevent bacterial infections, and restorative dentistry (implants, fillings, gold wire fixings, and supports) are among the many uses of Au.

Cobalt–Chromium Alloys

Medical implants made of Co-Cr alloys have been used since the 1930s. Compared to stainless steel, Co-Cr alloys offer superior corrosion resistance and wear resistance.[51] As this alloy contacts the human body, Cr creates a protective Cr_2O_3 coating, which makes it very biocompatible. Some implants, such as Co-Cr-Mo manufactured implants, discharge ions of Co and Cr into the bloodstream because of their metal-on-metal bearings.[52] After 4–5 years of implantation, some patients with metal-on-metal hip prosthesis have reported severe reactions because of cobalt toxicity. Treatment of the laser with the alloy and calcium phosphate coating of the prosthesis might be applied as one of the methods to make the process of osseointegration faster and further improve the surface characteristics of the implant and stimulate the development of new bone tissues.[53]

Stainless Steel

Stainless steel alloys consist of Fe and Ni alloys with chromium content ≥ 11%. By manipulating the doping and heat treatment of stainless steel, one can influence its mechanical properties. Owing to its biocompatibility, low cost, ease of manufacturing, and widespread availability, austenitic stainless steel, such as stainless steel 316L, is used in the majority of biomedical applications. Co-Cr alloys form a protective oxide layer on stainless steel surfaces.

Polymer-Based Materials

Figure 7 shows various types of 3D printing polymeric materials. The following sections present a detailed discussion on polymeric 3D printing materials.

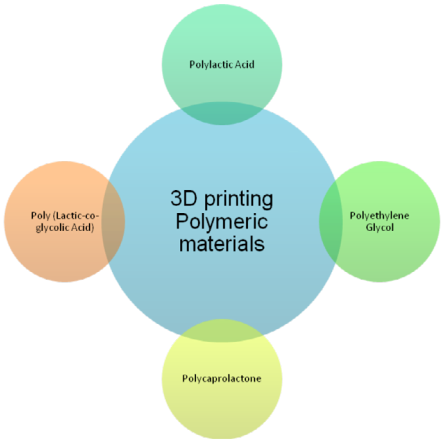

FIGURE 7. Various types of 3D printing polymer-based materials.

Polylactic Acid

Corn starch, tapioca roots, and sugarcane are some of the renewable natural resources used to make polylactic acid (PLA). It melts at the moderate temperatures of 160–180 °C, and is biodegradable.[54] Its mechanical qualities and high level of biocompatibility have made it a US Food and Drug Administration (FDA)-approved implantable medical device. Liu et al. etched and coated the PLA fused deposition modelling (FDM)-printed scaffold with polydopamine

(PDA) to investigate the topographic shift brought about by etching that affected cell adherence, growth, and proliferation.[55] Both in vitro and in vivo studies demonstrated that the etched and PDA-coated scaffolds were superior to the unetched scaffolds in terms of cell proliferation, growth, cell viability, and bone regeneration.

Polyethylene Glycol

A synthetic biocompatible polymer with hydrophilicity and solubility in a range of liquids, polyethylene glycol (PEG) is also known as polyethylene oxide (PEO). Compared to other materials, PEG's compressive modulus is higher because of its larger molecular weight. The mechanobiological evaluation of PEG and its composites involves combining tendon extracellular matrix (tECM) with PEG diacrylate (PEGDA) by SLA printing to produce a stronger and more porous scaffold.[56] While tECM makes the synthetic polymer more biocompatible, PEGDA provides the scaffold with its physical and mechanical strength.

Polycaprolactone

The US FDA has authorised polycaprolactone (PCL), a synthetic aliphatic polymer used in tissue regeneration. It is inexpensive and easy to obtain. Its biocompatibility and slow disintegration rate have made it a popular polymer-based material. PCL's decreased cytotoxicity and inflammation in vivo are due to its breakdown rate. Mechanically, two types of cervical cages are characterised: first, with a ring form, and the second with a porous rectangular shape, and their static and fatigue properties are SLS-printed. The structural properties are impacted by the geometry and design of the cages, as demonstrated by mechanical characterization through static and dynamic loading of cages.

Poly Lactic-Co-Glycolic Acid

Two different monomers, namely PLA and PGA, combine to form poly lactic-co-glycolic acid (PLGA). Its use as a biodegradable polymer in healthcare is approved by the FDA. Polycondensation or ring-opening of PLA and PGA are two methods for its synthesis. PLGA is very easy to process with good biocompatibility. The incorporation of nano-titania and PLA into a composite scaffold improves its mechanical characteristics and stimulates bone cell function by simulating macro- and nano-structures of real bone.[57] Liu et al. extruded a scaffold from the composite material using an aerosol-based printing process.[57] According to the authors, cell adhesion was highest for surfaces with roughness similar to that of real bone. In vitro tests showed that osteoblasts interacted with 3D scaffolds, infiltrated bone cells, and proliferated.

Ceramic Materials

Oxide ceramics contain metal oxides and are known for their excellent thermal and chemical stability. The following are some examples of ceramic materials used in bioimplant applications.

Alumina

Alumina (aluminium oxide [Al_2O_3]) is widely used due to its hardness, corrosion resistance, and electrical insulation properties. It is commonly found in cutting tools, substrates for electronics, and dental applications. Alumina is renowned for its hardness and wear resistance, making it ideal for applications such as dental implants and industrial cutting tools.[58] Its ability to maintain structural integrity at high temperatures allows it to be effectively processed using techniques such as SLS and binder jetting, enabling the creation of complex geometries that meet demanding performance requirements.

Zirconia

Zirconium oxide (ZrO_2) is a high-strength ceramic with low thermal conductivity, which makes it particularly suitable for applications requiring durability and resistance to thermal stress. Oxide ceramics, including zirconia, have very high melting points and are widely used in electronics, aerospace, and chemical processing. Zirconia is especially important in 3D printing for the dental field, where excellent mechanical properties, such as toughness, aesthetics, and biocompatibility, are desired. It is commonly used in crowns, bridges, and orthopaedic implants due to its durability and natural appearance. Advanced 3D printing techniques, such as SLA and DLP, allow high-resolution fabrication of dental restorations, expanding their role in biomedical applications.[59] Research on zirconia processing continues to optimize its properties and enhance clinical performance.

The 3D printed models can be prepared from diverse materials, such as metals, plastics, ceramics, etc. The materials that are usually compatible with particular processes include Ti, Co-Cr alloys, and stainless steel; they are usually compatible with electron beam melting, selective laser melting, and direct metal laser sintering. Some of the ceramic materials, such as Al_2O_3, hydroxyapatite, and calcium phosphate, are also used for 3D printing. JBT and MET are commonly used methods of printing ceramic materials. Polymeric materials, such as PLA, PCL, and polyethylene (PE), are widely used in the medical field. Natural polymers include collagen, alginate, silk, fibrin, hyaluronic acid, chitin, chitosan, gelatin, and polysaccharides.[60] Properties of natural polymers help to maintain the extracellular matrix composition of tissues and make them suitable for constructing scaffolds.

Despite their low mechanical strength, ceramic materials are very biodegradable and have excellent bioactivity.[61] Materials, such as Ti and stainless steel, are often used in the medical field. FDM is now the method of choice for fabricating models in 3D printing.[62] Compared to other methods, it offers several benefits, including affordability, user-friendliness, and thermal and mechanically sound products. Human tissues, bones, and blood vessels are created using 3D bioprinting technology and biomaterials. Hydrogels, bio-glasses, bio-ceramics, and other similar materials are used in bioprinting. Hence, the biomedical sector is strongly associated with 3D printing for creating scaffolds, implants, etc. Tissue engineering and organ transplantation are two areas where bioprinting is finding many uses. This method of bioprinting makes use of a variety of technologies, including thermal inkjet, micro extrusion, and laser-assisted printing.[63]

APPLICATIONS OF 3D PRINTING IN BIOMEDICAL IMPLANTS

The AM technology has many benefits that contribute largely to the manufacture of implants. The customization is one of the most outstanding advantages as it can produce patient-specific devices according to their anatomical requirements. Such a high degree of personalization has the potential to result in better surgical outcomes and patient satisfaction. Furthermore, AM helps to achieve waste reduction because of its layer-by-layer principle that helps to eliminate the wastage of materials, compared to old subtractive manufacturing.[13] This also makes the process sustainable as well as reduces production costs. Moreover, with AM, it is easy to conduct rapid prototyping, which means that it is easy to perform one or a few iterations of the device's design and form, and thus development cycles can be made faster. This hierarchical ability shortens the development of innovation, which results in more efficiently designed and higher-quality implants. The technology has revolutionized medical device manufacturing, as it is now possible to manufacture patient-specific implants and prosthetics to improve surgical registry and patient satisfaction. As illustrated in Figure 8, some uses of implants of 3D printing include hand and arm applications, bone and joint applications, implantable devices applications, and inside and outside use applications. Among the most remarkable strengths of 3D printing is the possibility to print individually fitted implants on the basis of the unique anatomical scan; this makes the process extremely precise. Thus, it is less prone to complications brought about by improperly designed and manufactured devices.[64] Moreover, 3D printing can also be used to aid rapid prototyping, in which the prototypes can be iterated and tested for developing new ideas without long lead times of manufacturing. This ability also helps in hastening the invention of new products in the fields of orthopaedic implants, dental products, and heart stents.[65] In this case, Ti cranial plates can be 3D printed in a shorter period, thus reducing the time previously needed for reconstruction surgeries using conventional methods. Additionally, the incorporation of bioprinting technologies has provided more opportunities in the production of functional tissues and organs.[66] By culturing living cells on top of one another with biomaterials, researchers are able to create tissue constructs that appear similar to natural organs. This can be used in the field of organ transplantation, where the availability of organs is very limited, thus solving the problem of grafting, and also contributing to the field of regenerative medicine.

FIGURE 8. Various implant applications of 3D printing.

Orthopaedic Implants

The development of AM technology has contributed to the quality and effectiveness of orthopaedic implants, resulting in increased improvement of surgical results and patient satisfaction, as shown in Figure 9. The material innovations present one of the greatest changes, and the use of biocompatible materials. In the same context, advancement in making Ti implants has resulted in high strength and also being favorable in terms of integrating with bone tissues. The materials used are safe to interact with human tissues, which also reduces possible rejection and complications. Moreover, advancement in the field of biocompatibility has led to the search for other bioactive ceramics and polymers. This has also contributed to the performance and durability of orthopaedic implants. Wu et al. investigated the possibilities of 3D printing in the design of orthopaedic implants with a focus on the ability to develop complex-geometry implants with patient specificity for high mechanical and biological performance.[67] The authors found these parameters suitable for the success of implants in terms of lower porosity and pore size, which results in bone ingrowth and the mitigation of stress shielding. García-Ávila et al.[68] presented a dynamic topology optimization method for the design of transtibial orthopaedic implants, using high-speed AM processes, such as continuous liquid interface production (CLIP). The authors explained the inclusion of biomechanical data using gait cycle forces into the design process, thus resulting in lower load distribution and high implant stability. The authors further demonstrated that significantly lightweight implants could be achieved by porous metamaterials formulated on triply periodic minimal surfaces (TPMS) and without the loss of isotropic behavior.

Fixation Devices

The use of fixation devices for orthopaedic and cranial surgeries is redefined by the nature of 3D printing technology. Additive manufacturing has significantly enhanced the customization, precision, and overall performance of critical medical components which includes plates, screws, pins, cranial fixation systems, and rods. These innovations have removed the shortcomings of conventional manufacturing through patient-specific solutions, greater functionality, and better surgical results.

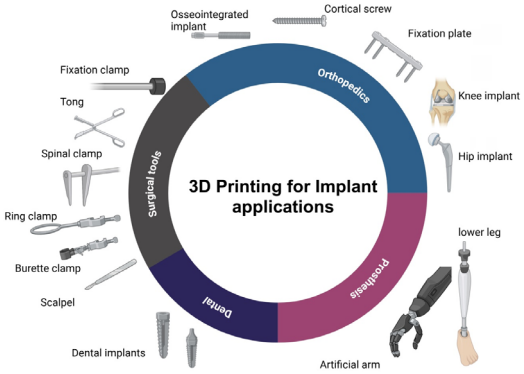

FIGURE 9. 3D printing in biomedical applications.

Plates

3D printing has benefited the production of plates used in fixing the bones. The conventional plates usually need adjustments by the surgeon during the surgery to generate the anatomical shape of the patient. This factor increased the length of the surgery and lowered its accuracy.[69] With the help of 3D printing, plates are made and adapted to the exact geometry of the bone, which is a good fit and distributes load more efficiently. The new technology with 3D printing makes it possible to print plates with complex internal lattice structures, of less weight, and of the same mechanical strength. Such small patient-specific plates reduce the irritation of neighboring tissues and accelerate recovery. Liu et al. studied the development of a 3D-printed

permanent implantable porous tantalum-coated bone plate that can be used to fix a fracture.[70] They also found that the porous coating of Ti improves osteogenesis and osseointegration, and is mechanically compatible with human bones. In animal studies, the rate of fracture healing is higher, as a better callus develops with Ti-coated plates, compared to conventional and porous Ti plates. The research highlighted the possibilities of combining 3D printing and chemical vapor deposition to develop superior orthopaedic implants. Oraa et al. discussed the case application of 3D technology in the field of orthopaedics, considering derotation tibial osteotomy.[71] The authors illustrated the process of creating and printing their own cutting guides and osteosynthesis plates using 3D printing. Their method showed accurate corrections in bone deformities using virtual surgery planning and personalized implants to achieve the best possible outcome of surgery. The method demonstrated the increasing use of 3D printing in customized orthopaedic care.

Screws and Pins

Bone stabilization requires screws and pins, which have to be designed using 3D printing so that they are better than the original ones. AM enables the screws and pins to be manufactured both lengthwise and width-wise perfectly, with the best pattern of threads and surface texture that would enhance their grip and stability on the bone. Second, high-tech and biocompatible materials, non-reactive to the human body, can be used to create these devices from Ti or composite polymers. Customized screws and pins are especially useful in complicated fractures or deformities where more standard components are unlikely to provide sufficient support. Figure 10 shows the fitting of Ti interbody cages and anterior plate fixation in the cervical spine. Miao et al.[72] examined the use of 3D printing technology in the calcaneal fracture repair of the paediatric population using percutaneous reduction and cannulated screws. The authors proved that preoperative planning using a 3D printing model improved surgical precision and results. Sampath Kumar reported that the angle of Böhler, calcaneal height, and length showed significant improvement following surgery.[73] In addition, the clinical outcome assessed by the American Orthopaedic Foot and Ankle Society (AOFAS) with a hindfoot score was 94.1, which indicates good postoperative function. Although a few complications were noted, both surgeons and patients expressed higher satisfaction. This study highlights the value of 3D printing in the visualization of fractures and supporting surgical planning.

FIGURE 10. Cervical spine X-ray illustrating anterior discectomy and fusion at C5–C7, utilizing Ti interbody cages and anterior plate fixation.[74] (Permission under the CC BY 4.0 license).

Fixation Devices

The neurosurgery cranial fixation devices are needed when cranial bones are fixed after trauma or surgery.[75] These devices have seen transformative improvement through 3D printing, where they have been subjected to radical innovations.[76] The benefit is the possibility to develop patient-specific devices that fit the specific shape of the skull, eliminating complications and guaranteeing a perfect fit. Moreover, custom prototypes of cranial fixation devices produced by 3D printing could be endowed with properties to promote osseointegration (porosity), resulting in better long-term results because of lighter weight and high strength.

Rods

Rods are an essential part of spine and long bone surgeries to ensure the structure and alignment of a patient. The geometries and surface finishes of rods are focused on using 3D printing to enhance their mechanical behaviors and compatibility with the body. Patient-specific rods can be adjusted to fit specific dimensions that correspond to the requirements and help in minimizing intraoperative

changes. Also, Ti alloys are used in rods because of their strength and lightweight properties, which minimize stress on the surrounding tissue. Figure 11 shows the integration of patient-specific implants and bone cements with distraction osteogenesis. The successful use of custom-designed parts was observed to achieve maintenance of alignment and gradual bone transport.[76]

It is a part of a larger pattern in orthopaedic and spinal surgery, in which the 3D-printed rods and implants are custom-designed to match specific anatomy. The use of rods to stabilize spinal and long bone surgeries is important for maintaining structural integrity and restoration of shape. 3D printing has made it possible to create rods that have new geometries and treatments to enhance the mechanical properties and compatibility with tissues. The rods are also customized to specific patients regarding length and curvature, so that less or no adjustment is needed during the procedure. Moreover, the material used to make rods (Ti alloys) makes them strong and, at the same time, light to reduce stress on neighboring tissues. Figures 11A and 11B indicate the intraoperative use of PSI and vancomycin-loaded Refobacin 12 bone cement used to execute the defect.[76] Manipulation of the wound after the operation was performed using vacuum sealing drainage (VSD), sparing skin grafting, and progressive cement removal as a part of the bone transport procedure. The X-rays indicate proper alignment of fractured fragments and had 1.74-mm valgus and 1.14-mm angles of anteversion. The Ilizarov fixator was stable (Figure 11C and 11D).

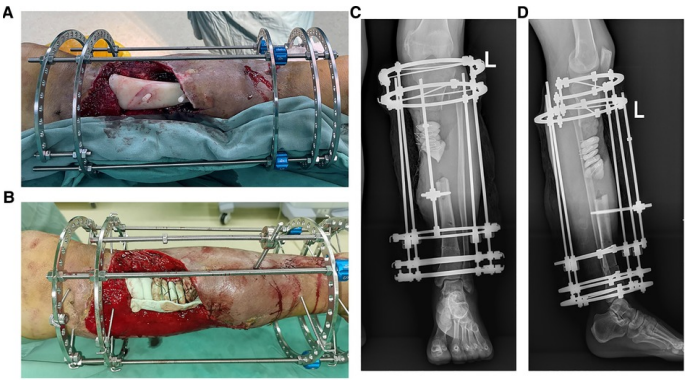

FIGURE 11. Intraoperative patient-specific instrument placement and postoperative X-rays in case 1 using Ilizarov distraction osteogenesis. (A) PSI maintains fracture alignment; (B) pie-shaped bone cements inserted for gradual removal during transport; (C) postoperative AP X-ray shows 1.74° valgus angulation; and (D) lateral X-ray shows 1.14° anteversion.[76] (Permission under the CC BY 4.0 license).

Joint Replacement Implants

Specifically, knee arthroplasties, acetabular cups, and other implants of joint replacement applications have gained a remarkable transformation, individualization, and effectiveness offered by AM. Various joint replacement implants are discussed as follows.

Knee Arthroplasties

3D printing has become a game-changer in knee arthroplasty by enabling the production of highly customized implants tailored to individual patients' anatomy. Traditional knee replacement procedures often rely on standardized implants that may not perfectly match a patient's unique bone structure, potentially leading to discomfort or reduced mobility. By employing 3D scanning and printing technologies, surgeons can now design implants that precisely replicate a patient's knee geometry. This customization enhances joint alignment, reduces wear and tear, and minimizes the risk of post-operative complications.[77] Figure 12 presents the overall process of designing and applying 3D-printed PSI into orthopaedic surgery.[78] A preoperative planning (Figure 12A–12D) is made using a CT scan and shows the precise modelling of the distal femur and proximal tibia of the patient, which is reconstructed accurately. The 3D models reconstructed (Figure 12E) are inserted with osteotomy markers that help in making surgical incisions. On the models (Figures 12F and 12G), the fit of PSI is checked to ensure accuracy prior to surgery. Throughout the process, the PSI is placed on the bone to advise capacities in the operation (Figures 12H and 12I), which increases precision in the surgery. As comparison of the scheduled and actual osteotomy volumes (Figure 12J) verifies, the bone cuts are very close to the preoperative plan, which proves that the PSI is effective in enhancing surgical results. Furthermore, the ability to preprint surgical guides based on patient-specific data allows for greater accuracy during the procedure, reducing operating time and improving the overall outcome.

FIGURE 12. Design and intraoperative use of 3D-printed PSI: (A–D) CT-based preoperative planning for femoral and tibial reconstruction; (E) 3D models of distal femur and proximal tibia with osteotomy markers; (F and G) PSI fit verification; (H and I) intraoperative placement of PSI; (J) real-time comparison of planned versus actual osteotomy volume.[78] (Permission under the CC BY 4.0 license).

Acetabular Cups

In hip replacement surgery, acetabular cups serve as a crucial component for restoring joint function and stability. 3D printing has introduced groundbreaking improvements in the design and functionality of these implants. By leveraging AM, acetabular cups can now incorporate porous structures that mimic the natural trabecular bone architecture. This porosity not only facilitates superior osteointegration that helps the bone grow into the implant but also guarantees a long-term stability and durability of the implant. Furthermore, advanced materials that cannot be (or are more difficult to) 3D printed are used; for example, Ti alloys offer a greater strength to biocompatibility as well as corrosion-resistance.[79] Such innovations increase the life duration of implants and decrease the chance of revision surgeries.

Prosthetics

3D printing has facilitated innovative solutions in several categories of prosthetics. AM techniques are of great use to develop lightweight prosthetics, customized prosthetic limbs, and bionic prosthetics with embedded electronics. These developments have not only made prosthetics more accessible and useful but also improved the lives of people with impaired limbs.

Lightweight Prosthetics

One of the contributions of 3D printing is to design lightweight and strong prosthetics. The conventional materials used in developing prosthetics are quite cumbersome, for instance, heavy metals or dense polymer, and are usually inconvenient to the individuals using them. Titanium alloys are mixed with other materials to produce advanced polymers and subsequently printed to attain low weight and increased strength.[80] Also, a lattice structure facilitated by 3D printing is of lesser weight and does not compromise the mechanical integrity of prosthetics. The innovation is especially useful for paediatric patients or for those who need prosthetics for longer periods, so that lightweight equipment is less tiring and comfortable for use in daily life situations.

Customized Prosthetic Limbs

One of the most essential characteristics of the contemporary prosthetic design is customization, and 3D printing has allowed the creation of highly customized prosthetic limbs. With the help of 3D scan technology, the design of the prosthetics is adjusted to the peculiarities of the patient's anatomy in order to make them fit and increase functionality. Such elaboration leads to better mobility and decreases discomfort due to poorly fitting instruments. Besides, this capability to weave aesthetic inclinations, for instance, color, texture, and style, contributes to the user's individualistic spirit and mental health. Customized prosthetics are especially impressive in the case of people who have complex needs, for example, athletes or people with partial limb deviations.

Bionic Prosthetics with Embedded Electronics

The next level of use in prosthetics through 3D printing is the creation of bionic prosthetics with wired electronics. Such devices combine sensors, actuators, and microprocessors that allow users to conduct complex life-simulated movements with high accuracy. 3D printing facilitates the incorporation of intricate internal components into the prosthetic framework, ensuring

compact and seamless designs. Moreover, the technology supports the creation of flexible, conductive materials for sensor placement and connectivity. The result is a new generation of prosthetics that responds to muscle signals or even neural inputs, allowing for intuitive control and interaction with the environment.[81] Such bionic prosthetics represent a significant leap toward restoring near-natural limb functionality for users.

Hip Implants

3D printing technology has emerged as a transformative force in the production of hip implants, significantly enhancing the customization and effectiveness of these critical orthopaedic devices.[79] Hao et al. compared X-rays taken one week after surgery with those taken 12 months later for radiographic evaluation.[82] The authors conducted the study on three different patients, and in all cases, implants were held firmly. The authors found no signs of implant loosening or osteolysis around the implants (Figure 13). The patient-specific acetabular cups and femoral stems are designed in accordance with the specifics of a patient. With the aid of cutting-edge imaging technology such as CT scans or MRIs, a surgeon is able to create implants that work seamlessly in a patient's hip joint and offer greater stability and decrease the probability of complications such as dislocation or problems with the loosening of implants. This not only improves the fit but also aids better osseointegration, or the process of bone fusing to the implant, thus leading to a long life and long use of hip replacement.

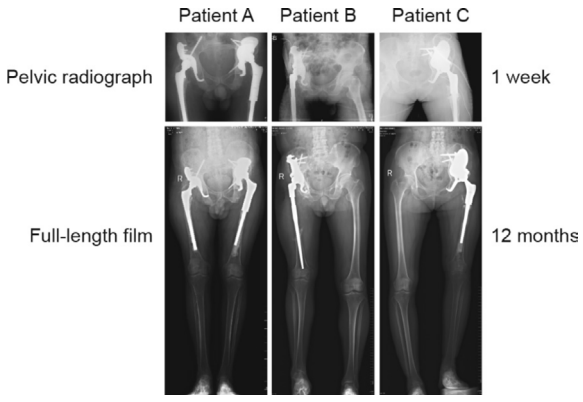

FIGURE 13. X-rays showing prosthesis evaluation after 1 week and 12 months that demonstrating stable fixation without any signs of loosening after 12 months.[82] (Permission under the CC BY-NC-ND license).

Spinal Implants

Porous Spinal Implants

Use of 3D printing technology in biomedical engineering has unlocked new possibilities in casting spinal porous Ti and other implants. These implants are developed with interconnective porous designs to resemble the natural architecture of the bone and vitalize osteogenesis and advance bone incorporation. The pore size and porosity are very significant, compared to mechanical properties and biological performance, which can be controlled precisely using techniques such as selective laser melting (SLM).[83]

Optimizing these parameters ensures that the implants provide sufficient mechanical support while facilitating nutrient exchange and cellular integration.[84] The recent studies have demonstrated that porous Ti scaffolds with pore sizes of around 600–700 μm and higher porosities are more conducive to osteogenic activity and bone formation, making them ideal for spinal applications where load-bearing and biocompatibility are paramount. Using a 3D printer, Li et al. designed and tested elastic two-component polymer-metal discs for the lumbar spine with varying stresses.[85] The layered structure with a 10-μm algorithm depicts the microscopic structure in Figure 14(a, b). Along the same lines of parallel grooves are the surface strands that have grown on the sheets. Surface strips with different structures enhance mechanical characteristics. According to the scanning electron micrographs, the cut sheets are sufficiently rough to adhere to a polymer cage that has been attached using adhesive bio resin. Arthroplasty, which involves the removal and replacement of damaged vertebrae, together with a bioactive ceramic covering, has been suggested as a solution to the problems caused by the current degenerative disc disease (DDD) therapies. In order to lessen the impact on the nearby components, bead connection techniques are devised.

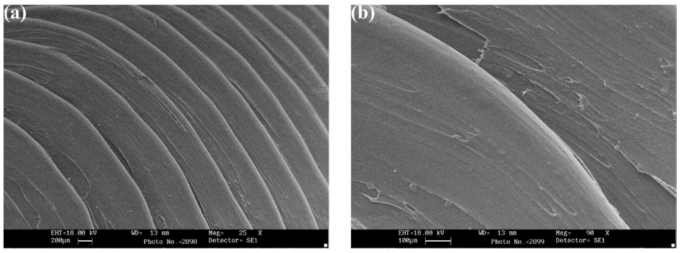

FIGURE 14. *Scanning electron microscope* (SEM) pictures of PLA polymer used to construct L4 and L5 intervertebral discs at (a) ×25 and (b) × 90.[85] (Permission under the CC BY-NC-ND license).

Interbody Fusion Devices

Customized interbody fusion devices represent a significant advancement in personalized spine care, leveraging 3D printing technology to create implants tailored to individual patients' anatomy. By utilizing medical imaging data and advanced manufacturing techniques, such as SLM and electron beam melting (EBM), these devices are designed to match the unique curvature and dimensions of a patient's spine. Owing to the presence of Ti in these implants, the strength-to-weight ratios are high and also favor biocompatibility. Ti alloys allow implants to use complex porous ways of manufacturing to promote osteoinduction and osteoconduction.[86] Customization is helpful in enhancing accuracy in surgery and achieves a better fit and embeds the implant with precision, resulting in improved clinical outcomes through reduced complications in the form of implant migration or subsidence. This is a patient-customized technique, which means a revolutionary change in spinal surgery because it is in line with the objectives of making the practice of medicine more personal, efficacious, and focused.

Dental Implants

The 3D printing technology is changing the face of dentistry, especially in the manufacturing of dental implants. This new technique makes it possible to produce individual implants adapted to individual anatomy for a closer fit and more convenience. However, standard-sized implants are produced with traditional treatment procedures that do not fit a patient, thus causing potential problems. Conversely, there are also 3D-printed dental implants, which are custom-designed by digital scanning and CAD, and tailored to enhance both aesthesis and functionality.[2] Besides increasing durability, the choice of material serves to improve osseointegration and the coupling of the implant and the jaw bone.[87] Moreover, the 3D printing technology saves clothing design and production time, and also curtails wastage, as minimal tooling and molds are required with such a process, which makes on-demand production possible. Such efficiency is translated into reduced costs and a faster turnaround period among dental laboratories so as to cater to patients in a better way.[88] Furthermore, 3D printing allows the creation of intricate shapes that are hard to attain by using conventional techniques. For example, it is possible to make implants with different porosities to ensure a natural bone structure in which implants would integrate and distribute the load in a better manner.[89] The capacity to build well-defined models also helps in preoperative planning, thus the dentist is able to simulate the process and enhance surgical precision. Consequently, the patients experience shorter recuperation periods and fewer after-surgery modifications, thus making their experience better.[90]

Shi et al. explored the application of 3D inkjet printing for fabricating zirconia ceramic teeth.[26] Their study utilized high-permeability 3 mol% yttria-stabilized tetragonal zirconia polycrystal (3Y-TZP as the primary material. The zirconia ceramic ink, with a 55 vol% solid phase, demonstrated shear-thinning behavior favorable for the printing process. After sintering at 1,500 °C for 54 h, the printed samples achieved a density of 98.5%, a hardness of 14.4 ± 0.1 GPa, and a transverse rupture strength of 520 ± 20 MPa, conforming to ISO 13356:2015 standards. This method proved to be efficient, cost-effective, and suitable for producing complex geometries, compared to traditional manufacturing methods.[91] Mohammed et al. developed the zirconia ceramics-based dental prostheses using DLP 3D printing, as shown in Figure 15.[28] Alqutaibi et al.[2] presented a detailed overview of advanced AM in the framework of implant dentistry with the focus on the contribution of 3D printing technologies, such as Vat photopolymerization (VPP), PBF, and multi jet fusion (MJT) to manufacture dental implants and prosthetics. They emphasized the benefits of such technologies which

is increased precision, minimized waste, and the possibility of creating complex geometries. The optimization of printable material and the necessity of post-processing to obtain the required mechanical and biological qualities were other observable issues[92].

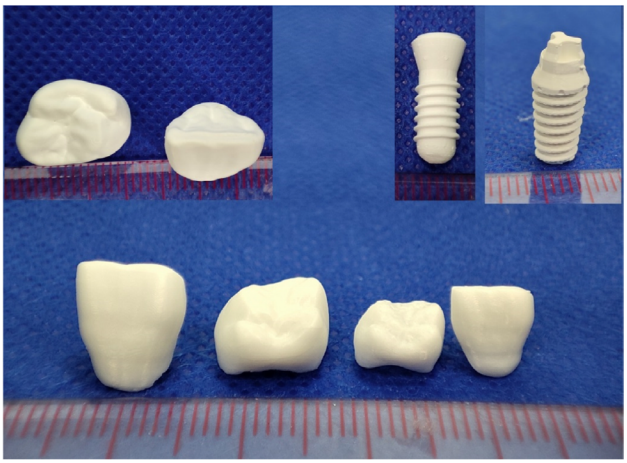

FIGURE 15. 3D-printed dental prostheses.[28] (Permission under the CC BY-NC-ND license).

Craniofacial Implants

The 3D printing technology has proved to be quite revolutionary in neurosurgery, especially regarding cranial implants used during cranioplasty procedures.[93] Such an innovative approach enables the production of individualized implants perfectly fitting to individual anatomical peculiarities of the patient, thus providing a great improvement in both functional and aesthetic results. It starts with high-resolution CT scans of the skull, which are consequently employed to make a complex 3D model. This is reflected to provide the complete mirror of the skull, making it symmetrical and fit, perfect as an implant. With the help of this technology, surgeons create patient-specific implants from biocompatible materials, such as Ti or polyether ether ketone (PEEK), which are known to be strong and resistant to corrosion and can be used with human tissue.

The advantages of employing 3D printing in cranial implants are numerous. It enables quick prototyping and production and cuts down the production time of implants, which previously took weeks instead of a few days. This expedited process is essential in emergency cases, where prompt intervention is required after traumatic brain injuries or brain surgery. Moreover, complex geometries in 3D-printed implants favour integration with the surrounding bones and reduce complications, such as stress shielding. Further, preoperative modelling techniques help surgeons to plan their strategy in a better manner, consequently shortening the surgery time and complications. It has been demonstrated that operating with 3D-printed molds achieves good results, such as a low level of bleeding and quick recovery.

Moreover, recent developments resulted in the FDA approving 3D-printed PEEK cranial implants, which is an important step in customized medicine and the increased usage of such technology in cranial reconstruction.[94] Mishchenko et al. explored the application of 3D printing and the usage of plasma electrolyte oxidation (PEO) to generate personalized Ti implant in the context of craniofacial reconstruction.[95] The experiment used Ti6Al4V alloy in producing customized implants, which were then processed using PEO to increase surface bioactivity. The conducted PEO process used electrolyte calcium phosphate at 250 V, subsequently resulting in the formation of a bioactive oxide layer, which enhanced osteoblast proliferation and osseointegration. Successful implantation in patients with craniofacial defects that entailed fewer postoperative complications and greater aesthetic and functional results was indicated in clinical application. In complex craniofacial structures, the significance of surface modifications in obtaining bone and soft tissue integration was mentioned by the authors. Yousefiasl et al. prepared 3D-printed bioactive chitosan-based scaffolds applicable to bone tissue engineering of craniofacial origin.[96] Such scaffoldings were supplemented by the concentration of hydroxyapatite, which enhanced the same in terms of porosity, bioactivity, as well as strength. The addition of hydroxyapatite enhanced osteoconductivity and cell survival, and 5% hydroxyapatite scaffolds were found to perform optimally in the presence of cell proliferation.

The study emphasized the potential of such scaffolds for regenerating craniofacial bone defects, affording their biocompatibility and ability to support stem cell growth

and differentiation. A case study was conducted by Mishchenko et al. on the improvement of surface properties of craniofacial reconstruction using 3D personalized implants.[95] In their study, a 48-year-old male (patient P) was admitted with a mandibular defect, which caused facial deformity, partial secondary adentia, and functional disability. The defect was due to failed ameloblastoma surgery, which necessitated segmental resection and tibial graft harvesting, but developed infection, graft necrosis, and exposure of the fixation plate. The delayed iliac crest segment was grafted, and a patient-specific, 3D-printed Ti implant treated with PEO was installed, as shown in Figure 16. Subjective use was evident postoperatively, covering aesthetic appearance, facial balance, lip seal, speech, and psychoemotional well-being. The biocompatibility of Ti implant guaranteed proper integration with lasting positive results regarding functioning and appearance, irrespective of high-risk infection zones and various comorbidities.

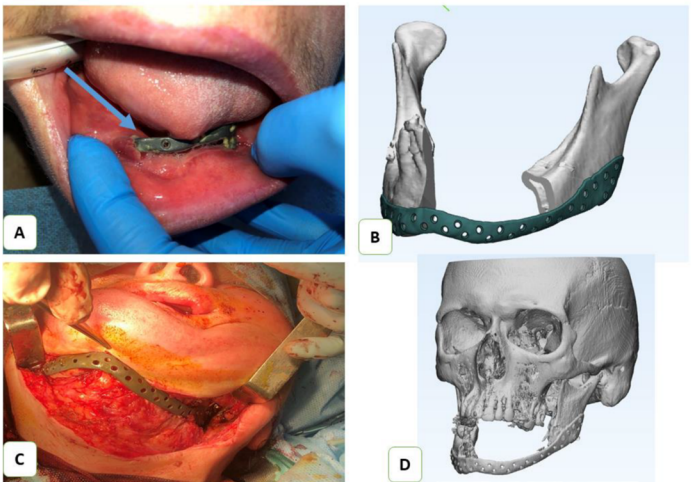

FIGURE 16. Patient P. A: Graft fragment erupted into the oral cavity (blue arrow); B: 3D model of the patient-specific implant (PSI); C: Intraoperative view of mucous membrane defect in the lower jaw; D: Postoperative CT scan showing restored mandible configuration and joint function.[95] (Permission under the CC BY-NC-ND license).

Cardiovascular Stents and Implants

3D printing technology is increasingly utilized in the production of stents, which are critical devices used to support blood vessels and maintain patency in various medical conditions, particularly cardiovascular diseases.[97] One of the primary applications of 3D printing in stent production is the ability to create customized stents that are tailored to the specific anatomy of individual patients. By using advanced imaging techniques, such as angiography and CT scans, healthcare providers design stents that fit precisely within the targeted blood vessel, ensuring optimal support and reducing the risk of complications, such as restenosis (re-narrowing of the vessel). This customization not only enhances the effectiveness of the stent but also improves patient comfort and outcomes.

Besides customization, 3D printing is also used to manufacture stents with geometries not possible through traditional models of manufacturing. This allows adding features such as variable strut thicknesses and distinctive lattice styles, which maximize flexibility and conformability as well as strength. The dynamics of blood flow and turbulence are improved by such designs, which result in improved healing responses. Additionally, 3D printing enables fast prototyping, which enables design to be iterated based on clinical feedback, resulting in more efficient end products. The possibilities of applications of biocompatible materials and drug-eluting coating also increase the functionality of 3D-printed stents by inducing healing and obviating thrombosis (blood clot formation).[98] The use of 3D printing in the production of stents is a great development in the field of vascular interventions, as it provides a customized solution that helps patients and surgical outcomes in a greater way.

With the current technology, such as angiography or CT scans, medical practitioners can make a stent that perfectly fits the target blood vessel, such that it provides optimum support and the chances of complications are minimized.

Hatami et al. examined the aspect of using 3D and 4D printing technologies to produce cardiovascular stents.[96] Their study emphasized the capability of these processing methods of AM to manufacture patient-specific stents in intricate geometries with superior biocompatibility and drug-releasing capabilities. The authors focused on

the future of 4D printing, where stents would change in real-time, reacting to environmental triggers, such as heat and moisture, supporting easy deployment and a smooth flow into the vascular system.

Yuan et al. developed 3D-printed melatonin-loaded esophageal stents (MESs) and used them to treat corrosive esophagitis (CE).[99] They tested stents of different designs by the SLA technique. A stent of Pagoda shape was found with better retention and drug-release characteristics. The MESs ensured that entry of melatonin to the oesophageal tissues was done effectively, thereby decreasing oxidative stress, inflammation, and oesophageal stenosis in a rat model. The results also showed that the stents are biocompatible and should be safely degraded in the gastrointestinal tract, which promises higher levels of therapeutic applications in oesophagus injuries.

Surgical Devices and Tools

The technology of 3D printing is being used increasingly for creating surgical equipment and tools, transforming the very nature of surgery, as well as for improving the overall care of patients.[100] Some of the most common uses include manufacturing modified surgical equipment to fit special surgical needs or the preferences of a surgeon. The customization enables instruments that are ergonomically perfect to fit in the surgeon's hands, thus leading to better dexterity and control of instruments while performing surgery. For example, 3D-printed surgical instruments can be made in such a way that they meet the needs of different surgical practices better because of their ergonomic handles and special tips that meet the demands of specific surgical techniques and improve precision and decrease fatigue during a long procedure.

The other important use of 3D printing in surgery is the anatomical model created during preoperative planning. Before the surgeon enters an operating room, patient-specific models based on imaging information (e.g., CT or MRI scans) are used, so that the surgeon can visualize all aspects of the complex anatomy. This advanced planning makes it possible to devise effective strategies and achieve more productive surgeries marked by shorter operation periods and fewer spillages. Moreover, they can be used as training models that enable medical professionals to practice surgical procedures in a simulated environment without involving actual patients. It is also possible to continually improve tools and models according to clinical feedback, with rapid prototyping capabilities providing tools and models to be at the cutting edge of innovation.

Kessler et al. studied the release of monomers in surgical guide resins produced with various 3D printing methods, and were focused on the elution of methanol and water.[101] They found that the release of monomers greatly varies in terms of printing method and the type of resins. Monomers, such as methyl methacrylate (MMA) and hydroxyethyl methacrylate (HEMA), among others, were found to be in high concentration in methanol and low concentrations in water. Notably, the maximum concentrations of the released monomers in Nextdent SG were obtained when these materials were fabricated using SLA devices. The result highlighted the most significant evidence of the type of printer and the material of resin when applied to reducing the amount of chemical exposure in surgical operations. Li et al. developed a photocurable gel that can have superior tear resistance to be used in 3D printing of flexible wearable devices and surgical mock-ups.[102] The gel utilized a double network with covalent and hydrophobic cross-linking that significantly improves its mechanical properties, such as toughness, tear resistance, and conductivity. The addition of sodium chloride and glycerol to the gel revealed better anti-drying and anti-freezing effects, which allowed using the gel in a wide range of environments. Their results demonstrated the possibilities of using such a gel to develop customized surgical models and wearable biomedical devices with enhanced durability and flexibility.

CHALLENGES IN ADDITIVE MANUFACTURING OF BIOMEDICAL IMPLANTS

Although AM has numerous benefits, there are various challenges to the universal use of the technology in producing implants. The first major impediment is regulatory barriers, because the process of regulating medical equipment slows down innovation and delays market entry of new products. Compared to conventional manufacturing methods, there are few limitations to the

materials that are used in AM.[103] Such limitations may limit the type of implants that could be produced efficiently. Besides, it is a significant challenge to provide quality control because the printing conditions change, and this process may influence the consistency and reliability of different batches of implants.

Regulatory and Standardization Issues

The regulatory landscape of AM in the biomedical sector is complex and evolving. Regulatory bodies such as the FDA have begun to establish guidelines for the approval of 3D-printed medical devices. However, these regulations are often not fully developed or standardized across different regions. The lack of clear guidelines leads to inconsistencies in product evaluation for safety and efficacy, thus potentially delaying the introduction of innovative technologies into the market. Furthermore, the absence of standardized testing protocols poses a significant barrier. Each AM technique produces varying results based on parameters, such as material choice, printer settings, and post-processing methods.[104]

Without standardized criteria for assessing the mechanical properties and biocompatibility of printed implants, it becomes challenging to ensure that devices meet necessary performance benchmarks.[105] Regulatory challenges can be resolved by investing in and developing new instruments, devices, and technology for patients (Figure 17). This inconsistency hinders collaborations between manufacturers and healthcare providers, as differing standards may complicate the integration of new technologies into existing medical practices.

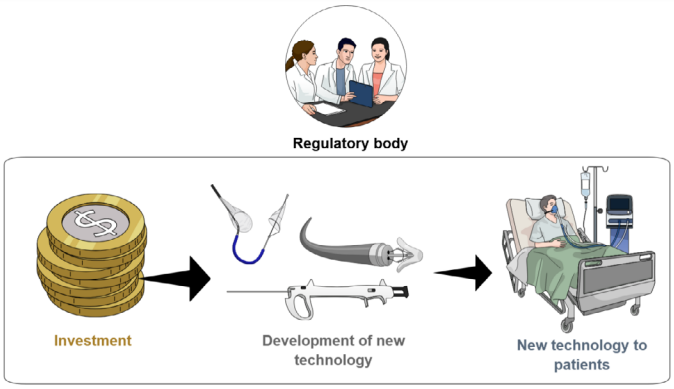

FIGURE 17. 3D printing in biomedical applications.

Material Limitations

Material selection is critical in the AM of biomedical implants. While AM allows for a wide range of materials, such as metals, polymers, and ceramics, each material has specific limitations that can impact its suitability for medical applications. For instance, biocompatibility is a primary concern, and materials must not elicit adverse biological responses when implanted in the body. Mechanical properties such as strength, elasticity, and the capacity to resist fatigue have to match the needs of the implant site. Generally, the performance of the existing materials is also lacking. Ti alloys, because of their strength-to-weight ratio and resistance to corrosion, may have poor osseointegration characteristics compared to natural bone.[106] Moreover, polymers that are applied to AM processes are not always provided with the mechanical strength required to be of load-bearing capacity or are subject to degradation due to prolonged exposure to the physiological environment. Consequently, the current research continues to consider the possible development of new biomaterials that fulfil the strict requirements of numerous uses and are compatible with AM.

Process Repeatability and Reliability

Repeatability and reliability of a process used in AM are another important issue. The AM processes are very variable compared to the established traditional manufacturing process, which usually adopts predictable, well-proven techniques. Such variations may cause discrepancies in the quality of the implants used, and this is truly daunting in biomedical applications where the safety of patients is at the forefront. A robust quality control is needed during the manufacturing process so as to enable it to tackle this problem. Adoption of real-time monitoring software that monitors important parameters such as temperature variations during print, the ability of layers to stick together, etc., may help to have consistent results. Advancements in simulation tools that predict the influence of process parameter variations on the final product properties are helpful in significantly improving manufacturing reliability. By providing insights into the expected outcomes, these tools enable manufacturers to optimize process parameters, reduce trial-and-error experimentation, and design their production systems

in the most efficient and cost-effective manner before large-scale implementation.

Besides, AM offers a lot of potential to transform biomedical implants by customization and efficiency, although there are some serious challenges. Regulatory and standardization questions are also important to achieve efficacy and safety in diverse markets.

Similarly, the material compromises faced are defeated by conducting new research to make implants more functional. Moreover, high standards of implant production require advanced techniques of monitoring and simulation to achieve high levels of repeatability and reliability in the implant production process, thereby supporting high-quality standards.[107] However, with these challenges addressed, the biomedical field can fully leverage its benefits through the use of AM technologies.

FUTURE TRENDS AND INNOVATIONS

The future of AM in medical implantology is promising with several exciting directions. The research relating to the future discovery of biocompatible materials could be focused on increasing the longevity of implants. Also, the usage of AM with digital technologies (e.g., advanced imaging techniques such as CT scans) can increase the level of customization because implants are now designed to the requirements of patients.[108] Moreover, point-of-care manufacturing has huge possibilities, and the manufacturing of tailor-made implants on demand has the possibility of transforming surgical procedures by removing delays and making the treatment more effective as a whole. With the help of the directions developed in the market, AM has a chance to leave a significant impact in the field of medical implantology by addressing current challenges.

Advanced Materials for Additive Manufacturing

In order to increase functionalities and the use of AM, the development of advanced materials is essential. With the growth of advanced AM technologies, the demands of new materials are increasing, which not only respond to the mechanical and thermal requirements of the processes used in multiple applications but also possess certain functionalities. Various studies on AM have dealt with nontraditional materials, such as metals, non-ceramics, composite polymers, and high-performance alloys. For instance, carbon fibers reinforced within polymer matrices have demonstrated much enhanced mechanical properties. Thus, it is possible to produce lightweight components with better mechanical strengths for automobile and aerospace applications.[109] Additionally, the future materials made from AM can support the manufacturing of multi-functional structures possessing a combination of different properties in the same component. This comprises the synthesis of biomaterials that are biocompatible and allow tissue integration in the case of medical implants and metamaterials that are naturally uneven in their mechanics. Investigation of these new materials is necessary to fill the existing gaps in AM.

Multi-Material Additive Manufacturing Processes

Multi-Material Additive Manufacturing (MMAM) technology is a remarkable improvement to the AM technology because this has enabled developers to manufacture parts with diverse material qualities in the same construct.[110] This allows more complicated shapes to be created that are able to optimize performance by using various materials in the areas where they can function the best. For instance, a combination of soft and hard materials can result in an implant replica in the natural behavior of biological tissues, leading to an improvement in comfort and functionality.

Multi-materials are introduced to support the techniques such as FDM and SLS. FDM has the potential to lay down different filaments with dual or multi-extrusion nozzles. SLS can stack timelines of dissimilar materials as a means of creating the desired material gradients.[111] The ability to process multiple materials provides not just more freedom to design but new avenues to customize and personalize products, such as biomedical engineering products. The ongoing research is expected to provide MMAM a dominant part in improving the practicality and usefulness of 3D printed implants.

Use of CAD Design in Additive Manufacturing

Additive manufacturing or 3D printing is largely affected by CAD. The integration of AM and CAD results in increased efficiency of product development.[112] Rapid prototyping with CAD leads to multiple design iterations, resulting in increased production in a short time and less cost. The process translates CAD models into machine-readable models to achieve successful printing results. Three prerequisites to produce quality printed parts are geometric accuracy, feature resolution, and surface roughness. Moreover, dedicated software applications help to make necessary optimizations in designs as far as additive processes are concerned, which deal with support structures, material consumption, etc. Finally, this results in unique and tailored solutions that are hard to achieve in traditional manufacturing.[113]

Optimization of the Additive Manufacturing Process using CAD

The potential of CAD is to optimize the AM process by improving efficiency and accuracy in designing. One of the primary functions of CAD in this context is converting 3D models into machine-readable formats, which results in efficient and accurate 3D printing.[114] This process is completed by preparing the model, part orientation, and using supporting structures to make the model stable during printing. Moreover, advanced CAD applications simplify the slicing process by slicing the 3D model into layers so that a 3D print can be built sequentially. These layers are adjusted in thickness based on experimental requirements, ensuring optimal print quality. A notable feature of CAD is to support for DfAM (Design Framework of Additive Manufacturing) principles for the optimization of designs. It promotes the designing of lightweight and intricate geometries that cannot possible to be produced by conventional production methods, resulting in high material wastage and expenses.[13] Also, compatibility with simulation systems enables engineers to check designs in different conditions for the best performance. Before commencing the full-scale production, the printing success can be demonstrated through preliminary trials and simulations. These achievements allow manufacturers to validate the process, optimize printing parameters, and ensure product quality and reliability prior to real production. Overall, the AM process, which includes design, production, and the final output, is greatly accelerated by CAD. This process significantly elevates innovation and efficiency in product development.

Integration with Artificial intelligence and digital twin technology

The integration of AM with artificial intelligence (AI) and digital twin (a virtual copy of a real system) technology transformed the approach for the products designed and manufactured, thereby optimizing the performance and efficiency.[115] Huge data sets can be processed using AI algorithms to determine patterns and to optimize parameters such as print speed, temperature, and material flow. Such optimization increases process efficiency, minimizes waste, and provides high product quality. The application of digital twins enables a manufacturer to simulate and track the real cycle of an AM process. Digital twins can be used to predict failures, prioritize maintenance activities, and gain knowledge for better performance, which is achieved using live data from sensors. This combination of AI with digital twins provides better decisions and also reduces the cycle time of innovation to iterate on new designs quickly. This results in a good prototype and tests the designs locally before committing to building a real one. The combination of advanced materials, multi-material processes, and AI integration can create a revolution in AM. These developments ensure that product performances boost the industry and reduce the problems of material constraints and process maintenance. As experimental advancements in AM progress, it can unlock new possibilities for innovative engineering and production methods.

Integration of 3D Printing with Artificial Intelligence in Cardiology

Advances in the field of cardiology are achieved through the introduction of AI and 3D printing, thus allowing a more precise, efficient, and customized treatment.[116] Imaging data acquired from different techniques like CT, MRI, and echocardiography can be enhanced through AI-based processing to ensure accurate models for 3D printing.

The cardiac structures are sorted out with the help of machine learning (ML) algorithms to allow the optimization of imaging resolution and create effective replications of

cardiovascular structures of the patient to show proper anatomy. Such accuracy is invaluable in preoperative planning, especially in complicated situations, so that the course of action is planned with more fidelity. AI also streamlines the 3D printing process by automating procedures in design or even material selection. Predictive algorithms allow tailoring the devices with patient-specific data, when it comes to designing stents and valves, which focus on the geometry of the heart and the dynamics of the blood flow. Monitoring after and during printing by AI results in quality control, and AI can even locate discrepancies. The combination of these innovations and the capability of AI to simplify the process has the potential to maximize results in cardiac care by providing efficient, speedy, and patient-centered solutions.

CONCLUSION

Additive manufacturing has transformed the medical implant manufacturing industry by providing highly customized and patient-specific solutions. The technology has made surgery more accurate and effective in different areas of medical practice, such as orthopaedics, dentistry, and craniofacial surgery. 3D printers are able to produce complex shapes with the help of advanced imaging and digital designs that were not possible with other traditional processes. 3D printing results in improved fitting of implants, shorter surgery period, as well as recovery, coupled with sustainable manufacturing methods that minimize material waste and production inefficiencies. However, even with these advancements, the adoption of 3D-printed implants still faces many challenges. The major obstacles are approval by regulatory bodies, material restrictions, and long-term biocompatibility. The ongoing research for new biomaterials and integration with imaging technologies addresses these issues for more precise and accessible solutions. As these innovations evolve, 3D printing is set to play a pivotal role in customized medicine, transforming surgical practices and enhancing patient care, thus marking a new era in the field of medical implantology.

AUTHOR CONTRIBUTIONS

Conceptualization and Methodology, V.S. and J.S.; Literature Review, V.S. and J.S.; Formal Analysis, V.S. and J.S.; Writing–Original Draft Preparation, V.S. and J.S.; Software, J.S.; Writing–Review & Editing, A.S. and J.S.; Visualization, V.S.; Supervision: J.S.

CONFLICTS OF INTEREST

The authors declare no conflicts of interest.

ETHICS APPROVAL AND CONSENT TO PARTICIPATE

Not applicable.

CONSENT FOR PUBLICATION

Not applicable.

REFERENCES

1. Jiménez, M., Romero, L., Domínguez, I.A., et al. Additive manufacturing technologies: An overview about 3D printing methods and future prospects. *Complexity*. 2019;2019(1):9656938. https://doi.org/10.1155/2019/9656938.
2. Alqutaibi, A.Y., Alghauli, M.A., Aljohani, MHA., et al. Advanced additive manufacturing in implant dentistry: 3D printing technologies, printable materials, current applications and future requirements. *Bioprinting*. 2024;42:e00356. https://doi.org/10.1016/j.bprint.2024.e00356.
3. Kumar, S.A. and Tushar, J. Review of 3D printing applications in biomedical engineering: A comprehensive analysis. *J Clin Biomed Sci.* 2024;14(4):129–137. http://dx.doi.org/10.58739/jcbs/v14i4.110.
4. Li, J., Liang, D., Chen, X., et al. Applications of 3D printing in tumor treatment. *Biomed Technol*. 2024;5:1–13. http://dx.doi.org/10.1016/j.bmt.2023.03.002.
5. Gupta, R.S., Lal, B., Bhagat, A.C., et al. Medical imaging for patient-specific implants. In: *Biomedical Implants*, Dwivedi, R.K., Chauhan, P.S., eds. CRC Press: Boca Raton, FL; 2024. pp. 39–60. https://doi.org/10.1201/9781003375098-4.
6. Doganay, M.T., John, C.C., Tozluyurt, A., et al. 3D printed materials for combating antimicrobial resistance. *Mater Today*. 2023;67:371–398. http://dx.doi.org/10.1016/j.mattod.2023.05.030.

7. Derakhshanfar, S., Mbeleck, R., Xu, K., et al. 3D bioprinting for biomedical devices and tissue engineering: A review of recent trends and advances. *Bioactive Mat*. 2018;3:144–156. https://doi.org/10.1016/j.bioactmat.2017.11.008.
8. Huang, G., Zhao, Y., Chen, D., et al. Applications, advancements, and challenges of 3D bioprinting in organ transplantation. *Biomater Sci*. 2024;12(6):1425–1448. http://dx.doi.org/10.1039/d3bm01934a.
9. Song, Y., Ghafari, Y., Asefnejad, A., et al. An overview of selective laser sintering 3D printing technology for biomedical and sports device applications: Processes, materials, and applications. *Opt Laser Technol*. 2024;171:110459. http://dx.doi.org/10.1016/j.optlastec.2023.110459.
10. John, P., Antony, I.R., Whenish, R., et al. A review on fabrication of 3D printed biomaterials using optical methodologies for tissue engineering applications. *Proc Inst Mech Eng Part H J Eng Med*. 2022;236(11):1583–1594. http://dx.doi.org/10.1177/09544119221122856.
11. Bhatti, S.S., and Singh, J. 3D printing of biomaterials for biomedical applications: A review. *Int J Interact Des Manuf*. 2023; http://dx.doi.org/10.1007/s12008-023-01525-z.
12. Kennedy, S.M., Vasanthanathan, A., Jeen, R.R., et al. Impact of mechanical engineering innovations in biomedical advancements. *Vitr Model*. 2024;3(1):5–18. http://dx.doi.org/10.1007/s44164-024-00065-4.
13. Javaid, M., Haleem, A., Singh, R., et al. Role of additive manufacturing applications towards environmental sustainability. *Adv Ind Eng Polym Res*. 2021;4(4):312–322. https://doi.org/10.1016/j.aiepr.2021.07.005.
14. Jadhav, T., Kamble, N., Padave, P. A review on additive manufacturing for bio-implants. *Int J Eng Res Technol*. 2019;8(11):609–614.
15. Olakanmi, E.O. Selective laser sintering/melting (SLS/SLM) of pure Al, Al–Mg, and Al–Si powders: Effect of processing conditions and powder properties. *J Mater Process Technol*. 2013;213(8):1387–1405. https://doi.org/10.1016/j.jmatprotec.2013.03.009.
16. Olakanmi, E.O., Cochrane, R.F., Dalgarno, K.W. A review on selective laser sintering/melting (SLS/SLM) of aluminium alloy powders: Processing, microstructure, and properties. *Prog Mater Sci*. 2015;74:401–477. https://doi.org/10.1016/j.pmatsci.2015.03.002.
17. Way, A.C. SLS reliability considering autogenous self-sealing in tension governed reinforced concrete water retaining structures. PhD Thesis, Stellenbosch University, Stellenbosch, South Africa, 2021.
18. Ravi, P., and Patel, P. Stereolithography (SLA) in pharmaceuticals. In: *Additive Manufacturing in Pharmaceuticals*. Banerjee, S. Springer: Cham, Switzerland; 2023; pp. 97–123. https://doi.org/10.1007/978-981-99-2404-2_3.
19. Chen, Y.W., Moussi, J., Drury, J.L., et al. Zirconia in biomedical applications. *Expert Rev Med Devices*. 2016;13(10):945–963. https://doi.org/10.1080/17434440.2016.1230017.
20. Mzali, S., Elwasli, F., Mezlini, S., et al. Experimental investigation of tribological behavior of FDM-PLA surfaces. *Proc Inst Mech Eng Part L J Mater Des Appl*. 2025;239(4):760–775. https://doi.org/10.1177/14644207241312974.
21. Bhandari, S., Lopez-Anido, R.A., Gardner, D.J. Enhancing the interlayer tensile strength of 3D printed short carbon fiber reinforced PETG and PLA composites via annealing. *Addit Manuf*. 2019;30:100922. https://doi.org/10.1016/j.addma.2019.100922.
22. Wendels, S., and Avérous, L. Biobased polyurethanes for biomedical applications. *Bioact Mater*. 2021;6(4):1083–1086. https://doi.org/10.1016/j.bioactmat.2020.10.002.
23. Mousa, H.M., Abdal-Hay, A., Bartnikowski, M., et al. A multifunctional zinc oxide/poly(lactic acid) nanocomposite layer coated on magnesium alloys for controlled degradation and antibacterial function. *ACS Biomater Sci Eng*. 2018;4(6):2169–2180. https://doi.org/10.1021/acsbiomaterials.8b00277.
24. Song, J., Winkeljann, B., Lieleg, O. Biopolymer-based coatings: promising strategies to improve the biocompatibility and functionality of materials used in biomedical engineering. *Adv Mater Interfaces*. 2020;7: 2000850. https://doi.org/10.1002/admi.202000850.
25. Zub, K., Hoeppener, S., Schubert, U.S. Inkjet printing and 3D printing strategies for biosensing, analytical, and diagnostic applications. *Adv Mater*. 2022;34(31):2105015. https://doi.org/10.1002/adma.202105015.
26. Shi, Y., and Wang, W. 3D inkjet printing of the zirconia ceramic implanted teeth. *Mater Lett*. 2020;261:127131. https://doi.org/10.1016/j.matlet.2019.127131.
27. Swetha, S., Sahiti, T.J., Priya, G.S., et al. Review on digital light processing (DLP) and effect of printing parameters on quality of print. *Interactions*. 2024;245(1):178. https://doi.org/10.1007/s10751-024-02018-5.
28. Mohammed, M.K., Alahmari, A., Alkhalefah, H., et al. Evaluation of zirconia ceramics fabricated through DLP 3d printing process for dental applications. *Heliyon*. 2024;10(17):e36725. https://doi.org/10.1016/j.heliyon.2024.e36725.

29. Murchio, S. Hierarchical multifunctional cellular materials for implants with improved fatigue resistance and osteointegration. PhD Thesis, University of Trento, Trento, Italy, 2023. https://iris.unitn.it/handle/11572/379289.

30. Mostafaei, A., Elliott, A.M., Barnes, J.E., et al. Binder jet 3D printing—process parameters, materials, properties, modeling, and challenges. *Prog Mater Sci*. 2021;119:100707. https://doi.org/10.1016/j.pmatsci.2020.100707.

31. 31. Banothu, D., Kumar, P., Reddy, R. Advancements in 3D printing for metal bio-implants: a comprehensive bibliometric and scientometric analysis. *J. Mechanic. Continua Math. Sci*. 2024;19:9–28. https://doi.org/10.26782/jmcms.2024.11.00002.

32. Singh, A.B. Transforming healthcare: a review of additive manufacturing applications in the healthcare sector. *Eng Proc*. 2024;72(1):2. https://doi.org/10.3390/engproc2024072002.

33. Placone, J.K., Engler, A.J. Recent advances in extrusion-based 3D printing for biomedical applications. *Adv Healthc Mater*. 2018;7(8):1701161. https://doi.org/10.1002/adhm.201701161.

34. Yuan, X., Zhu, W., Yang, Z., et al. Recent advances in 3D printing of smart scaffolds for bone tissue engineering and regeneration. *Adv Mater*. 2024;36(34):2403641. https://doi.org/10.1002/adma.202403641.

35. Svetlizky, D., Das, M., Zheng, B., et al. Directed energy deposition (DED) additive manufacturing: physical characteristics, defects, challenges and applications. *Mater Today*. 2021;49:271–295. https://doi.org/10.1016/j.mattod.2021.03.020.

36. Ahmad, M., Javaid, M., Haleem, A. Enhancing biocompatible metal alloy fabrication for bio implants through laser-based additive manufacturing (LBAM). *Biomed Anal*. 2024;1(1):73–85. https://doi.org/10.1016/j.bioana.2024.02.001.

37. Kundu, M., Kadambi, P., Dhatrak, P. Additive manufacturing of bio-implants using functionally graded materials. In: *AIP Conference Proceedings*. International Conference on Recent Innovations in Science and Technology (RIST 2021) 19–20 June 2021, Malappuram, India, 2021, Paul, V., Deepanraj, B, eds., AIP Publishing: Melville, New York; 2022. https://doi.org/10.1063/5.0082039.

38. Tilton, M., Lewis, G.S., Manogharan, G.P. Additive manufacturing of orthopedic implants. In: *Orthopedic Biomaterials: Progress in Biology, Manufacturing, and Industry Perspectives*. Li, B.Y. Webster, T. Springer: Cham, Switzerland 2018; pp. 21–55. https://doi.org/10.1007/978-3-319-89542-0_2.

39. Rakić, B., Ratković, A., Mrvić, J. Potential impact of 3D printing in redesigning supply chain–example of medical industry. In *International Symposium (symorg 2016) Reshaping The Future Through Sustainable Business Development And Entrepreneurship*, Zlatibor, Serbia, June 10–13, 2016; University of Belgrade, Faculty of Organizational Sciences: Belgrade, Serbia, 2016.

40. Sharma, V., Singh, J.P., Hussan, K., et al. Machine learning approach for predicting the machining characteristics of additive manufactured ABS material. *Proc Inst Mech Eng C J Mech Eng Sci.* 2024; 239(1):129–144. https://doi.org/10.1177/09544062241283330.

41. Jiang, L. Application and innovation of 3D printing in medical equipment maintenance. *Glob Clin Eng J.* 2024;6(4):15–23. https://doi.org/10.31354/globalce.v6i4.181.

42. Ballor, J., Li, T., Prima, F., et al. A review of the metastable omega phase in beta titanium alloys: the phase transformation mechanisms and its effect on mechanical properties. *Int Mater Rev*. 2023;68(1):26–45. https://doi.org/10.1080/09506608.2022.2036401.

43. Velásquez-García, L.F., Kornbluth, Y. Biomedical applications of metal 3D printing. *Annu Rev Biomed Eng*. 2021;23(1):307–338. https://doi.org/10.1146/annurev-bioeng-082020-032402.

44. Khulief, Z. Tribological, Electrochemical, and Tribocorrosion Behaviour of New Titanium Biomedical Alloys. PhD thesis, University of Sheffield: Sheffield, UK, 2018.

45. Li, G., Liu, S., Xu, Z., et al. Recent advancements in liquid metal enabled flexible and wearable biosensors. *Soft Sci*. 2023;3(4):37. https://doi.org/10.20517/ss.2023.30.

46. Yang, X., Yu, Y., Lai, Q., et al. Recent development and advances on fabrication and biomedical applications of GA-based liquid metal micro/nanoparticles. *Compos B Eng.* 2023;248:110384. https://doi.org/10.1016/j.compositesb.2022.110384.

47. Gupta, C.P. Role of iron (Fe) in body. *IOSR J Appl Chem.* 2014;7(11):38–46. https://doi.org/10.9790/5736-071123846.

48. Gąsior, G., Szczepański, J., Radtke, A. Biodegradable iron-based materials—what was done and what more can be done? *Materials (Basel)*. 2021;14(12):3381. https://doi.org/10.3390/ma14123381.

49. Pasternak, K., Kocot, J., Horecka, A.. Biochemistry of magnesium. *J Elem*. 2010;15(3):601–616. https://doi.org/10.5601/jelem.2010.15.3.601-616.

50. Grimwade, M. The metallurgy of gold. *Interdiscip Sci Rev.* 1992;17(4):371–381. https://doi.org/10.1179/isr.1992.17.4.371.

51. Bandyopadhyay, A., Traxel, K.D., Avila, J.D., et al. In: *Biomaterials Science*. Wagner, W.R., Shelly, E., eds. Elsevier: Amsterdam, the Netherlands; 2020; pp. 257–269. https://doi.org/10.1016/B978-0-12-816137-1.00020-9.

52. Milošev, I. CoCrMo alloy for biomedical applications. In: *Biomedical Applications*. Djokić, S.S. Springer: Cham, Switzerland; 2012; pp. 1–72. https://doi.org/10.1007/978-1-4614-3125-1_1.

53. Sahasrabudhe, H., Bose, S., Bandyopadhyay, A. Laser-processed calcium phosphate reinforced CoCrMo for load-bearing applications: processing and wear induced damage evaluation. *Acta Biomater.* 2018;66:118–128. https://doi.org/10.1016/j.actbio.2017.11.022.

54. de Albuquerque, T.L., Júnior, J.E.M., de Queiroz, L.P., et al. Polylactic acid production from biotechnological routes: a review. *Int J Biol Macromol.* 2021;186:933–951. https://doi.org/10.1016/j.ijbiomac.2021.07.074.

55. Liu, S., Qin, S., He, M., et al. Current applications of poly(lactic acid) composites in tissue engineering and drug delivery. *Compos B Eng.* 2020;199:108238. https://doi.org/10.1016/j.compositesb.2020.108238.

56. Chen, Z., Du, C., Liu, S., et al. Progress in biomaterials inspired by the extracellular matrix. *Giant*. 2024;19:100323. https://doi.org/10.1016/j.giant.2024.100323.

57. Liu, H., and Webster, T.J. Enhanced biological and mechanical properties of well-dispersed nanophase ceramics in polymer composites: from 2D to 3D printed structures. *Mater Sci Eng C.* 2011;31(2):77–89. https://doi.org/10.1016/j.msec.2010.07.013.

58. Ben-Nissan, B., Choi, A.H., Cordingley, R. Alumina ceramics. In: *Bioceramics and their Clinical Applications*. Elsevier: Amsterdam, the Netherlands; 2008. pp. 223–242. https://doi.org/10.1533/9781845694227.2.223.

59. Lin, L., Fang, Y., Liao, Y., et al. 3D printing and digital processing techniques in dentistry: a review of literature. Adv Eng Mater. 2019;21(6):1801013. https://doi.org/10.1002/adem.201801013.

60. Sionkowska, A. Collagen blended with natural polymers: recent advances and trends. *Prog Polym Sci.* 2021;122:101452. https://doi.org/10.1016/j.progpolymsci.2021.101452.

61. Sharma, S., Sudhakara, P., Singh, J., et al. Critical review of biodegradable and bioactive polymer composites for bone tissue engineering and drug delivery applications. *Polymers (Basel)*. 2021;13(16):2623. https://doi.org/10.3390/polym13162623.

62. Buj-Corral, I., Tejo-Otero, A., Fenollosa-Artés, F. Use of FDM technology in healthcare applications: recent advances. In: *Fused Deposition Modeling Based 3D Printing*. Dave, H.K. Davim, J.P. Springer Cham: Switzerland, 2021;277–297. https://doi.org/10.1007/978-3-030-68024-4_15.

63. Li, J., Chen, M., Fan, X., et al. Recent advances in bioprinting techniques: approaches, applications and future prospects. *J Transl Med*. 2016;14:1–15. https://doi.org/10.1186/s12967-016-1028-0.

64. Mulcahy, N.J. *Exploring the Feasibility of 3D Printing in the Treatment of Diabetic Foot Ulcers*. University of Limerick: Limerick, Ireland; 2024.

65. Beshchasna, N., Saqib, M., Kraskiewicz, H., et al. Recent advances in manufacturing innovative stents. *Pharmaceutics*. 2020;12(4):349. https://doi.org/10.3390/pharmaceutics12040349.

66. Leberfinger, A.N., Dinda, S., Wu, Y., et al. Bioprinting functional tissues. *Acta Biomater*. 2019;95:32–49. https://doi.org/10.1016/j.actbio.2019.01.009.

67. Wu, Y., Liu, J., Kang, L., et al. An overview of 3D printed metal implants in orthopedic applications: present and future perspectives. *Heliyon*. 2023;9(7): e17718. https://doi.org/10.1016/j.heliyon.2023.e17718.

68. García-Ávila, J., González-Gallegos, C.P., Segura-Ibarra, V., et al. Dynamic topology optimization of 3D-printed transtibial orthopedic implant using tunable isotropic porous metamaterials. *J Mech Behav Biomed Mater.* 2024;153:106479. https://doi.org/10.1016/j.jmbbm.2024.106479.

69. Wong, K.C. 3D-printed patient-specific applications in orthopedics. *Orthop Res Rev.* 2016;8:57–66. https://doi.org/10.2147/ORR.S99614.

70. Liu, B., Ma, Z., Li, J., et al. Experimental study of a 3D printed permanent implantable porous Ta-coated bone plate for fracture fixation. *Bioact Mater.* 2022;10:269–280. https://doi.org/10.1016/j.bioactmat.2021.09.009.

71. Oraa, J., Fiz, N., González, S., et al. Derotation tibial osteotomy with custom cutting guides and custom osteosynthesis plate printed with 3D technology: case and technical note. *Ann 3D Print Med.* 2023;9:100093. https://doi.org/10.1016/j.stlm.2022.100093.

72. Miao, K., Wang, J., Yu, K., et al. Percutaneous reduction and cannulated screw fixation assisted by 3D printing technology of calcaneal fractures in children. *J Orthop Sci.* 2022;29(1):236-242. https://doi.org/10.1016/j.jos.2022.12.004.

73. Kumar, S.V., Marimuthu, K., Subramani, S., et al. Prospective randomized trial comparing open reduction and internal fixation with minimally invasive reduction and percutaneous fixation in managing displaced intra-articular calcaneal fractures. *Int Orthop.* 2014;38:2505–2512. https://doi.org/10.1007/s00264-014-2501-0.

74. Kia, C., Antonacci, C.L., Wellington, I., et al. Spinal implant osseointegration and the role of 3D printing: an analysis and review of the literature. *Bioengineering*. 2022;9(3):108. https://doi.org/10.3390/bioengineering9030108.

75. Siracusa, V., Maimone, G., Antonelli, V. State-of-art of standard and innovative materials used in cranioplasty. *Polymers (Basel).* 2021;13(9):1452. https://doi.org/10.3390/polym13091452.

76. Zheng, H., Wang, L., Jiang, W., et al. Application of 3D printed patient-specific instruments in the treatment of large tibial bone defects by the Ilizarov technique of distraction osteogenesis. *Front Surg.* 2023;9:985110. https://doi.org/10.3389/fsurg.2022.985110.

77. Choudhari, A., Gupta, A.K., Kumar, A., et al. Wear and friction mechanism study in knee and hip rehabilitation: a comprehensive review. In: *Applications of Biotribology in Biomedical Systems.* Kumar, A., Kumar, A., eds. Springer Cham: Switzerland, 2024;345–432. https://doi.org/10.1007/978-3-031-58327-8_13.

78. Wang, J., Wang, X., Sun, B., et al. 3D-printed patient-specific instrumentation decreases the variability of patellar height in total knee arthroplasty. *Front Surg*. 2023;9:954517. https://doi.org/10.3389/fsurg.2022.954517.

79. Meng, M., Wang, J., Huang, H., et al. 3D printing metal implants in orthopedic surgery: methods, applications and future prospects. *J Orthop Transl*. 2023;42:94–112. https://doi.org/10.1016/j.jot.2023.08.004.

80. Saroia, J., Wang, Y., Wei, Q., et al. A review on 3D printed matrix polymer composites: its potential and future challenges. *Int J Adv Manuf Technol.* 2020;106:1695–1721. https://doi.org/10.1007/s00170-019-04534-z.

81. Gentile, C., and Gruppioni, E. A perspective on prosthetic hands control: from the brain to the hand. *Prosthesis.* 2023;5(4):1184–1205. https://doi.org/10.3390/prosthesis5040083.

82. Hao, Y., Wang, L., Jiang, W., et al. 3D printing hip prostheses offer accurate reconstruction, stable fixation, and functional recovery for revision total hip arthroplasty with complex acetabular bone defect. *Engineering.* 2020;6(11):1285–1290. https://doi.org/10.1016/j.eng.2020.04.013.

83. Dziaduszewska, M., and Zieliński, A. Structural and material determinants influencing the behavior of porous Ti and its alloys made by additive manufacturing techniques for biomedical applications. *Materials (Basel).* 2021;14(4):712. https://doi.org/10.3390/ma14040712.

84. Borah, J., and Chandrasekaran, M. Experimental investigation and development of artificial neural network modeling of 3D printed PEEK bio implants and its optimization. *Research Square (preprint) 2023*; posted 14 Sep, 2023. https://doi.org/10.21203/rs.3.rs-3204960/v1.

85. Li, X., Heidari, A., Nourbakhsh, S.M., et al. Design and fabrication of elastic two-component polymer-metal disks using a 3D printer under different loads for the lumbar spine. *Polym Test.* 2022;112:107633. https://doi.org/10.1016/j.polymertesting.2022.107633.

86. Lewallen, E.A., Riester, S.M., Bonin, C.A., et al. Biological strategies for improved osseointegration and osteoinduction of porous metal orthopedic implants. *Tissue Eng B Rev.* 2015;21(2):218–230. https://doi.org/10.1089/ten.teb.2014.0333.

87. Bandyopadhyay, A., Mitra, I., Goodman, S.B., et al. Improving biocompatibility for next generation of metallic implants. *Prog Mater Sci.* 2023;133:101053. https://doi.org/10.1016/j.pmatsci.2022.101053.

88. Schito, M., Peter, T.F., Cavanaugh, S., et al. Opportunities and challenges for cost-efficient implementation of new point-of-care diagnostics for HIV and tuberculosis. *J Infect Dis.* 2012;205(Suppl 2):S169–S180. https://doi.org/10.1093/infdis/jis044.

89. Wu, S., Liu, X., Yeung, K.W.K., et al. Biomimetic porous scaffolds for bone tissue engineering. *Mater Sci Eng R Rep.* 2014;80:1–36. https://doi.org/10.1016/j.mser.2014.04.001.

90. Bernard, H., and Foss, M. Patient experiences of enhanced recovery after surgery (ERAS). *Br J Nurs.* 2014;23(2):100–106. https://doi.org/10.12968/bjon.2014.23.2.100.

91. Sidhu, S.S., Chanda, A., Abdel-Hady, G.M. Advances and perspective in bio-implants for commercialization. *Front. Bioeng. and Biotech*. 2023;11:1306077. https://doi.org/10.3389/fbioe.2023.1306077.

92. Mahajan, A., Devgan, S., Zitoune, R. *Additive Manufacturing of Bio-Implants.* Springer: Cham, Switzerland; 2024. https://doi.org/10.1007/978-981-99-6972-2.

93. Jegadeesan, J.T., Baldia, M., Basu, B. Next-generation personalized cranioplasty treatment. *Acta Biomater.* 2022;154:63–82. https://doi.org/10.1016/j.actbio.2022.10.030.

94. Pathak, K., Saikia, R., Das, A., et al. 3D printing in biomedicine: advancing personalized care through additive manufacturing.

Explor Med. 2023;4(6):1135–1167. https://doi.org/10.37349/emed.2023.00200.

95. Mishchenko, O., Kopchak, A., Chernohorskyi, D., et al. Craniofacial reconstruction using 3D personalized implants with enhanced surface properties: technological and clinical aspects. *Appl Surf Sci Adv.* 2023;16:100437. https://doi.org/10.1016/j.apsadv.2023.100437.

96. Yousefiasl, S., Sharifi, E., Salahinejad, E., et al. Bioactive 3D-printed chitosan-based scaffolds for personalized craniofacial bone tissue engineering. *Eng Regen*. 2023;4(1):1–11. https://doi.org/10.1016/j.engreg.2022.09.005.

97. Ullah, M., Bibi, A., Wahab, A., et al. Shaping the future of cardiovascular disease by 3D printing applications in stent technology and its clinical outcomes. *Curr Probl Cardiol*. 2024;49(1):102039. https://doi.org/10.1016/j.cpcardiol.2023.102039.

98. Liu, J., Mohd Rafiq, N.B., Wong, L.M., et al. Surface treatment and bioinspired coating for 3D-printed implants. *Front Chem.* 2021;9:768007. https://doi.org/10.3389/fchem.2021.768007.

99. Yuan, T., Liu, D., Li, Q., et al. 3D printing of melatonin-loaded esophageal stents for treatment of corrosive esophagitis. *Appl Mater Today*. 2024;37:102161. https://doi.org/10.1016/j.apmt.2024.102161.

100. Jabeen, F. Bio implants—a review. J Adv Med Dent Sci Res. 2018;6(1):169. https://doi.org/10.21276/jamdsr.

101. Kessler, A., Reichl, F.X., Folwaczny, M., et al. Monomer release from surgical guide resins manufactured with different 3D printing devices. Dent Mater. 2020;36(11):1486–1492. https://doi.org/10.1016/j.dental.2020.09.002.

102. Li, H., An, J., Bao, Q., et al. Photocurable 3D printing high-strength gels for flexible wearable devices and surgical models. *Polymer (Guildf)*. 2023;286:126392. https://doi.org/10.1016/j.polymer.2023.126392.

103. Sharma, S., Jain, A., Gupta, V., et al. Additive manufacturing of bio-implants. In: *Additive Manufacturing for Biomedical Applications: Recent Trends and Challenges.* Dixit, A. Kumar, A., eds. Springer; Cham, Switzerland; 2024; pp. 39–54. https://doi.org/10.1007/978-981-97-5456-4_3.

104. Chua, C.K., Wong, C.H., Yeong, W.Y. *Standards, Quality Control, and Measurement Sciences in 3D Printing and Additive Manufacturing.* Academic Press: Cambridge, MA; 2017. https://doi.org/10.1016/B978-0-12-813489-4.00008-8.

105. Limaye, N., Veschini, L., Coward, T. Assessing biocompatibility & mechanical testing of 3D-printed PEEK versus milled PEEK. *Heliyon.* 2022;8(12):e12314. https://doi.org/10.1016/j.heliyon.2022.e12314.

106. Abd-Elaziem, W., Darwish, M.A., Hamada, A., et al. Titanium-based alloys and composites for orthopedic implants applications: a comprehensive review. *Mater Des.* 2024;241:112850. https://doi.org/10.1016/j.matdes.2024.112850.

107. Martinez-Marquez, D., Terhaer, K., Scheinemann, P., et al. Quality by design for industry translation: three-dimensional risk assessment failure mode, effects, and criticality analysis for additively manufactured patient-specific implants. *Eng Rep*. 2020;2(1):e12113. https://doi.org/10.1002/eng2.12113.

108. Guzzi, E.A., and Tibbitt, M.W. Additive manufacturing of precision biomaterials. *Adv Mater.* 2020;32(13):1901994. https://doi.org/10.1002/adma.201901994.

109. Das, T.K., Ghosh, P., Das, N.C. Preparation, development, outcomes, and application versatility of carbon fiber-based polymer composites: a review. *Adv Compos Hybrid Mater.* 2019;2:214–233. https://doi.org/10.1007/s42114-018-0072-z.

110. Verma, A., Kapil, A., Klobčar, D., et al. A review on multiplicity in multi-material additive manufacturing: process, capability, scale, and structure. *Materials (Basel).* 2023;16(15):5246. https://doi.org/10.3390/ma16155246.

111. Wu, Y., An, C., Guo, Y. 3D printed graphene and graphene/polymer composites for multifunctional applications. *Materials (Basel).* 2023;16(16):5681. https://doi.org/10.3390/ma16165681.

112. Vido, M., de Oliveira, N.G.C., Lourenço, S.R., et al. Computer-aided design and additive manufacturing for automotive prototypes: a review. *Appl Sci.* 2024;14(16):7155. https://doi.org/10.3390/app14167155.

113. Gao, W., Zhang, Y., Ramanujan, D., et al. The status, challenges, and future of additive manufacturing in engineering. *Comput Des.* 2015;69:65–89. https://doi.org/10.1016/j.cad.2015.04.001.

114. Top, N., Şahin, İ., Gökçe, H., et al. Computer-aided design and additive manufacturing of bone scaffolds for tissue engineering: state of the art. *J Mater Res.* 2021;36:3725–3745. https://doi.org/10.1557/s43578-021-00156-y.

115. Delgado, J.M.D., and Oyedele, L. Digital twins for the built environment: learning from conceptual and process models in manufacturing. *Adv Eng Informatics.* 2021;49:101332. https://doi.org/10.1016/j.aei.2021.101332.

116. Wang, D.D., Qian, Z., Vukicevic, M., et al. 3D printing, computational modeling, and artificial intelligence for structural heart disease. *Cardiovasc Imaging.* 2021;14(1):41–60. https://doi.org/10.1016/j.jcmg.2019.12.022.

Received September 12, 2024, accepted June 30, 2025, publication date for online-first December 20, 2025.

Original Research Article

Performance Comparison of AlexNet and GoogLeNet on Pneumonia Chest X-Rays

S. Pravin Kumar*, B. Panchami, Vishal Narayanan and Suke Bhargav

Sri Sivasubramaniya Nadar College of Engineering, Chennai, Tamil Nadu, India.

* Corresponding Author Email: pravinkumars@ssn.edu.in

ABSTRACT

Detecting pneumonia on chest radiographs is crucial for precise clinical intervention. Efficient diagnostic tools are necessary to assess a large number of X-rays and improve patient outcomes. This study uses 6,796 chest X-ray images, consisting of both pneumonia and healthy conditions, to test the classification performance of two deep learning models, GoogLeNet and AlexNet. Both models demonstrated high sensitivity; however, AlexNet exhibited higher accuracy, specificity, and F-score. AlexNet also showed a higher validation accuracy at 98.08% compared to GoogLeNet's accuracy of 97.87%. Therefore, the results indicate that AlexNet model show better accuracy than the GoogLeNet model.

Keywords—*Pneumonia, Chest-X-rays, CNN, AlexNet vs GoogleNet, Performance comparison.*

INTRODUCTION

Pneumonia is a disease in the respiratory systems as a result of microorganism infections, that can lead to fluid accumulation and inflammation in the lungs.[1] Timely medical interventions and treatment depends on accurate and early diagnosis of this disease. Chest X-rays remain a widely used tool to detect pneumonia, with typical signs appearing as white or hazy infiltrates compared to healthy lung tissue.[2,3] Although CT scans are the gold standard, chest X-rays are more accessible, especially in resource-limited settings.

Challenges persist, including the rise of multidrug-resistant pathogens, diagnostic delays during pandemics, and the shortage of radiologists in rural or underdeveloped areas.[4] Deep neural networks are shown to be effective in the interpretation of images and can provide potential solutions to these problems.

Specifically, convolutional neural networks (CNNs), can extract diagnostic features automatically from X-ray images and improve diagnostic accuracy. However, their adoption is still limited by the requirement for large labeled datasets, considerable computational resources, and model interpretability.

This study compares the performance of two CNN models, AlexNet and GoogLeNet, for automatic detection of

pneumonia from chest X-rays, along with their diagnostic capabilities and practical implications.

LITERATURE REVIEW

CNNs have been extensively used for detecting pneumonia in chest X-rays and shown to be efficient with better diagnostic speed and accuracy. Several recent studies have proposed deep learning models for medical image classification applications.

For example, Çınar used a ResNet50 model that uses skip connections to improve feature extraction. In contrast, our study compares the performance of the two popular CNN architectures, AlexNet and GoogLeNet, on a dataset of 6,796 chest X-ray images.[5] AlexNet outperformed GoogLeNet, with a validation accuracy of 98.08%, specificity of 96.64%, and an F-score of 92.18%. These results show that AlexNet, despite its relatively simpler architecture, can be effective compared to more complex models like ResNet50.

Militante et al. introduced adaptive deep learning techniques to improve pneumonia detection across different datasets.[6] While these adaptive models offer flexibility, our study focuses on a comparison of classical models under similar experimental conditions. Our evaluation shows that AlexNet shows stable performance with better validation accuracy. This makes it more suitable for clinical settings where consistency and reproducibility are crucial.

Ullah et al. investigated how modifications in the GoogLeNet architecture enhanced its performance in pneumonia detection.[7] However, our findings indicate that even unmodified AlexNet performs exceptionally well. This suggests that complex modifications may not be necessary for effective pneumonia classification.

Reshan et al. used lightweight models like MobileNet for use in mobile health applications.[8] While it is shown valuable for low-resource settings, their accuracy remains lower than that achieved by AlexNet in our study, which shows clinical-grade performance and reliability.

Militante et al. further demonstrated the efficiency of adaptive architectures. However, it involved higher computational overhead costs.[6] Our work, by contrast, uses simpler classic models that are easy to deploy and maintain. AlexNet showed its potential for real world diagnostic applications through its high specificity and precision.

The trials on the Kaggle pneumonia dataset, with models such as VGG16, DenseNet, and Inception, reported an accuracy of approximately 86%. In comparison, our AlexNet implementation showed 98.08% accuracy and high F-score. This implies its ability to learn complex patterns in radiographic images.

Rajpurkar et al. and Lakhani & Sundaram have also demonstrated that deep CNNs can achieve high sensitivity and specificity for pneumonia detection and other thoracic diseases.[9,10] These studies demonstrate the feasibility of CNN models for medical diagnostics and thus validating our architectural choice.

AlexNet, introduced by Krizhevsky et al., consists of five convolutional and three fully connected layers.[11] ReLU activations and dropout layers, enable it for faster convergence and regularization, respectively. Through GPU acceleration, it can be benefitted with effective feature extraction and efficient training for medical imaging applications.

In contrast, GoogLeNet uses inception modules to learn multiscale representations through parallel convolutions of different kernel sizes.[12] The inclusion of 1 × 1 convolutions allows for a deeper, but at the same time computationally efficient networks. While GoogLeNet achieved lower error rates than AlexNet on ImageNet dataset, our results show that AlexNet performs better for pneumonia classification in chest X-rays.

Table 1 provides an overview of the performance of AlexNet and GoogLeNet across various medical imaging tasks. For example, Singh & Talwekar reported GoogLeNet achieving 100% accuracy and AlexNet 99.7% for sleep apnea detection.[13] Similarly, AlexNet outperformed GoogLeNet in seizure detection and showed competitive results in white blood cell classification and cancer drug response prediction.[14,15]

TABLE 1. Comparison of the performance of AlexNet and GoogLeNet in various applications reported in the literature.

Methods	Key findings	Publication
An automatic detection method of obstructive sleep apnea is proposed using single-channel electrocardiogram (ECG) using AlexNet and GoogLeNet models.	AlexNet and GoogLeNet were compared for obstructive sleep apnea detection using single-channel ECG. GoogLeNet achieved 100% accuracy, while AlexNet reached 99.7%.	13
Compared against the least absolute shrinkage and selection operator (LASSO) model for multiclass drug responsiveness prediction.	Better performance of both models compared to LASSO.	15
Compared against fine-tuned models with customized CNN for the detection of parasites from the stool sample.	GoogleNet has an ROC area under the curve (AUC) of 0.99, while AlexNet achieves a perfect ROC AUC of 1.00.	16
Face recognition application.	GoogLeNet learns features faster with fewer iterations, while AlexNet achieves 100% accuracy after 30 iterations.	17
Seizure detection from EEG.	AlexNet outperformed GoogLeNet in seizure detection with an accuracy of 95.61% compared to 94.99%. Both networks were evaluated alongside SqueezeNet, which achieved an accuracy of 94.09%.	14
WBC classification.	The paper compares AlexNet and GoogleNet for WBC classification, showing that the hybrid model outperforms both individually, achieving 99.73% accuracy and 0.99 F1-score.	18
Handwriting recognition.	GoogLeNet showed highest accuracy, while LeNet-5 was fastest. AlexNet's performance was not specifically addressed in the paper.	19
Brain tumor detection.	AlexNet and GoogLeNet were compared for brain tumor detection; GoogLeNet outperformed with 99.45% accuracy and 99.75% sensitivity, being faster and more accurate than AlexNet.	20
Both GoogLeNet and AlexNet were tested on sketches, showing limited recognition compared to humans. Efficacy varied across classes, highlighting differences in generalization abilities.	Poor recognition for both networks compared to humans.	21

AlexNet and GoogLeNet have shown effectiveness in soft tissue analysis, particularly in breast cancer detection. For instance, Zhang et al. reported training accuracies of 100% for both models using photoacoustic tomography, with testing accuracies of 87.69% (AlexNet) and 91.18% (GoogLeNet).[22] Pacal found AlexNet (79.5%) outperformed GoogLeNet (75.6%) on ultrasound images.[23] Samee et al. consistently observed better accuracy from AlexNet across varied mammogram conditions, while Yu et al. reported accuracies of 79% (AlexNet) and 81% (GoogLeNet) using transfer learning.[24,25] Khafaga's meta-heuristic-based study noted GoogLeNet slightly outperformed AlexNet (96.1% vs. 94.6%).[26]

Beyond breast imaging, CNNs have been widely used in medical image analysis. Chen et al.[5] reviewed CNN progress in disease detection, also achieving 94.5% accuracy for brain tumor segmentation using a modified U-Net. Alshmrani et al. used RetinaNet with ResNet-10 for pneumonia detection, reporting 96.45% accuracy.[27] Other studies on CheXpert, VinDr-CXR, and PulmoNet confirmed CNNs' promise in pulmonary disease diagnosis, though with slightly lower accuracies than our models. Wang & Yang reached 93.2% accuracy using 3D CNNs for COVID-19 detection.[28] In skin lesion classification, Bazgir et al. achieved 85.94% with Inception-v3.[29]

Given these successes, this study evaluates the performance of AlexNet and GoogLeNet for pneumonia detection on chest X-ray images.

Theoretical Framework

Pneumonia's diagnosis begins with obtaining chest X-ray images from the patient. Acquired X-ray images must be preprocessed before being used in the machine learning models, as this will eliminate variations that could negatively affect the algorithm. The steps involved in preprocessing include standardizing the image by correcting for patient positioning, adjusting exposure settings, and mitigating noise from factors such as motion artifacts or inconsistent use of grids.

The preprocessed images are used as input to the machine learning model for training. The model learns to find patterns indicative of pneumonia by dataset analysis of labelled images. The performance of this model is validated with different qualitative and quantitative tests. Testing is carried out on a separate set of images not seen by the model during the training phase. This phase is critical for evaluating the model's efficacy and generalizability. To determine the effectiveness of the model in discriminating between healthy and diseased states, accuracy, precision, recall, and the area under the receiver operating characteristic curve (ROC)are used as evaluation metrices.

Validation takes place simultaneously with the training process, utilizing a small portion of the data for adjusting the model's parameters and avoiding overfitting. Overfitting occurs when a model memorizes specific details in the training set instead of learning overall trends, leading to decreased performance on unfamiliar data. Monitoring the performance of the model on the validation subset is part of the validation process. This monitoring guides decisions on making model adjustments, like determining when to halt training to prevent overfitting. Figure 1 is depicted in the illustration.

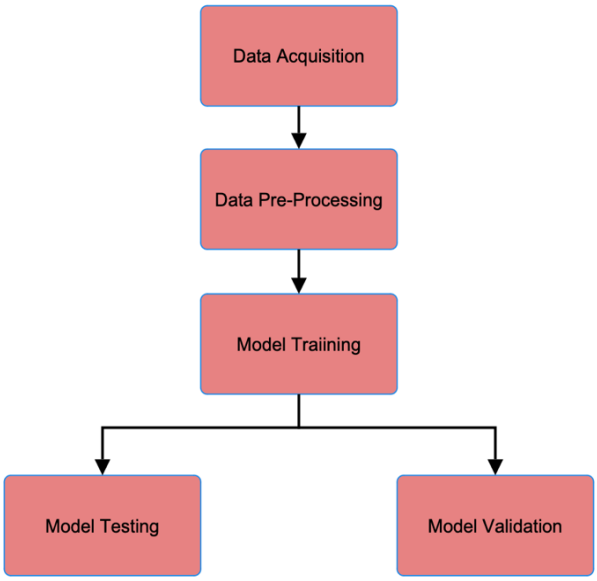

FIGURE 1. Workflow for diagnosis of pneumonia: From X-Ray images to trained CNN model.

RESEARCH METHODOLOGY

Dataset

Different deep learning models utilized to train on the Kaggle dataset containing images of chest radiograph of patients diagnosed with pneumonia. This publicly available dataset was collected from Guangzhou Women and Children's Medical Centre. It consists of images from young patients between the ages of 1 and 5, who received front and back chest X-rays as part of their regular medical check-ups. Before being added to the dataset, every radiograph went through a thorough quality control procedure. This was a crucial step to guarantee the integrity and suitability of the images for the machine learning task. Radiographs that did not meet the quality standard because of factors such as poor image clarity or legibility were excluded. In total, there are 5,856 X-Ray images in JPEG format. The dataset is organized into three main groups: training, test, and validation (Table 2). Each group contains two subcategories: Pneumonia and Normal (Figure 2).

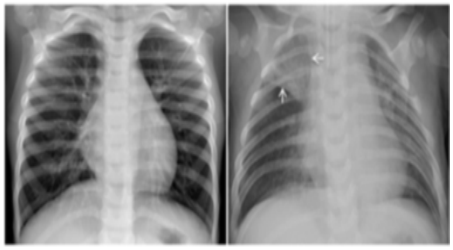

FIGURE 2. Example chest X-rays showing (Left) normal and (Right) pneumonia conditions.

TABLE 2. Dataset organization.

	Pneumonia	Normal	Total
Training	3875	1341	5216
Test	1162	402	1564
Validation	8	8	16
Total	5045	1751	6796

Moreover, to affirm the clinical validity of the images, two experienced physicians independently reviewed the chest X-rays. This review process was aimed at confirming the presence of features characteristic of pneumonia in the "Pneumonia" labelled images and ensuring the absence of such features in the "Normal" ones. The common signs on chest X-ray used to label that as pneumonia are listed in Table 3.

TABLE 3. Common signs of pneumonia.

Sign	Description
Consolidation	Area of increased density in lung tissue, often indicating infection or inflammation.
Infiltrates	Cloudy or hazy areas because of fluid or inflammatory cells accumulating in the lung.
Air Bronchograms	Visible air-filled bronchi surrounded by denser lung tissue.
Lobar Atelectasis	Collapse of a lung lobe, resulting in a white-out appearance in that specific area.
Pleural Effusion	Accumulation of fluid in the pleural space, seen as a blunted costophrenic angle or meniscus-like shadow.
Cavities or Abscesses	Well-defined round or oval areas of lucency within the lung.
Increased Interstitial Markings	Thickening of lung interstitium, seen as fine lines or reticular opacities.
Pneumothorax	Presence of air in the pleural space, causing lung collapse and a visible pleural line.
Nodules or Masses	Abnormal growths within lung tissue, which may be infectious or neoplastic.

Dataset Quality and Relevance

This study utilizes a dataset comprising 6,796 high-resolution chest radiographs. It consists of both pneumonia-positive and healthy cases, to evaluate the performance of deep learning models in pneumonia detection. The performance of the deep learning models developed largely depends on the quality of the dataset with which it is trained.

To test the reliability and benchmark, the dataset needs to be trained and tested with different models, including established architectures such as AlexNet and GoogLeNet. The results from the classical models can be used to compare the performance of other advanced models.

Image Quality and Resolution

It is evident that, higher the resolution better the intrinsic details are preserved in the X-ray images. This enables the deep learning models to detect subtle features associated with pneumonia. For example, slight variations in lung opacity or structural abnormalities are captured in high resolution images. They also do not suffer from the noise and artifacts that might otherwise affect the model's learning process, which. leads to more reliable and consistent performance.

Class Labels and Subdivision

The dataset used in this study is annotated by medical experts, as shown in Table 2. Each image is assigned to either one of the two classes: pneumonia or normal. This binary classification method allows us to carry out a simple training process for differentiating between these two conditions. The dataset is partitioned into three subsets: training, validation, and testing. The training subset is used to train the model, so that it learns distinguishing the features of pneumonia and healthy lungs.

The validation set is used to fine-tune hyperparameters and avoid overfitting. This provides a measure of how well the model generalizes to unseen data. The test set subjected to data augmentation is reserved specifically for final evaluation. This enables an unbiased assessment of the model's performance on entirely unseen data.

Usage of sufficiently large volume of image subsets minimizes the preprocessing work required, enables direct image input to the model, and allows for a more straight forward workflow.

Following segregation and verification for its quality and accuracy, the images were then processed using a batch processing pipeline. This step applies to a series of transformations to standardize and enhance the images and optimize them for model training. Preprocessing steps include resizing images to a uniform scale, adjusting brightness and contrast, and, where applicable, augmenting the dataset to enhance the model's capacity to generalize from training data to unseen data.

Data Preprocessing

During the preprocessing, bilinear interpolation is used to resize all X-ray images to a standard resolution. As explained, the objective image resizing is to maintain high resolution and image details, which are important for detecting anomalies in chest X-rays. Bilinear interpolation provides smoother results than nearest-neighbor interpolation by determining new pixel values using a weighted average of the original image's nearest neighbors. This method calculates the new pixel intensity values, $I(x,y)$,for the coordinates (x,y) in the resized image, by computing a weighted average of the pixel values in proximity in the original image ($I'(i,j)$).

Mathematically, the bilinear interpolation is represented as Equation (1):[30]

$$I(x,y)=\sum_{i,j} I'(i,j).h(x-i,y-j) \quad (1)$$

where $I'(i,j)$ are the pixel values in the original image, and (h) is the interpolation kernel which modulates the influence of each original pixel based on its spatial relationship to the new location.

After resizing, z-score normalization is used to standardize the intensity values within each image. It changes the pixel values according to the image-specific mean (μ) and standard deviation (σ):[31]

$$Inorm(x,y)=\frac{\left[I(x,y)-\mu\right]}{\sigma} \quad (2)$$

This normalization process ensures uniformity in the distribution of data, which enables the CNN model to learn from the structural content of the images instead of being influenced by intensity variations.

Although z-score normalization is commonly applied, its application to medical imaging, particularly in standardizing intensity values across high-resolution radiographs needs to be highlighted. This standardization reduces variability because of different medical imaging conditions and enhances the model's ability to focus on structural variations between healthy and unhealthy tissues.

Additionally, histogram equalization is applied to improve the contrast of the image, it redistributes pixel intensity values to expand the dynamic range and highlight important features in X-ray images that could suggest pneumonia. The process ensures that critical diagnostic features are highlighted to improve the detection capability of the model.

The data is augmented to introduce a range of variations within the dataset, which included image rotations and flips. Such transformations are governed by rotation matrices (R), defined as:[32]

$$R=\begin{pmatrix} cos\theta & -sin\theta \\ cos\theta & cos\theta \end{pmatrix} \quad (3)$$

where (θ) denotes the angle of rotation. This step is useful to prevent overfitting and improve the performance of CNN. It contributes to effective pattern recognition in various clinical scenarios.

Data augmentation steps including rotation through rotation matrices discussed above introduce variations within the dataset. This approach helps the model exposed to a wide range of possible scenarios and subsequently enhances its generalization capabilities. The mathematical basis for rotation matrices provides precision in augmenting the data. It makes the model robust against different clinical conditions.

The overall effect of these preprocessing steps, such as resizing, normalization, contrast enhancement, and data augmentation, is helpful in refining the dataset for optimal quality. It ensures standardized and enhanced images suitable for training the CNN model for accurate detection of pneumonia.

Training Models

The CNN architecture was designed to focus on the subtle features corresponding to pneumonia in chest X-rays. It uses a deep layer structure to extract complex features, along with regularization techniques such as dropout and batch normalization to minimize overfitting. This custom design for pneumonia conditions differentiates this model from generic CNN architecture.

To make use of existing feature extraction capabilities, we initialized both AlexNet and GoogLeNet with pretrained weights from ImageNet. Fine-tuning these models on the pneumonia dataset allowed efficient adaptation to domain-specific patterns in pneumonia detection.

The final layers of both architectures were modified to suit the binary classification task (pneumonia vs. normal). Specifically, we adjusted the fully connected and output layers to better fit the dataset characteristics.

A dynamic learning rate adjustment was implemented to improve convergence and prevent issues such as vanishing gradients or entrapped into local minima which are common pitfalls in deep learning optimization.

The models were trained using the following hyperparameters:

- Learning rate: 0.001
- Epochs: 20
- Minibatch size: 300
- Dropout rate: 0.1

Using the configuration above, AlexNet achieved 98.08% accuracy, and outperformed that of GoogLeNet, which achieved 97.87%.

The minibatch size of 300 improved the training stability by providing reliable gradient estimates and thereby smoother convergence. The dropout layer, with a 0.1 rate, played a critical role in reducing overfitting by forcing the network to learn more generalized features.

AlexNet

Introduced by Krizhevsky et al., AlexNet was a breakthrough in CNN design, winning the ImageNet Large Scale Visual Recognition Challenge (ILSVRC) with nearly half the error rate of competing models.[11]

The architecture (Figure 3) consists of five convolutional layers followed by three fully connected layers, totaling approximately 60 million parameters. Its key features are summarized in Table 4.

TABLE 4. AlexNet architecture overview.

Layer	Description
ReLU Activation Functions	Uses rectified linear unit (ReLU) activation functions. These functions accelerate training by avoiding the vanishing gradient problem. ReLU activation ensures faster convergence and better gradient flow during backpropagation.
Pooling Layer	It reduces the feature maps dimensions. By downsampling, it extracts essential features while minimizing computational complexity. The output of this layer serves as input to subsequent convolutional layers.
Fully Connected Layer	Acting as a bridge between preceding layers, the fully connected layer integrates extracted features. It facilitates high-level feature representation and decision-making.
Overfitting Mitigation Strategies	AlexNet incorporates methodologies to combat overfitting: Dropout Layer: Prevents the network from memorizing specific patterns by randomly deactivating neurons during training. Data Augmentation: The dataset is artificially augmented using label-preserving transformations. This augmentation expands the dataset, enhancing the model's generalization capability.

The key contributions of AlexNet to the advancement of deep learning include the introduction of ReLU activation functions. The ReLU function is defined as:

$$f(x) = max(0, x) \tag{4}$$

This simple yet effective function sped up the training process because it mitigated the vanishing gradient problem commonly observed with traditional activation functions such as the sigmoid or tanh.

AlexNet also implemented a pooling layer, particularly max pooling, to downsample the feature maps, reducing their dimensions while preserving the most important information. This operation helps to reduce the computational load for subsequent layers. The max pooling operation employs the following formula for a 2D feature map:

$$M(x, y) = max_{\{a,b \in N(i,j)\}} I(a, b) \tag{5}$$

where $M(x, y)$ is the output of the max pooling operation, $I(a, b)$ represents the input pixel values within the neighborhood $N(i, j)$ around the point (i, j) in the feature map.

To address overfitting, AlexNet introduced the use of dropout layers, which randomly set a subset of activations to zero during training to prevent the network from becoming too reliant on any one feature. This can be represented as:

$$r_j^{(i)} \sim Bernoulli(p) \tag{6}$$

$$y_j^{(i)} = r_j^{(i)} * a_j^{(i)} \tag{7}$$

where $r_j^{(i)}$ is a random variable drawn from a Bernoulli distribution with probability (p), and $a_j^{(i)}$ is the activation of neuron (j) at layer (l). The value of (p) typically ranges from 0.5 to 1, representing the probability that a given neuron will be retained.

Moreover, AlexNet utilized data augmentation techniques, like image translations and horizontal reflections, to artificially enhance the size of the training dataset. The transformations could be represented by transformation matrices applied to the pixel coordinates of the images, thereby increasing the variety of training examples and improving the ability of the model to generalize to unseen data.

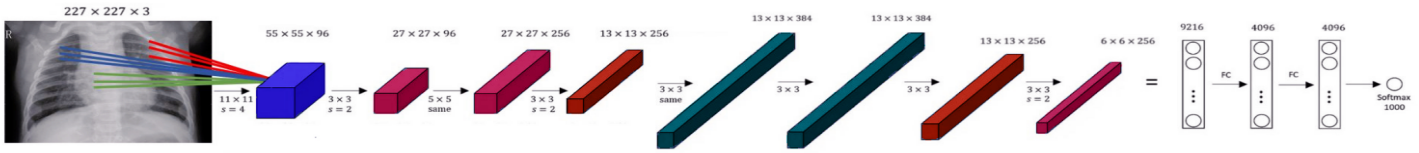

FIGURE 3. AlexNet architecture.

In practice, AlexNet accepts input images with dimensions of 227 × 227 × 3, where 227 × 227 corresponds to the height and width of the image, and 3 signifies the RGB color channels. We employed AlexNet for pneumonia detection through feature transfer learning. It provides an advantage of leveraging backbone models initially trained on large-scale general-purpose datasets, instead of relying solely on domain-specific pretrained models. The idea is to transfer rich feature representations learned from general-purpose models to medical tasks. AlexNet automatically learns features in a hierarchy, capturing both low-level details (edges, textures) and high-level patterns (shapes, structures).

GoogLeNet

GoogLeNet, another landmark innovation in the field of CNNs, expanded upon the foundations laid by architectures such as AlexNet. Designed to optimize depth and breadth within the network while mitigating the issue of overfitting, GoogLeNet introduced a novel architectural element as seen in Figure 4, known as the inception module.

The inception module forms the core of GoogLeNet, leveraging a network-in-network architecture to enable the model to benefit from multiscale processing. Rather than a linear stack of layers, the inception module applies multiple filter sizes within the same level of the network, allowing it to capture information at various resolutions. Symbolically, these can be represented by convolutional operations over the input and then aggregating the outputs. For instance, convolutional operations within an inception module might look like:

$$I_{output} = [IF_{1\times1}, IF_{3\times3}, I * F_{5\times5}] \quad (8)$$

where $F_{n\times n}$ represents a filter of size ($n\times n$), and (I) is the input to the inception module. The brackets indicate concatenation of the outputs of the convolution operations with filters of different sizes.

GoogLeNet also incorporates global average pooling toward the end of the network instead of fully connected layers, reducing the total number of parameters and helping to counter overfitting. The global average pooling operation can be denoted as:

$$I_{gap}(c) = \frac{1}{H\times W}\sum_{i=1}^{H}\sum_{j=1}^{W} I_{ij}(c) \quad (9)$$

where $I_{ij}(c)$ represents the activation of a feature map (c) at the spatial location (i, j), and (H) and (W) denote the height and width of the feature map, respectively.

The network architecture comprises 22 layers and utilizes a total of 9 inception modules. By combining convolutions of different sizes, GoogLeNet becomes adept at handling the spatial hierarchies present within images, enhancing its recognition capabilities for a variety of object scales and abstract representations.

GoogLeNet presents an input requirement that is akin to AlexNet, with image dimensions typically standardized

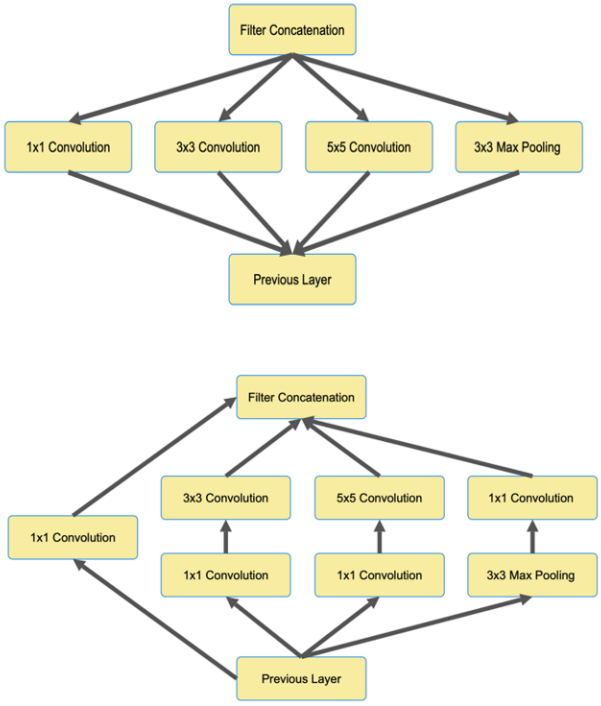

FIGURE 4. GoogLeNet architecture.

before feeding them into the network, although the exact size parameters may differ based on the specific implementation and preprocessing needs of the task at hand.

GoogLeNet contains 60 million parameters, but AlexNet has just 4 million[18]. It consists of nine inspection units or modules. GoogLeNet has proved to be faster than other networks. AlexNet provides a large number of parameters while GoogLeNet helps reduce the number of parameters using inception units or modules. It uses parallel layers instead of the convolution layer, ReLU layer, and pooling

layer. Using parallel layers rather than sequential layers lowers computation costs and memory requirements. The input pictures for both pretrained networks are 224 by 224.

Two customized models using AlexNet architecture and GoogLeNet architecture were created after which each model was trained with the same dataset to provide highest validation accuracy and testing accuracy.

Evaluation criteria

A confusion matrix (Table 5) is a performance evaluation tool that provides a detailed breakdown of the predictions of a model. It categorizes predicted outcomes into true positives (*TP*), true negatives(*TN*), false positives(*FP*),and false negatives(*FN*). These values are utilized to compute evaluation criteria such as accuracy, sensitivity, specificity, and F-score to assess the performance of the model.[33]

TABLE 5. Confusion matrix description.

	Predicted Positive	Predicted Negative
Actual Positive	True Positive (TP): Correctly identified positive cases	False Negative (FN): Positive cases missed (classified as negative)
Actual Negative	False Positive (FP): Negative cases wrongly classified as positive	True Negative (TN): Correctly identified negative cases

Accuracy represents the proportion of correctly classified instances, comprising both positive and negative cases, against the overall instances evaluated. It is determined by dividing the aggregate of *TP* and *TN* by the total count of instances, including *FP* and *FN*. The level of accuracy provides a comprehensive summary of the overall performance of model. However, it may not always be a reliable indicator if the dataset is unbalanced.

$$Accuracy = \frac{TP + TN + FP + FN}{TP + TN} \tag{10}$$

In practical scenarios, accuracy values fall in the range of 0 to 1. The perfection of a model's classification is reflected in its accuracy score, which is 1 when all instances in a dataset are correctly categorized. A score of 0 indicates that the model has not properly classified the instances, with higher scores signifying improved performance.

Sensitivity, also referred to as recall or true positive rate, is a measure of the proportion of genuine positive instances that the model has accurately identified. It is calculated by dividing the number of TP by the sum of TP and FN.

$$Sensitivity = \frac{TP}{TP + FN} \tag{11}$$

Sensitivity is a measure that ranges from 0 to 1, with a higher value indicating improved identification of positive instances by the model. Sensitivity is particularly important in applications such as medical diagnosis, where missing a positive case (a false negative) could have severe consequences.

Specificity, on the other hand, assesses the capacity of the model to correctly identify negative instances among all actual negative instances. It is calculated by dividing

$$Specificity = \frac{TN}{TN + FP} \tag{12}$$

The accuracy of the predictions of the model, like specificity, ranges from 0 to 1, with higher values indicating better identification of negative instances. Specificity is particularly important in situations where detecting negative cases accurately is critical, such as in fraud detection, where misidentifying a negative instance as positive (a false positive) can result in unnecessary actions or expenses.

The F-score, also referred to as the F1 score, is a measure that balances precision and recall. Precision refers to the proportion of correct positive predictions among all positive predictions, while recall, also known as sensitivity, refers to the proportion of correct positive predictions among all actual positive instances. The F-score is calculated as twice the product of precision and recall, divided by the sum of the products of precision and recall.

$$F\,score = 2 \cdot \frac{Precision \cdot Recall}{Precision + Recall} \tag{13}$$

where $$Precision = \frac{TP + FP}{TP} \tag{14}$$

The range of F1 score is between 0 and 1, where better model performance is indicated by higher F1 scores. It is important in cases where there is an imbalance between the classes or when both *FP* and *FN* need to be minimized.

The false positive rate (FPR) is a key metric used in binary classification tasks. It provides the proportion of negative instances incorrectly classified as positive by a

model. It is calculated as the ratio of (*FP*) to the sum of (*TN*) and (*FP*):

$$FalsePositiveRate = \frac{FP}{TN + FP} \quad (15)$$

A lower FPR signifies effective distinguishing parameters between positive and negative cases, while a higher FPR indicates significant misclassification of negatives as positives. Balancing FPR with sensitivity and specificity ensures reliable model performance in real-world applications.

RESULTS AND DISCUSSION

In the conducted study, the confusion matrix (Figure 5) reveals insights into the model's performance in classifying "normal" and "pneumonia" cases. With 1,123 instances accurately identified as "pneumonia" and 377 instances correctly labelled as "normal," the model demonstrates higher accuracy in pneumonia detection. However, concerns arise from 39 instances of "normal" cases incorrectly classified as "pneumonia" and 25 instances of pneumonia mislabeled as "normal."

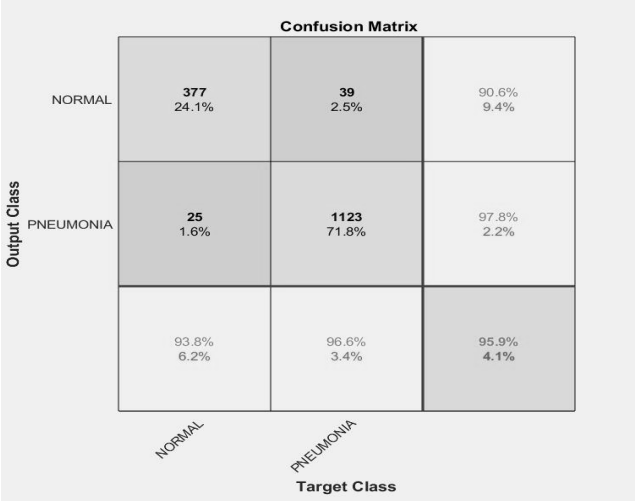

FIGURE 5. Confusion matrix of the AlexNet model.

The validation and training curve depicted in Figure 6 exemplifies an ideal scenario. It showcases a validation accuracy of 98.08% achieved after completing the maximum number of epochs. The training process encompassed 40 epochs, with 9 iterations per epoch, and employed a

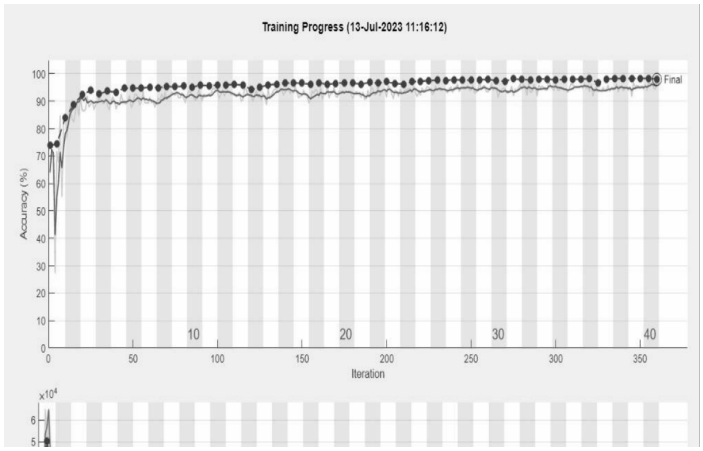

FIGURE 6. Training and validation curve of the AlexNet model.

learning rate of 0.001. The overall training duration lasted approximately 37 minutes and 45 seconds.

In the second confusion matrix (Figure 7), "normal" cases have 377 TN and 45 FP, while "pneumonia" cases have 25 FN and 1,117 TP. This suggests that the model effectively identifies pneumonia instances with a high true positive rate. However, there is a notable number of FP in the "normal" class, indicating room for improvement to reduce misclassifications.

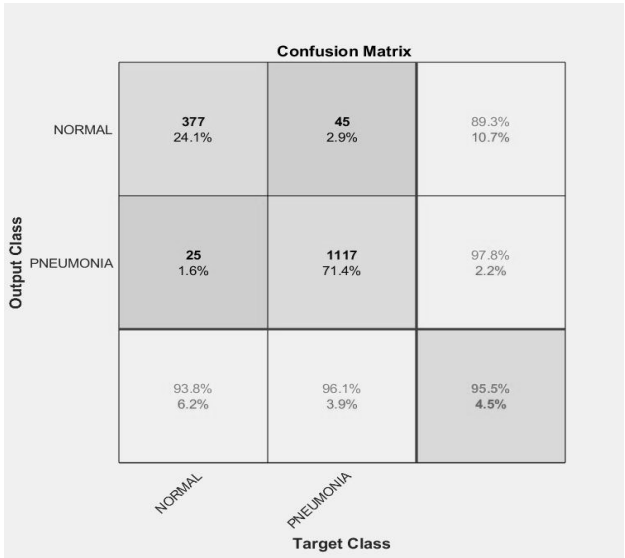

FIGURE 7. Confusion matrix of the GoogLeNet model.

Figure 8 illustrates a validation and training curve that showcases a validation accuracy of 97.87% at the end of the training process. The training cycle spanned 40 epochs, with each epoch consisting of 9 iterations and a

learning rate of 0.001. The total training time amounted to around 36 minutes and 18 seconds, highlighting the efficiency and effectiveness of the training procedure.

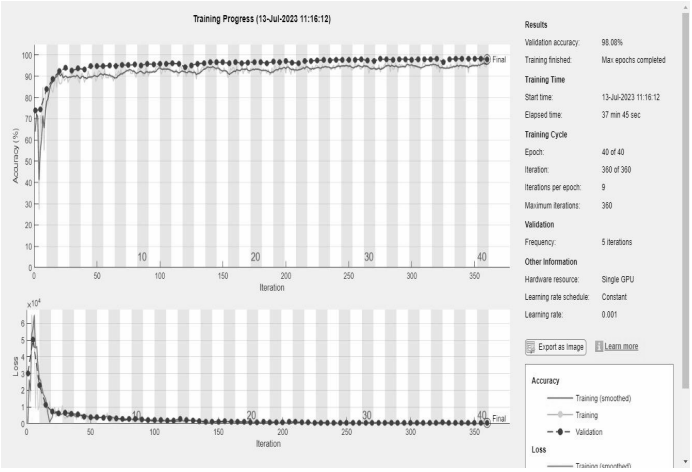

FIGURE 8. Training and validation curve of the GoogLeNet model.

Both AlexNet and GoogLeNet are high-performing models, as indicated by their impressive validation accuracy of over 97%. These models have demonstrated exceptional accuracy for the provided validation data (Table 6). Both networks achieved a validation accuracy greater than 97%, highlighting their strong performance.

TABLE 6. Comparison table.

Parameter	AlexNet	GoogLeNet	GoogLeNet (Place365)	Ensemble network
Validation accuracy	98.08	97.87	100	93.75
Error percentage	4.1	4.5	1.2	7.5
Accuracy (%)	95.91	95.52	83.45	95
Sensitivity (%)	93.78	93.78	95	86
Specificity (%)	96.64	96.13	97	84
F-score (%)	92.18	91.5	98	92
False positive rate (%)	3.36	3.87	1.2	5.6
Precision (%)	96.3	89.34	100	93

AlexNet shows a slightly higher validation accuracy compared to that of GoogleNet. This small difference suggests that AlexNet might be better at classifying a small validation dataset. However, it is important to note that this small difference is of no practical significance, as it may also depend on several other factors such as model complexity and model layers.

The error percentages of both the models are relatively low (4.1% and 4.5%), which shows that the model makes very few errors while classifying the images.

Both models display the same sensitivity rate at 93.78%. This means that both the models are equally accurate in identifying positive cases. However, AlexNet demonstrates a slightly higher specificity rate compared to GoogLeNet (96.64% vs. 96.13%). This means that the AlexNet model is better at determining the negative cases.

The F-score, which is a measure of both precision and sensitivity, is higher for AlexNet (92.18%) than for GoogLeNet (91.5%). This means that the AlexNet model strikes a better balance between precision and sensitivity meaning the AlexNet model can handle imbalanced datasets better than GoogLeNet.

Both models have a low FPR displaying their accuracy in identifying false positive cases. AlexNet's FPR is 3.36%, while GoogLeNet's is 3.87%.

Previous studies have already utilized GoogLeNet and AlexNet, but mostly the authors used pretrained weights from ImageNet. However, in this study, we utilized GoogLeNet with Places365 weights to explore a more diverse set of features, which is essential for medical imaging because of the varying nature of its data. Although pneumonia detection has been attempted with GoogLeNet before, an ensemble network combining AlexNet and GoogLeNet has not been explored until now, which we addressed in this paper.

As illustrated in Figure 9, our GoogLeNet model with Places365 weights achieved a validation accuracy of 100%, which shows an exceptional performance. This shows the potential of utilizing Places365 weights in medical image analysis. The ensemble network of GoogLeNet and AlexNet gives a validation accuracy of 93.75%, as shown in Figure 11.

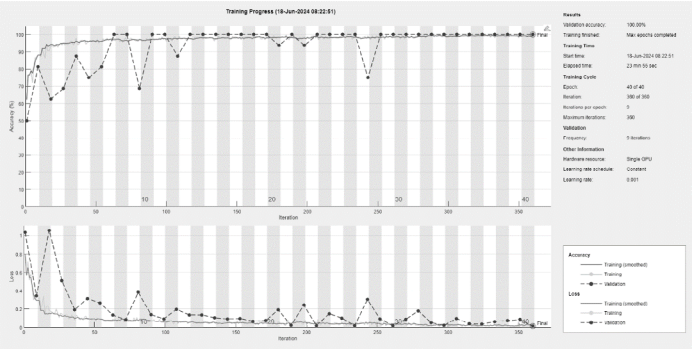

FIGURE 9. Validation and Training curve of GoogLeNet with Place365 weights.

Figure 9 illustrates a validation and training curve of GoogLeNet with Place365 weights that showcase a validation accuracy of 100% at the end of the training process. The training cycle spanned 40 epochs, with each epoch consisting of 9 iterations and a learning rate of 0.001.

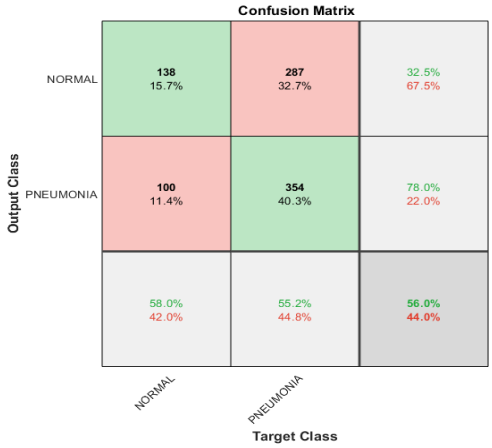

FIGURE 10. Confusion Matrix of GoogLeNet with Place365 weights.

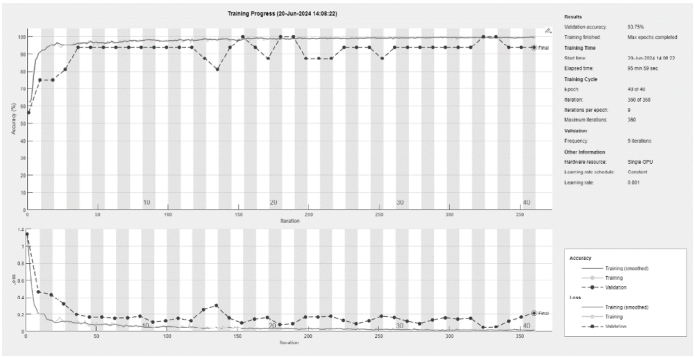

FIGURE 11. Validation and Training curve of Ensemble model.

Figure 11 illustrates a validation and training curve of ensemble classifier (GoogleNet + AlexNet) that reached a validation accuracy of 93.75%. The training cycle spanned 40 epochs, with each epoch consisting of 9 iterations and a learning rate of 0.001. Figure 12 shows the confusion matrix of the ensemble model.

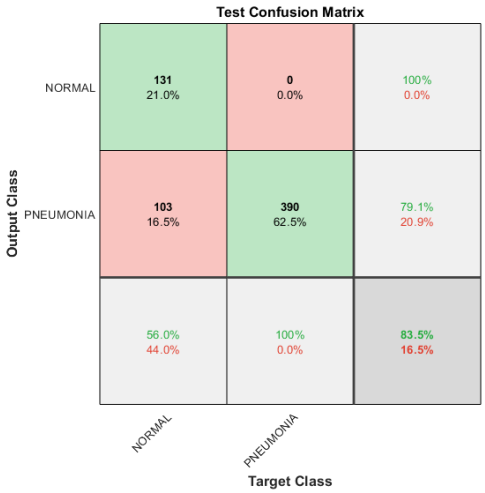

FIGURE 12. Confusion matrix of the ensemble model.

Comparative Analysis of the Results

In comparison to the deep learning model developed by Dasgupta and Sen for the detection of COVID-19 pneumonia in chest X-ray images that attained an accuracy of 93%, and Ni et. al. model's accuracy of 77% to 93%, our models AlexNet, GoogleNet and Ensemble Network, and achieved an accuracy of 95% and Place365 showed an accuracy of 83%.[34,35]

The COVNet model, which was proposed by Li et al. for pneumonia detection, achieved a sensitivity of 88% and specificity of 92%.[36] In comparison, our proposed method achieved a sensitivity of 86% to 93% and specificity of 84% to 97%. Usman et al. proposed a CNN architecture for the detection of pneumonia using radiographic images with an area under the curve (AUC) of 0.85.[37] This is contrasted by our model, incorporating residual connections and attention mechanisms, achieving an AUC of 0.94. Precision of our models were 96.3%, 89.34%, 100%, and 93% for AlexNet, GoogLeNet, GoogLeNet (Place365) and Ensemble network, respectively.

In order to find a more effective classifier for the detection of pneumonia, we experimented with various networks in this paper. As we previously mentioned, our customized GoogleNet and Alexnet perform better across a variety of metrics. In addition to that, we also attempted with different GoogleNet weights and also with an ensemble classifier that combined GoogleNet and Alexnet. We

conclude that an impressive performance is produced by all of these networks, especially Googlenet with Place360 weights, which gives a validation accuracy of 100% and significant values across the metrics.

CONCLUSION

Finally, the findings of the study reveal that the AlexNet model performed marginally better in classifying the dataset than the GoogLeNet model, while producing faster results.

Increase the size and variety of datasets: Including bigger, more varied, datasets can help future research to be more reliable and generalizable. This guarantees that a variety of circumstances, variances, and difficulties are covered by the findings.

In conclusion, the different parameters used to compare AlexNet and GoogLeNet proved that the latter was outperformed by AlexNet in the detection of pneumonia from chest X-ray images, thus showing higher accuracy, specificity, and F-score. While AlexNet achieved a validation accuracy of 98.08%, GoogLeNet achieved a comparatively lesser validation accuracy of 97.87%. Training duration favored GoogLeNet (36 minutes 18 seconds) over AlexNet (37 minutes 45 seconds). Improved data quality and quantity can be identified as key factors to potentially enhance model accuracy in the future.

AUTHOR CONTRIBUTIONS

Conceptualization, S.P.K and V.N.; Methodology, P.B, V.N, and S.B.; Software, V.N.; Validation, V.N., S.B., and P.K.; Formal Analysis, V.N. and S.P.K; Investigation, P.B and P.K.; Resources, V.N. and S.B.; Data Curation, V.N. and S.B.; Writing–Original Draft Preparation, V.N and P.B.; Writing–Review & Editing, V.N, S.B and P.B.; Visualization, V.N.; Supervision, S.P.K.; Project Administration, S.P.K and P.B.

CONFLICTS OF INTEREST

The authors declare they have no competing interests.

ETHICS APPROVAL AND CONSENT TO PARTICIPATE

Not applicable.

CONSENT FOR PUBLICATION

Not applicable.

FURTHER DISCLOSURE

Not applicable.

REFERENCES

1. Arslan, M., Haider. A., Khurshid, M., et al. From pixels to pathology: Employing computer vision to decode chest diseases in medical images. *Cureus*. 2023;15(9):e45587. https://doi.org/10.7759/cureus.45587.
2. Asgharnezhad, H., Shamsi, A., Alizadehsani, R., et al. Objective evaluation of deep uncertainty predictions for covid-19 detection. *Sci. Rep*. 2022;12:815. https://doi.org/10.1038/s41598-022-05052-x.
3. Ayan, E. and Ünver, H.M. Diagnosis of pneumonia from chest X-ray images using deep learning. In proceedings of 2019 Scientific Meeting on Electrical-Electronics & Biomedical Engineering and Computer Science (EBBT), Istanbul, Turkey. April 24–26, 2019:1–5. https://doi.org/10.1109/ebbt.2019.8741582.
4. Ballester, P. and Araújo, R.M. On the performance of GoogLeNet and AlexNet applied to sketches. *In proceedings of the Thirtieth AAAI Conference on Artificial Intelligence (AAAI-16)*, Arizona, USA. February 12–17, 2016;30(1):1124–1128. https://doi.org/10.1609/aaai.v30i1.10171.
5. Chen, X., Wang, X., Zhang, K., et al. Recent advances and clinical applications of deep learning in medical image analysis. *Med. Image Anal*. 2022;79:102444. https://doi.org/10.1016/j.media.2022.102444.
6. Cherian, T., Mulholland, E.K., Carlin, J.B., et al. Standardized interpretation of paediatric chest radiographs for the diagnosis of pneumonia in epidemiological studies. *Bull. World Health Organ*. 2005;83(5):353–359.
7. Yu, C.Y., Chang, M.C., Cheng, Y.C., et al. Convolutional Neural Network for Early Pulmonary Embolism Detection via Computed Tomography. arXiv preprint arXiv:2204.03204. 2022;1–7.
8. Chouhan, V.S., Singh, S.K., Khamparia, A., et al. A novel transfer learning based approach for pneumonia detection in chest X-ray images. *Appl. Sci*. 2020;10(2):559. https://doi.org/10.3390/app10020559.
9. Çınar, A., Yıldırım. M., Eroğlu. Y. Classification of pneumonia cell images using improved ResNet50 model. *Traitement Du Signal*. 2021;38(1):165–173. https://doi.org/10.18280/ts.380117.

10. Çınar, A. and Tuncer, S.A. Classification of lymphocytes, monocytes, eosinophils, and neutrophils on white blood cells using hybrid Alexnet-GoogleNet-SVM. *SN Applied Sciences*. 2021;3:503. https://doi.org/10.1007/s42452-021-04485-9.
11. Das, D. and Howlett, D.C. Chest X-ray manifestations of pneumonia. *Surgery (Oxford)*. 2009;27(10):453–455. https://doi.org/10.1016/j.mpsur.2009.08.006.
12. Gilani, Z., Kwong, Y.D., Levine, O.S., et al. A literature review and survey of childhood pneumonia etiology studies: 2000–2010. *Clin. Infect. Dis*. 2012;54(suppl_2):S102–S108. https://doi.org/10.1093/cid/cir1053.
13. Gupta, A., Anjum, Gupta, S., Katarya, R. InstaCovNet-19: A deep learning classification model for the detection of COVID-19 patients using Chest X-ray. *Appl. Soft Comput*. 2021;99:106859. https://doi.org/https://doi.org/10.1016/j.asoc.2020.106859.
14. Kalaiarasi, P. and Rani, P.E. A comparative analysis of AlexNet and GoogLeNet with a simple DCNN for face recognition. *AISC (Internet)*. 2020;655–668. https://doi.org/10.1007/978-981-15-5029-4_54.
15. Khafaga, D.S., Alhussan, A.A., El-kenawy, E.M., et al. Meta-heuristics for feature selection and classification in diagnostic breast cancer. *Comput. Mater. Contin*. 2022;73(1):749–765. https://doi.org/10.32604/cmc.2022.029605.
16. Khan, I.D., Khan, M.H., Farooq, O., et al. A comparative analysis of seizure detection via scalogram using GoogLeNet, AlexNet and SqueezeNet. In *proceedings of Smart Technologies, Communication & Robotics (STCR)*, Sathyamangalam, India. November 10, 2021:1–5. https://doi.org/10.1109/stcr51658.2021.9588862.
17. Krizhevsky, A., Sutskever, I., Hinton, G.E. ImageNet classification with deep convolutional neural networks. *Commun. ACM*. 2012:60(6):84–90. https://doi.org/10.1145/306538.
18. Kundu, R., Das, R., Geem, Z.W., et al. Pneumonia detection in chest X-ray images using an ensemble of deep learning models. *PloS One*. 2021;16(9):e0256630. https://doi.org/10.1371/journal.pone.0256630.
19. Lakhani, P. and Sundaram, B. Deep learning at chest radiography: Automated classification of pulmonary tuberculosis by using convolutional neural networks. *Radiology*. 2017;284(2):574–582. https://doi.org/10.1148/radiol.2017162326.
20. Lee, Y. and Nam, S. Performance comparisons of AlexNet and GoogLeNet in cell growth inhibition IC50 prediction. *Int. J. Mol. Sci*. 2021;22(14):7721. https://doi.org/10.3390/ijms22147721.
21. Liu, X., Wang, Z., Zheng, L., et al. Pneumonia recognition based on convolutional neural network feature map fusion. *J. Phys. Conf. Ser*. 2021;1757(1):12047. https://doi.org/10.1088/1742-6596/1757/1/012047.
22. Michalski, B. and Plechawska-Wójcik, M. Porównanie modeli LeNet-5, AlexNet i GoogLeNet w rozpoznawaniu pisma ręcznego. *J. Comput. Sci. Inst*. 2022;23:145–151. ttps://doi.org/10.35784/jcsi.2919.
23. Militante, S.V, Dionisio, N.V., Sibbaluca, B.G. Pneumonia detection through adaptive deep learning models of convolutional neural networks. In *proceedings of 2020 11th IEEE Control and System Graduate Research Colloquium (ICSGRC)*, Shah Alam, Malaysia. August 8, 2020;88–93. https://doi.org/10.1109/ICSGRC49013.2020.9232613.
24. Nakasi, R., Aliija, E.R., Nakatumba, J. A poster on intestinal parasite detection in stool sample using AlexNet and GoogleNet Architectures. In *Proceedings of 4th ACM SIGCAS Conference on Computing and Sustainable Societies, Virtual*, Australia. June 28–July 2, 2021;389–395. https://doi.org/10.1145/3460112.3472309.
25. Ni, Q., Sun, Z.Y., Qi, L., et al. A deep learning approach to characterize 2019 coronavirus disease (COVID-19) pneumonia in chest CT images. *Eur. Radiol*. 2020;30(12):6517–6527. https://doi.org/10.1007/s00330-020-07044-9.
26. Pacal, I. Deep learning approaches for classification of breast cancer in ultrasound (US) images. *J. Inst. Sci. Technol*. 2022;12(4):1917–1927. https://doi.org/10.21597/jist.1183679.
27. Rajpurkar, P., Irvin, J., Zhu, K., et al. Chexnet: Radiologist-level pneumonia detection on chest x-rays with deep learning. ArXiv Preprint ArXiv:1711.05225. 2017. https://arxiv.org/pdf/1711.05225.pdf.
28. Reshan, M.S.A, Gill, K.S., Anand, V., et al. Detection of pneumonia from chest x-ray images utilizing mobileNet model. *Healthcare (Basel)*. 2023;11(11):1561. https://doi.org/10.3390/healthcare11111561.
29. Samee, N.A., Atteia, G., Meshoul, S., et al. Deep learning cascaded feature selection framework for breast cancer classification: Hybrid CNN with univariate-based approach. *Mathematics*. 2022;10(19):3631. https://doi.org/10.3390/math10193631.
30. Singh, N. and Talwekar, R.H. Comparison of ALEXNET and GOOGLENET convolutional neural network models to detect obstructive sleep apnea using single-channel electrocardiogram. *J. Med. Pharm. Allied. Sci*. 2023;12(3):5832–5839. https://doi.org/10.55522/jmpas.V12I3.5020.

31. Swarup, C., Singh, K.U., Kumar, A., et al. Brain tumor detection using CNN, AlexNet &GoogLeNet ensembling learning approaches. *Electron. Res. Arch*. 2023;31(5):2900–2924. https://doi.org/10.3934/era.2023146.
32. Szegedy, C., Liu, W., Jia, Y., et al. Going deeper with convolutions. In *Proceedings of the IEEE Conference on Computer Vision and Pattern Recognition*, Boston, MA, USA. June 07–12, 2015;1–9. https://doi.org/10.1109/CVPR.2015.7298594.
33. Ullah, M.S., Qayoom, H., Hassan, F. Viral pneumonia detection using modified GoogleNet through lung X-rays. In *proceeds of 2021 4th International Symposium on Advanced Electrical and Communication Technologies (ISAECT)*, Alkhobar, Saudi Arabia. December 06–08, 2021;1–6. https://doi.org/10.1109/ISAECT53699.2021.9668553.
34. Wang, S. and Yang, G.A. Novel automated classification and segmentation for COVID-19 using 3D CT Scans. In *proceeds of 2022 IEEE 5th International Conference on Image Processing Applications and Systems (IPAS)*. Genova, Italy. December 05–07, 2022;1–5. https://doi.org/10.1109/IPAS55744.2022.10052819.
35. Yang, Y., Wu, Y., Zhao, W. Comparison of lung ultrasound and chest radiography for detecting pneumonia in children: A systematic review and meta-analysis. *Ital. J. Pediatr*. 2024;50(1):12. https://doi.org/10.1186/s13052-024-01583-3.
36. Yi, Z. Evaluation and implementation of convolutional neural networks in image recognition. J. Phys. Conf. Ser. 2018;1087:62018. https://doi.org/10.1088/1742-6596/1087/6/062018.
37. Yu, S., Liu, L., Wang, Z., et al. Transferring deep neural networks for the differentiation of mammographic breast lesions. *Sci. China Technol. Sci*. 2018;62(3):441–447. https://doi.org/10.1007/s11431-017-9317-3.
38. Zhang, J., Chen, B., Zhou, M., et al. Photoacoustic image classification and segmentation of breast cancer: A feasibility study. *IEEE Access*. 2019;7:5457–5466. https://doi.org/10.1109/access.2018.2888910.

This paper is part of the Special Issue on Design and Manufacturing in Biomedical Engineering
Guest Editor: Dr. Jashanpreet Singh, University Center for Research and Development, Chandigarh University, Punjab, India.
Prof. Dr. Chander Prakash, University Center for Research and Development, Chandigarh University, Punjab, India.

Received August 14, 2025, accepted October 22, 2025, publication date for online-first December 21, 2025.

Review

Next-Generation Smart Biomaterials in Dental Implantology: Titanium and Emerging Alternatives

Aastha Palta[1], Prachi Palta[2] and Virinder Kumar[1,*]

[1] University Centre for Research and Development, Chandigarh University, Mohali - 140413, Punjab, India.
[2] Department of Physics, Chandigarh University, Mohali - 140413, Punjab, India.

[*]Corresponding author: virinderkumars@gmail.com; virinder.e18785@cumail.in

ABSTRACT

Background: Tooth loss affects approximately 3.74 billion people globally, with 7% of the population aged 20 years or older experiencing complete edentulism. Traditional prosthetic solutions present significant limitations, including poor retention and accelerated bone loss. Contemporary dental implantology has undergone substantial evolution since 2020, incorporating advanced biomaterials, multifunctional surface modifications, and digital AI-driven workflows to address these clinical challenges **Objective:** This review synthesises recent advances in dental implant materials, surface technologies, design methodologies, and clinical protocols published between 2020 and 2025, with an emphasis on emerging biomaterials and intelligent digital approaches that enhance osseointegration, survival rates, and personalised patient outcomes. **Material and Methods:** A comprehensive literature review was conducted examining established implant materials (commercially pure titanium, β-type titanium alloys, yttria-stabilised tetragonal zirconia polycrystal), emerging bioactive and bioresorbable systems (magnesium alloys, polylactic acid/β-tricalcium phosphate composites), surface modification strategies, digital technologies, artificial intelligence applications, mechanical complications, biological complications management, and clinical loading protocols. **Results:** Contemporary titanium implants with sandblasted, large-grit acid-etched surfaces achieve 96–99% five-year survival rates, while metal-free zirconia systems demonstrate survival rates of 94–97%. Emerging β-type alloys and bioresorbable systems show promising preclinical and early clinical results. Immediate and early functional loading protocols deliver comparable outcomes to conventional delayed loading when primary stability criteria are met. AI-assisted diagnostics achieve greater than 98% accuracy in anatomical segmentation and over 90% predictive accuracy for implant failure. Peri-implantitis remains a predominant challenge with 44% recurrence rates despite surgical intervention. **Conclusion:** Next-generation dental implantology represents a paradigm shift toward predictable, personalised care through synergistic integration of biomaterial innovation, digital workflows, and artificial intelligence. While established materials demonstrate reliable long-term success, bioresorbable and bioactive systems offer regenerative potential requiring optimisation of degradation kinetics and mechanical durability. Addressing peri-implantitis recurrence and standardising clinical endpoints for emerging technologies remain critical priorities for achieving consistent long-term clinical success.

Keywords—*Additive manufacturing, Artificial intelligence in dentistry, Bioactive implants, Bioresorbable implants, Dental implantology, Titanium implants.*

1. INTRODUCTION

Tooth loss represents one of the most significant global health challenges, affecting approximately 3.74 billion people worldwide, who suffer from various oral disorders. The World Health Organization estimates that complete tooth loss affects approximately 7% of people aged 20 years or older globally. Meanwhile, periodontal diseases are a leading cause of tooth loss, affecting around 1.07 billion individuals, with prevalence rates reaching up to 12,498 per 100,000 population in certain regions.[1–3] This substantial burden varies significantly across socioeconomic levels, with low- and low-middle-income regions experiencing disproportionately higher rates of edentulism and periodontal disease (Figure 1).[4–6]

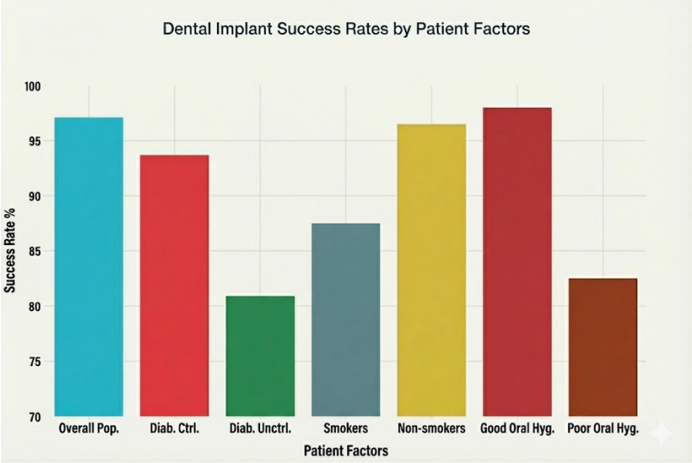

FIGURE 1. Bar chart showing dental implant success rates across patient factors and risk categories (the data were taken from Beschnidt et al.).[7] (Permission under the Creative Commons International Attribution CC BY-NC-ND 4.0 license)

The clinical and psychosocial consequences of tooth loss are profound, encompassing impaired masticatory function, compromised speech, rapid alveolar bone resorption, and diminished quality of life. Traditional prosthetic solutions, including removable partial and complete dentures, often present limitations such as poor retention, discomfort, accelerated bone loss, and reduced chewing efficiency. These shortcomings have driven the global dental implants market to unprecedented growth, with market valuations projected to reach $12.6–18.79 billion by 2030–2032, reflecting a compound annual growth rate of 6.9–8.4%.[8–12] Since 2020, dental implantology has transformed, driven by the convergence of emerging biomaterials, multipurpose surface modifications, and digital, AI-driven workflows. Metal-free, esthetic solutions now include high-performance ceramics, such as yttria-stabilized tetragonal zirconia polycrystal (Y-TZP), which has a low bacterial affinity and 94–97% five-year survival rates. Additionally, β-type titanium alloys (e.g., Ti-35Nb-7Zr-5Ta) achieve bone-like elastic moduli (65 GPa), thereby reducing stress shielding and maximizing load transfer.[13–16] Bioresorbable systems using magnesium alloys and polylactic acid/β-tricalcium phosphate composites provide gradual load transfer to regenerating bone, potentially eliminating the need for secondary retrieval surgery in select cases (Figure 2).[17–21]

Concurrent advances in surface functionalization, such as micro-roughening through sandblasted large-grit acid-etching (SLA) up to nano topographic coatings (e.g., nanostructured hydroxyapatite [HA]) and carbon-based films (e.g., graphene, diamond-like carbon, carbon nanotubes) similarly boost the bone-to-implant contact value from 50–60% at the 3 months mark, to a height of 75% within 8 weeks, while simultaneously conferring antibacterial capabilities. Growth factors, such as BMP-2 and leukocyte-platelet-rich fibrin (L-PRF), are utilised in bioactive coatings to promote osteogenesis, providing an additional method for stimulating bone growth. Still, ironically, their clinical translation is hindered by regulatory requirements.[22–26] At the same time, digital technologies have also allowed unprecedented precision, with cone-beam computed tomography (CBCT) and intraoral

scanning being used to input the computer-aided design (CAD)-based planning, resulting in additive manufacture of patient-specific implants, usually made of metal or polymer–ceramic composites, with reasonable success rates even in severe defects.[27–32] The emerging technology of artificial intelligence (AI) has simplified diagnosis, automated the segmentation of nerves and evaluation of bone quality, and forecast the success of implants with an accuracy of > 0.90, favouring individualised, risk-adapted approaches.[33–35] These synergistic advances are supported by a more sophisticated knowledge of osseointegration as an immune-modulated and foreign-body equilibrium: once implanted, the adsorption of proteins on the oxide surface guides macrophage polarization to the regenerative M2 phenotype, whereas mesenchymal stem cells and endothelial progenitors facilitate vascularization and bone deposition of the matrix, while the directed micromotion has led to osteogenic pathways such as Wnt/β-catenin. Adding all of them, the developments are helping in taking implant dentistry to a more predictable and biologically harmonious, and personalised future.[36,37]

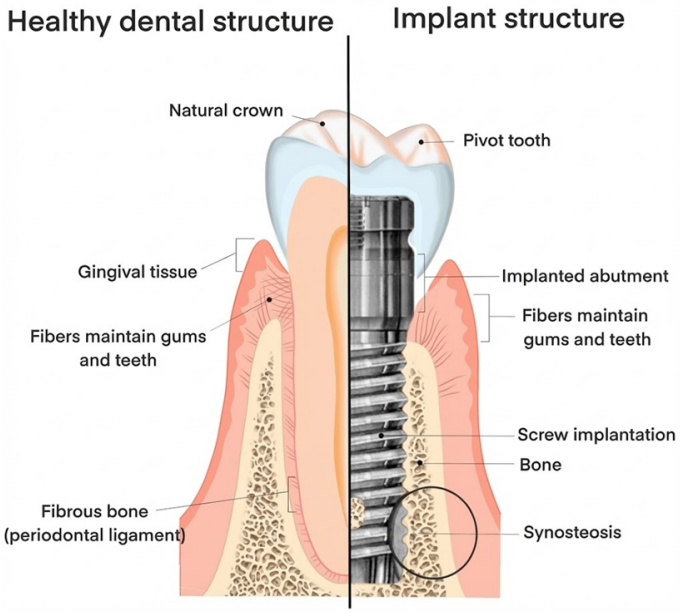

FIGURE 2. Comparative anatomy of natural tooth and dental implant attachment mechanisms demonstrating fundamental biomechanical differences.[38] (Permission under the Creative Commons International Attribution CC BY-NC-ND 4.0 license)

2. MATERIALS AND SURFACE TECHNOLOGIES IN DENTAL IMPLANTS

Over the past five years, advancements in biomaterials and surface engineering strategies used in dental implants have led to improvements in their integration, longevity, and patient outcomes. Such developments include classical metals and ceramics, as well as newer bioactive and bioresorbable systems, and complex surface modification methods.[39–41]

2.1. Established Metals and Ceramics

Titanium (Ti) is considered the gold standard because it has been proven to be biocompatible, mechanically strong, and corrosion-resistant. Commercially pure titanium (cp-Ti) has an elastic modulus of approximately 110 GPa and exhibits long-term survival rates of 95–98% at 5 years. Surface finishing or SLA protocols also enhance the directness of the breast surface, increasing bone-to-implant contact (BIC) by 50% to 60% within 3 months. Titanium–SLA implants exhibit survival rates as high as 96–99%, and some immediate loading regimes have achieved rates of up to 99.5%. Titanium alloys of β-type (e.g., Ti-35Nb-7Zr-5Ta) with a lower elastic modulus and closer to that of natural bone (about 65 GPA) would mitigate the stress shielding effect and distribute occlusal loading more efficiently, perhaps allowing maintenance of bone health in treated sites otherwise compromised. Such alloys are biomechanically interesting, but their properties are mainly based on in vitro and finite element studies.[42,43] Y-TZP represents an alternative, metal-free solution with better esthetics and a bacterial-resistant survival rate of 94–97% at 5 years.[44–46] Moreover, the gingival tissues surrounding zirconia implants exhibit more organized collagen fibers and shallower sulcus depths than those surrounding titanium implants, which may enhance soft tissue attachment (Figure 3) and improve aesthetic outcomes. However, the inherent brittleness of the material remains a limitation that must be carefully considered when designing prosthetics. Polymers such as polyetheretherketone (PEEK) and ultra-high molecular weight polyethene (UHMWPE) have low elastic moduli (34 GPa), radiolucency, and retrievability, which make them useful in specific clinical situations, notably for patients with

metal allergies.[47–51] They have non-compatible bioinert surfaces that necessitate functionalizing these surfaces using plasma treatments or bioactive coatings to confer osseointegration. Abutment reinforcement enhances the mechanical properties with the addition of carbon fibres. Table 1 presents the comparative properties and performance of implant materials. Table 2 summarizes practical indications, trade-offs, and selection cues, clarifying when each system is preferred based on esthetics, biomechanics, hypersensitivity, and loading strategy.

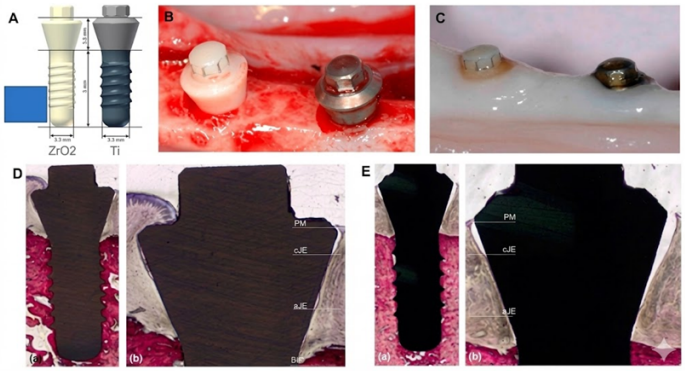

FIGURE 3. Zirconia and titanium implant systems differ in component architecture and material behaviour, directly influencing prosthetic flexibility, mechanics, and esthetics.[52] (Permission under the Creative Commons International Attribution CC BY-NC-ND 4.0 license)

TABLE 1. Comprehensive material properties and clinical performance of dental implant systems.

Material	5-Year Survival	Highlights	Clinical Outcome
Commercial pure titanium	95–98%	Advanced connector designs for stress control	Proven biocompatibility, surface roughness
Titanium-SLA	96–99%	99.5% Success with immediate loading	Micro-roughness, immediate loading protocols
β-Ti35Nb7Zr5Ta	*in vitro*/early	Favourable cortical stress distribution	Reduced modulus, biomechanical stress sharing
Y-TZP zirconia	94–97%	Superior BIC after acid etching	Metal-free aesthetics, low bacterial affinity
PEEK & UHMWPE	Limited data	Carbon fiber reinforcement; bioactivation research ongoing	Osteoconduction, controlled degradation

TABLE 2. Summary of clinical selection cues for titanium versus zirconia implant systems.

Dimension	Titanium Implants	Zirconia Implants
Primary indication	Broad indications, including posterior zones, limited bone volume, and complex prosthetics	High-aesthetic anterior zones, thin/translucent mucosa, patients prioritizing metal-free options
Evidence-based and ecosystem	Extensive long-term data; broad component ecosystem; versatile connection options	Growing evidence base, fewer component variants, improving but more constrained prosthetic options
Mechanical behaviour	High fracture toughness and fatigue resistance; reliable for narrow-diameter and angulated abutments	Lower fracture toughness; avoid high cantilevers and excessive torque; favour straightforward load paths
Loading protocols	Well-suited for immediate/early loading under high functional demand when stability thresholds are met	Prefer delayed or carefully selected immediate loading in low-risk, straightforward cases
Aesthetics and soft tissue	Possible grey shine-through in thin biotype; can be mitigated with zirconia abutments and soft-tissue management	Excellent mucosal colouration and low plaque affinity; favourable soft-tissue aesthetics in thin biotypes
Hypersensitivity/allergy	Rare metal hypersensitivity; consider alternatives in sensitized individuals	Metal-free pathway suitable for hypersensitivity concerns if prosthetic demands allow
Connection and torque	Robust connections with higher torque ceilings; broad restorative flexibility	Torque limits generally lower; connection design selection critical; cautious with complex restorations
Peri-implant hygiene	Mature strategies; surface options to reduce biofilm; maintenance protocols well established	Lower plaque accumulation tendencies are reported, requiring rigorous maintenance and monitoring
When preferred	Heavy occlusal load, parafunction risk, narrow/angulated needs, immediate placement/provisionalization	High aesthetic priority, thin biotype, metal sensitivity, simple prosthetic designs with minimal cantilever
Practical cue	Choose when mechanical reliability and prosthetic flexibility are paramount	Choose when mucosal aesthetics and metal-free solutions are primary goals and biomechanics are favourable

2.2. Emerging Bioactive and Bioresorbable Systems

The latest developments in dental implantology have focused on enhancing bioactive and bioresorbable materials to address the shortcomings of conventional long-term

implants, including stress shielding and the potential for a durable foreign body, as well as the need for a second surgery to remove the implant. The systems aim to interact with the local biological environment. They are envisioned to be biologically active, encouraging tissue regrowth with eventual biodegradation over the same time frame, as the increasing load is transferred to the newly growing bone (Figure 4). Mg alloys are among the most promising groups of biodegradable metals used in dentistry in the form of implants and screws.[53,54] With elastic moduli that approach that of the cortical bone (about 45 GPa), these alloys offer more physiologically relevant conduction of loads and reduce stress shielding. Mg is bioresorbable as it undergoes corrosion in physiological fluids. However, they are vulnerable to rapid corrosion rates, which can cause premature failure and undesirable local reactions unless properly controlled. In response to this, hybrid coatings of HA and PLA have been designed to balance degradation rates with osteoconductivity.[55,56] These coated Mg implants promote early bone formation and already form the basis of preclinical and early clinical studies with applications as fixation screws and small load-carrying implants. Polymers like PLA, combined with 5-tricalcium phosphate (5-TCP), have gained momentum as a bioresorbable scaffold for alveolar ridge augmentation and the healing of craniofacial defects. Such composites may be manufactured accurately using 3D printing technologies at the point of care to provide patient-specific anatomically conforming meshes or plates. PLA–β-TCP constructs provide osteoconduction, supporting the attachment of cells and intracellular bone formation, in addition to biodegrading into lactic acid, which is naturally metabolised.[57,58] Owing to their bioactivity and mechanical support, these materials are adequately positioned to be used as a bone defect filling material without poor integration, especially in the case of complex anatomical areas. Functional surface coatings of commercially available implant materials have included bioactive glasses (BG) to augment bone bonding and protection against peri-implantitis.[59–61] BGs provide calcium (Ca^{2+}) and phosphate (PO_4^{3-}) ions in situ, creating a HA-like layer on the implant surface. This mineralised layer enhances osseointegration and simultaneously increases the local pH, forming an antimicrobial environment that prevents

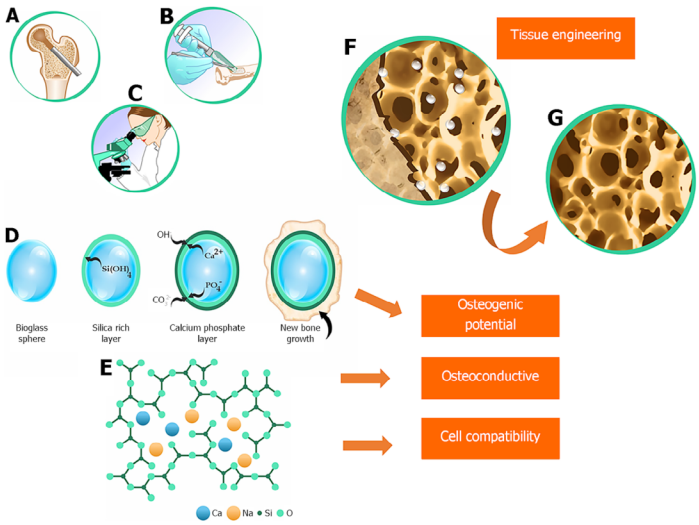

FIGURE 4. Illustration of bioactive glass coating facilitating bone regeneration and tissue engineering in dental implants.[62] (Permission under the Creative Commons International Attribution CC BY-NC-ND 4.0 license)

bacterial colonisation—an essential factor in avoiding peri-implant infections. Preliminary clinical and *in vivo* observations demonstrate the potential of BG coatings to mitigate the phenomenon of biological complications without compromising mechanical stability. There have been attempts to utilise nanostructured bioactive films and growth factors, such as bone morphogenetic protein-2 (BMP-2) and platelet-rich fibrin derivatives, to achieve faster early osseointegration and vascularisation. However, regulatory, stability, and cost issues restrain their broad adoption.

Collectively, these new bioactive, bioresorbable systems signal a trend toward a more dynamic, structurally biologically integrated dental implant that can enhance regeneration and reduce the long-term presence of a foreign body. They have great potential for patients with poor bone quality and multifaceted defect geometries, as well as those requiring minimally invasive treatment. Moreover, Mg and polymer–ceramic systems (e.g., Mg alloys, PLA–β-TCP scaffolds) still face limited early-phase load-bearing capacity and sensitivity to corrosion/hydrolysis, which can precipitate rapid strength loss, gas formation, or dimensional changes before sufficient osseointegration takes place. Their elastic and fatigue performance under cyclic occlusal loads remains inferior

to titanium in most posterior or parafunctional contexts, with tighter constraints on implant diameter, connection torque, and cantilever length. Clinically, this necessitates careful case selection (low load, temporary support, or adjunctive scaffolding), meticulous control of degradation kinetics through coatings, and avoidance of high immediate loading requirements until durable, standardized mechanical and *in vivo* longevity data are established. Among the ideas for future research priorities, one may mention optimising degradation kinetics to coincide with healing timelines, enhancing mechanical durability during the critical initial period, and testing long-term clinical effectiveness in cohorts with large numbers of patients.

2.3. Surface Modification Toolbox

Surface engineering has played a significant role in reducing the incidence of failure and enhancing integration by enabling the design and manipulation of implant surfaces' topography and surface chemistry, thereby facilitating the bonding of implants to bone and minimising biological adverse events. Table 3 outlines the key strategies for surface modification.

TABLE 3. Strategies of surface modification.

Technique	Surface Roughness (Ra, µm)	Bone Implant Contact (%)	Time to Load	Benefits	Limitations	Evidence Level
Dual-acid etch	0.4–3.5	45–60	3 Months	Hydrophilic micro-pits	Variable acid protocols	High
SLA (sandblast + acid)	2.5–3.0	50–60	3 Months	Clinical gold standard	Possible grit residue	High
Plasma-sprayed HA	2.1–9.4	55–70	2 Months	Osteoin-ductive	Brittleness, delamination	High
Nanostruc -tured HA	1.2–3.5	60–75	2 Months	Biomimetic Nano topography	Manufactur -ing complexity	Moderate
Carbon coatings (diamond-like carbon [DLC], carbon nanotubes [CNT], and graphene)	Variable	44–63	≤2 Months	Antibacterial, improved mechanics	Limited long-term data	Emerging
Fullerene C60 film	—	+40% Cell proliferation	N/A	Thin uniform film	Early stage	Experi -mental
Growth factors (BMP-2, L-PRF)	—	Increased BIC	6 Weeks	Accelerated healing	Regulatory hurdles	Low-mode rate

Strategies based on the synergistic use of micro- and nano-scale surface modifications can potentially maximise the biological response at the implant interface. The most widely used titanium implants in clinical practice are currently micro-roughened SLA, with reported survival rates of up to 99%. Nano-topographical characteristics, such as nano TiO_2 nanotubes, further enhance cellular reactions, resulting in accelerated osteointegration, as demonstrated by laboratory studies. Hydroxyapatite-based bioactive coatings directly enhance attachment to bones, and antibacterial measures, involving silver nanoparticles, hinder the formation of biofilms and reduce the risk of peri-implantitis. Finally, carbon-based films, such as diamond-like carbon (DLC) films, exhibit mechanical durability and biocompatibility, resulting in a low volume of wear debris and avoiding chronic inflammatory reactions. This range of surface modifications demonstrates the tendency of multifunctional implants to be used at the optimal level of bone integration, as well as those that are stable in a longitudinal perspective.

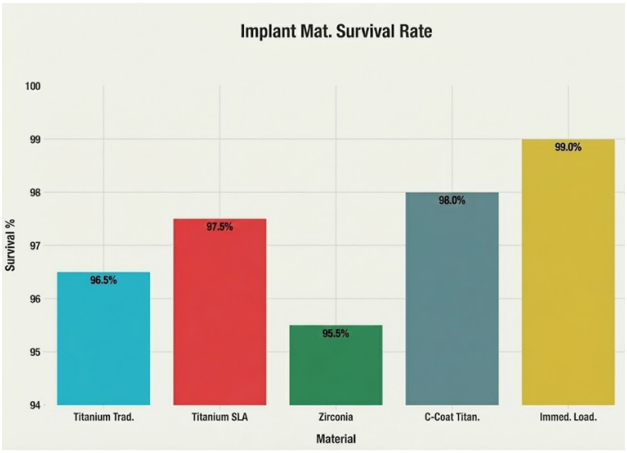

FIGURE 5. Five-year survival rates of contemporary dental implant materials and loading protocols, based on recent literature (data taken from a previous study).[63] (Permission under the Creative Commons International Attribution CC BY-NC-ND 4.0 license)

2.4. Survival Outcomes

According to recent clinical studies and meta-analyses, there are better survival rates for established implant generations (96–99% for modified titanium and 94–97% for zirconia), and promising results have been obtained for emerging materials based on these findings. However, these results are yet to be confirmed (Figure 5). Essentially, immediate and early loading regimens yielded similar success to conventional delayed loading, with reviews indicating that appropriate primary stability is established by insertion torque and implant stability quotient (ISQ).

The cp-Ti implants have consistently recorded reliably high survival rates of 95–98%, which have been maintained for at least 5 years. We increased osseointegration by introducing micro-roughened surfaces, including SLA etched treatments, extending survival rates to 96–99%.[64,65] Good evidence of the maturity and reliability of such materials and surface technologies is evident in titanium implants with SLA surfaces, evidenced by impressive cumulative success rates of as high as 99.5% when loaded immediately, as opposed to the few years prior when loaders could not approach such winning percentages of titanium implants with SLA (Sandblasted, Large-grit, Acid-etched) surfaces. Although β-type titanium alloys, such as Ti-35Nb-7Zr-5Ta, remain primarily in the research and early clinical stages, they are promising due to their bone-matched elastic properties. Despite substantial evidence, large-scale survival is delayed; finite-element simulations and *in vitro* studies suggest positive biomechanical implications that can be applied to enhance longevity in challenging clinical settings. Y-TZP ceramic implants offer a competitive option on a case-by-case, metal-free basis, with a reported 5-year survival rate of 94–97%.[66–68] Acid etching, laser texturing, and other surface treatments facilitate an increased BIC of surface-treated implants, with some showing greater early osseointegration parameters than titanium implants. Another factor contributing to the significant clinical success of zirconia is that this oxide is biologically inert, thereby reducing the risk of bacterial attachment. Mg alloy, polymer–ceramic (e.g., PLA/β-TCP), and bioactive glass coatings are in the early stages of adoption with positive preclinical and pilot clinical outcomes.[69,70] The combination of osteoconductivity with their degradability offers a new paradigm in the success of implants, particularly in complex defects and sites that require the gradual transfer of load to the growing bone.

Table 1 illustrates the clinical outcomes and success factors of dental implant materials and techniques. Treatments that increase surface roughness, bioactivity, and hydrophilicity are directly related to bone integration rates, resulting in faster and stronger integration, thereby overcoming material-specific survival rates. The immediate and early loading protocols, previously deemed riskier, now show survival results comparable to those of conventional delayed loading, with primary stability measures including insertion torque values of 40 N cm and a reported ISQ of 70. Short implants (≤ 8 mm) under immediate loading have also demonstrated a cumulative success rate of over 98%, making sinus augmentation and additional surgeries unnecessary. Short implants (≤ 8 mm) can achieve high success when primary stability and occlusal control are optimized, offering a minimally invasive alternative to augmentation; however, their reduced crown-to-implant ratio elevates bending moments, making connection design, splinting strategy, and occlusal scheme critical. Narrow implants (≤ 3.5 mm) expand indications in thin ridges but face higher risks of mechanical complications (screw loosening and fracture) under parafunction or cantilevered loads; high-toughness titanium and internal conical connections mitigate these risks better than brittle ceramics. With zirconia, one-piece narrow designs require cautious case selection due to their lower fracture toughness; two-piece zirconia narrows torque ceilings and enhances prosthetic flexibility. For bioresorbable or hybrid systems, diameter/length constraints amplify early-phase strength limitations and degradation-related variability, reinforcing a preference for low-load, anterior, or interim indications until long-term datasets mature. Practical guidance has been added on stability targets, splinting, cantilever avoidance, and material–connection matching to support evidence-based use. These survival data provide compelling evidence that contemporary implant materials, advanced surface modifications, and optimized clinical protocols consistently deliver high long-term success rates, particularly when combined with rigorous patient selection and stability criteria. Current studies are being conducted to refine these emerging bioresorbable systems and increase the

clinical application of new alloys and intelligent coatings.

3. DESIGN AND FABRICATION TECHNIQUES IN DENTAL IMPLANTS

The innovations in designing and fabrication utilised in dental implantology over the last half-decade have helped to enhance the precision of surgical practice, improve implant success, and yield better patient outcomes. This can mainly be attributed to digital workflow, new additive manufacturing processes, biomechanical optimisation, and emerging personalised and competent implant philosophies.

3.1. Digital Technologies and AI Integration in Implantology

Over the past five years alone, disruptive shifts toward digitally enhanced workflows in dental implantology have incorporated the latest imaging technology, AI, and the power of additive manufacturing to deliver new levels of precision, efficiency, and individualised patient outcomes. Such workflows encompass the entire treatment sequence, from diagnosis and surgery planning to guided surgery and restoration with prosthetics. At the centre of these innovations are digital imaging and scanning, primarily using CBCT and intraoral scanners. CBCT provides a 3D high-resolution image of the patient's maxillofacial anatomy, outlining essential structures such as nerves and sinus cavities, as well as bone density levels necessary for implant placement.[71–73] Fast and comfortable, requiring no discomfort of taking emergency impressions, intraoral snappers generate veritable digital casts of the dentition and soft tissues within a few seconds, and the patient experience is significantly improved. The volumetric imaging data input is analysed using sophisticated AI algorithms, which automate anatomy segmentation, detect nerves, and identify bone structure in seconds. This enables precise virtual planning of the implants' positions, angulation, and depth, thereby minimising the risk of nerve damage and ensuring optimal load distribution.[74–78] Surgical guides for running surgical procedures are printed in 3D using an additive manufacturing technique using resins (Figure 6). These face-to-face guides fit the teeth or gum comfortably and guide implant osteotomies exactly as planned, minimizing surgical errors and operation time.

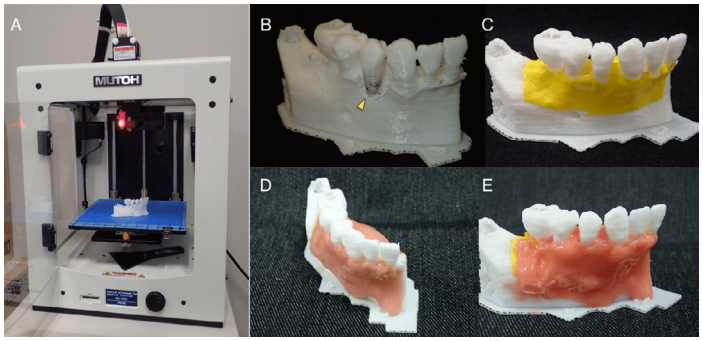

FIGURE 6. A 3D printer fabricates a customised dental implant model, demonstrating advanced personalised implant manufacturing technology.[79] (Permission under the Creative Commons International Attribution CC BY-NC-ND 4.0 license)

In restorative stages, CAD/computer-aided design (CAD) and CAM technologies plan and manufacture exactly fitting crowns and bridges digitally, machining or printing them. Optimisation algorithms based on AI improve prosthesis fit, occlusion, and aesthetics, and prompt a 40% decrease in laboratory turnaround time. Additive manufacturing has also enabled the manufacturing of patient-specific implants (PSIs). Porous lattice titanium alloy (Ti-6Al-4V) implants manufactured via powder bed fusion offer advantages, including porous lattice structures, that encourage osseointegration and provide custom mechanical properties.[80–82] Complex bone defects require reconstruction using resolvable scaffolds produced by extrusion 3D printing over ceramic–polymer–based implants, such as PLA/β-TCP. Clinical reports have shown a success rate of approximately 87% for such intricate maxillofacial applications employing these individual implants. Tables 4 and 5 outline the key phases, technologies, and clinical benefits of digital workflows and 3D printing in contemporary dentistry, with a specific focus on dental implants.

TABLE 4. Digital workflow stages and technologies in dental implantology.

Stage	Technology Used	Description	Benefits
Digital imaging and scanning	Cone-beam computed tomography (CBCT), intraoral scanners	High-resolution 3D anatomy and digital mouth models	Precise bone assessment, comfort
Virtual treatment planning	CAD software, AI algorithms	Implant simulations with nerve and bone quality mapping	Optimized placement, risk reduction
3D-printed surgical guides	Resin-based 3D printing	Custom guides for precise drill direction	Surgical accuracy, reduced time
CAD/CAM for prosthetics	Digital milling and printing	Crowns and bridges are designed and fabricated digitally	Improved aesthetics, faster restoration

TABLE 5. 3D Printing Techniques, Materials, and Clinical Outcomes in Implant Dentistry.

3D Printing Technique	Material Used	Application	Advantages	Clinical Success/ Outcome
Powder bed fusion (selective laser melting)	Titanium alloy (Ti-6Al-4V)	Patient-specific metal implants	Porous structure, mechanical strength, biocompatibility	87% Success in maxillofacial reconstructions
Extrusion printing (Arburg plastic free forming)	Polymer-ceramic (PLA/β-TCP)	Resorbable scaffolds and alveolar augmentation	Patient-specific, osteoconductive, degradable	Promising integration in pilot studies
Resin-based 3D printing	Surgical guide resins	Custom surgical guides	Precision fit reduces surgery time	Widely adopted, it enhances placement accuracy

Artificial intelligence in dental implants has also transformed the workflow, enabling automation, precision, and prediction across diagnosis, planning, surgical guidance, and prosthesis planning, as shown in Table 6. Generative design algorithms combine AI and subsequent optimisation of implant macro- and micro-geometries, relying on patient-specific finite element models. Such designs promote a balance between mechanical strength, stress utilisation, and osseointegration topographical details, downplaying the planning bias and enhancing great functional results. These customised implants also precisely fit irregular or damaged bone structures when used in conjunction with additive manufacturing, providing enhanced load transfer and reducing micromotion. Robots equipped with AI-based navigation software strengthen the accuracy of surgery, as demonstrated by pilot studies, which show accuracy in implant placement within 0.5 mm. The reason is that these systems reduce variability caused by hand, lessen trauma, and allow partial invasive procedures. Allowing AI to provide feedback on-the-fly to correct the drilling trajectory and depth can maximise primary stability and prevent the encounter of anatomical hazards. In addition to surgery, AI perfects the architecture and adaptation of prosthesis parts, including abutments and caps. Algorithms can maximise occlusal contacts, marginal fit, and esthetic outcomes, minimising the need for adjustments and remakes. This saves as much as 40% of chair time and minimises patient dissatisfaction by improving function and cosmesis.

TABLE 6. AI Applications in Dental Implantology: Functions, Benefits, and Performance Outcomes.

AI application	Description	Benefits	Accuracy/ outcome
Anatomical segmentation	Automated nerve and bone structure detection in CBCT scans	Enhances accuracy, reduces risk	> 98% Accuracy in nerve identification
Bone quality assessment	Prediction of bone density and morphology	Personalizes implant choice	High predictive accuracy (AUC > 0.90)
Failure risk prediction	Forecasts the likelihood of implant complications	Supports personalized risk management	Predictive models with AUC > 0.90
Surgical navigation	Real-time AI-guided implant placement during surgery	Improves precision, reduces surgical trauma	Placement accuracy within 0.5 mm (pilot)
Prosthetic design optimization	AI fine-tunes abutment and crown morphology	Better fit, reduced chair time	40% reduction in lab turnaround time

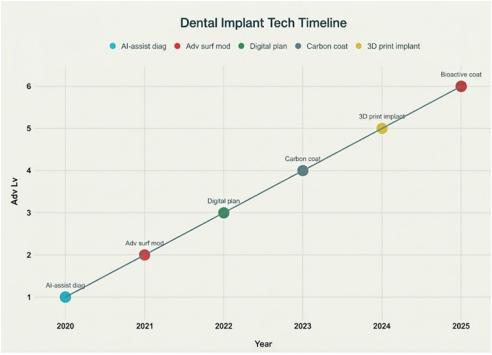

FIGURE 7. Timeline of transformative technological developments in dental implantology, highlighting the convergence of digital workflows and advanced biomaterials (the data were taken from a previous study).[83] (Permission under the Creative Commons International Attribution CC BY-NC-ND 4.0 license)

These technological developments in digital imaging, AI, 3D printing, and CAD/CAM technologies have brought dental implantology to an era of customised, efficient, and highly predictable treatment (Figure 7). They decrease operative complications, streamline implant placement, reduce treatment duration, and enhance aesthetic and functional outcomes. Advances in the future are expected to be presented by augmented and virtual reality in serving as intraoperative guidance, generative AI in designing implants, and additional incorporation of bioactive materials in the context of digital fabrication.

3.2. Mechanical Failure and Wear in Dental Implants

The long-term success of dental implants is still a factor of mechanical failure and wear. Although the future holds promise for improvements in biomaterials, implant design, and surgical procedures, complications such as screw loosening, ceramic chipping, implant fracture, and wear-induced corrosion still occur at varying rates, which can ultimately undermine the integrity of osseointegration and prosthetic stability. This is one of the most frequent mechanical complications in 6–12% of implants within 5 years. It is generally caused by micromovements between the implant and the abutment interface, commonly resulting from prosthetic misfit or inadequate load torque generated during installation. The loosening of screws may cause microleakage of bacteria, peri-implant inflammation, and prosthetic failures.[84–89] Mitigation measures involve optimising screw preloading through torque control, internal hex, or tri-channel connectors to enhance mechanical interlocking and minimise micro-movement, as well as fine digital processes for aligning the fit of parts. Ceramic chipping is a typical complication in zirconia-based restoration. It is encountered in most cases (4–8%), often in conjunction with parafunctional habits (e.g., bruxism), occlusal loading, or less-than-ideal prosthetic framework design. There has been a significant reduction in the use of monolithic zirconia crowns that do not require bonding layers of ceramics. Moreover, the personalisation of occlusal forces distribution with the help of occlusal analysis and occlusal adjustment guided by AI ensures the prevention of risks associated with chipping and posterior restoration.

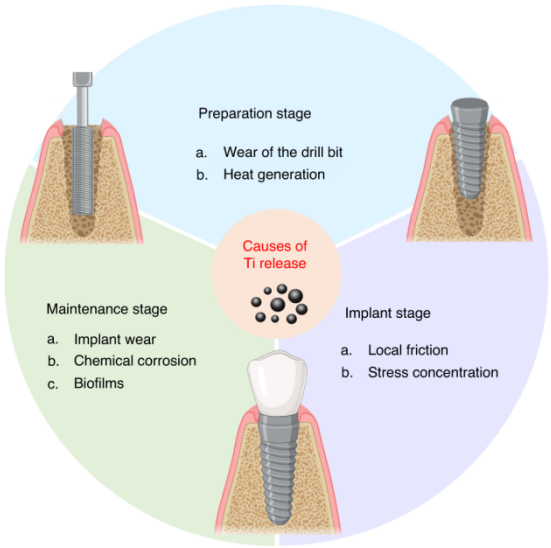

FIGURE 8. Causes of titanium release during dental implant preparation, implant, and maintenance stages.[90] (Permission under the Creative Commons International Attribution CC BY-NC-ND 4.0 license)

Although relatively uncommon (< 1%), implant fractures may be initiated by overload, particularly in implants with narrow diameters or poor bone quality. β-type titanium alloys produce more elastic moduli, unlike other types of alloys; the closer they are to those in the bone, the less the stress concentrations and hence the possibility of fracture (Figure 8).[91–95] Another effective preventive measure is prosthetic splinting, which decompresses occlusal forces and spreads them to several implants. Table 7 presents common failure modes in dental implants, including

prevalence, causes, and mitigation strategies. The release of titanium particulates due to wear or corrosion has been suspected of inducing peri-implant inflammation and peri-implantitis. The sources of wear debris could be micromotion between the implant and abutment or abrasion. To minimise the release of particles and biological impact, wear and chemical degradation resistance are improved by surface coatings, such as zirconia or carbon-based films (DLC and graphene). They are also antibacterial in nature and help fight the presence of biofilms.

TABLE 7. Common Failure Modes in Dental Implants: Prevalence, Causes, and Mitigation Strategies.

Failure Mode	5-Year Prevalence	Primary Causes	Mitigation Strategies
Screw loosening	6–12%	Micromotion, component misfit	Preload optimization, internal-hex/tri-channel connectors
Ceramic chipping	4–8%	Bruxism, framework design	Monolithic zirconia crowns, AI-balanced occlusal design
Implant fracture	< 1%	Overload, narrow diameter	β-type alloys, prosthetic splinting
Wear debris/ corrosion	-	Titanium particle release	Zirconia/carbon coatings for wear resistance

Finite-element analyses have played a significant role in identifying stress concentration zones and making design adjustments to distribute loading more evenly. Implant–abutment connections, such as Morse-taper, improve the dispersal of forces to the cortical bone.[96] Still, they can increase stress within components of the abutment, requiring the patient to choose with caution. Problems in mechanical failure often occur due to biological and prosthetic factors, indicating that more integrated treatment solutions should incorporate biomechanics, materials science, and treatment strategies to address these issues. The current standard of care involves prevention through optimised implant design, accurate surgical placement facilitated by digital workflow, and prosthetic planning that is also accurate based on AI analysis.

3.3. Bioactive and Bioresorbable Implants in Dental Implantology

Recent trends in the development of dental implants over the last 5 years have led to the conception of bioactive and bioresorbable materials as a crucial technology, focusing on accelerating the speed of biological adhesion and reducing the long-term foreign body burden. These advances signify a paradigm change toward nonactive, fixed objects to activate interactive systems that enable bone growth and support bone remodelling at the same rate of healing. Mg alloys have been a preferred choice of biodegradable dental implants because their elastic modulus (about 45 GPa) is similar to that of the cortical bones, effectively avoiding stress shielding effects. Mg alloys can biodegrade through an orderly corrosion process, thereby liberating Mg ions that are known to induce bone tissue development and angiogenesis.[97–101] Nonetheless, rapid corrosion presents issues such as local gas formation and early mechanical failure. To address this, synthesised methods for complex hybrid coatings that consist of HA and PLA have emerged (Figure 9). Such coatings slow the biodegradation rate and promote osteogenesis, stabilizing implant function during the critical early osseointegration phase. Early animal and pilot human studies have demonstrated positive findings regarding implant fixation and bone regeneration, particularly for small load-bearing and screw-like implants.

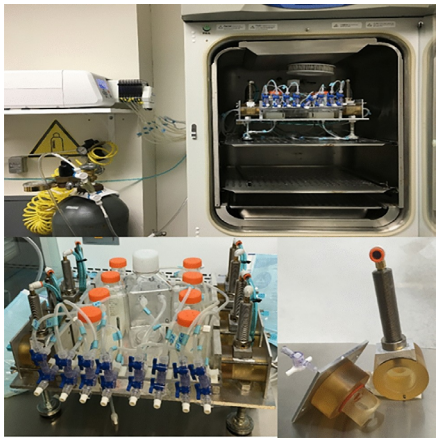

FIGURE 9. Laboratory setup for testing orthopaedic implants with fluid systems to evaluate bone formation on implant surfaces.[102] (Permission under the Creative Commons International Attribution CC BY-NC-ND 4.0 license)

A combination of PLA and β-TCP has gained popularity in producing bioresorbable scaffolds using advanced 3D printing technology.[103–106] The composites serve as osteoconductive scaffolding for alveolar ridge distension and craniofacial remodelling. Patient-specific geometries can be printed in 3D to enable an accurate anatomic fit, thereby accelerating the integration of functions. These materials resorb over time into natural metabolites (e.g., lactic acid) and gradually transfer the loads to the regenerating bone while acting as temporary mechanical support. Components of surface coatings, such as BG, facilitate bone bonding by dissolving and releasing calcium and phosphate ions, thereby encouraging the growth of an HA-like mineral layer.[107–110] This mineralised layer can promote osseointegration and raise the local pH, creating an antimicrobial environment that prevents bacterial colonisation and peri-implantitis (Figure 10). Preliminary clinical and animal studies suggest that BG coatings could be used to minimise biological complications due to their minimal impact on mechanical performance.

To further accelerate early bone growth and vascularisation of implants, an experimental coating has been developed that incorporates osteoinductive factors, such as BMP-2 and L-PRF (Figure 11).[112–119] They are promising, but regulatory hurdles, manufacturing costs, and difficulty achieving stable formulations with predictable controlled release kinetics constrain their clinical translation. Table 8 presents the emerging biodegradable and bioactive systems for dental implantology.

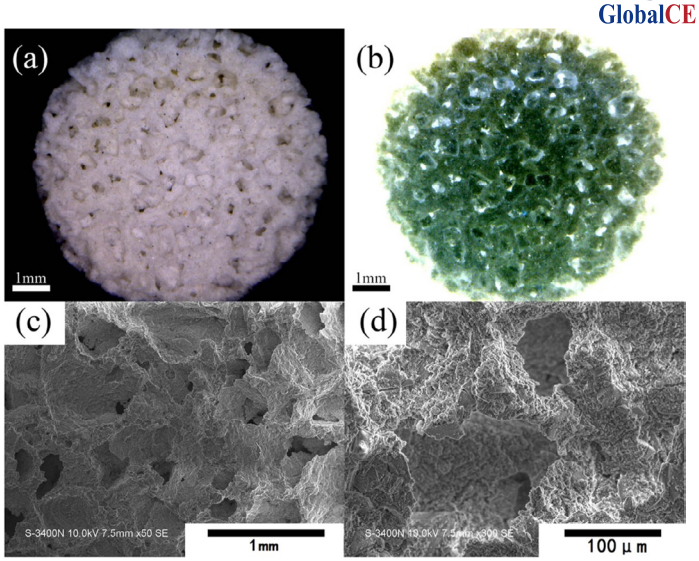

FIGURE 10. Optical and scanning electron microscope (SEM) images of mesoporous bioactive glass scaffolds showing porous microstructure relevant to bioresorbable bone implants.[111] (Permission under the Creative Commons International Attribution CC BY-NC-ND 4.0 license)

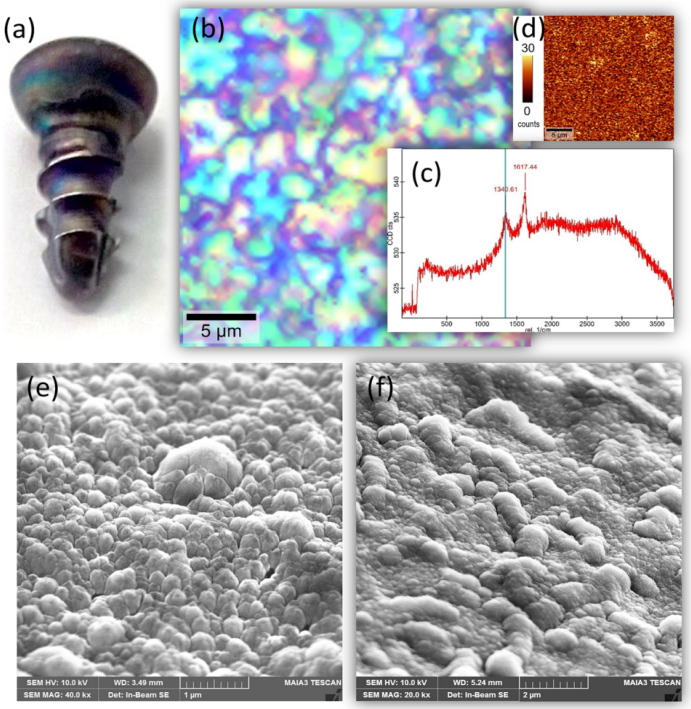

FIGURE 11. Microscopic and spectroscopic characterization of nanocrystalline coatings on Ti-6Al-4V implant screw, showing surface morphology and chemical fingerprinting relevant to bioactive implant coatings.[120] (Permission under the Creative Commons International Attribution CC BY-NC-ND 4.0 license)

TABLE 8. Emerging biodegradable and bioactive systems for dental implantology.

Material/ System	Key Properties	Advantages	Current Status/ Evidence
Magnesium alloys	Elastic modulus about 45 GPa; biodegradable	Bone-matched stiffness; osteogenic ion release	Preclinical & pilot clinical; coatings moderate corrosion
PLA/β-TCP composites	Osteoconductive polymer-ceramic blend	Patient-specific 3D-printable scaffolds; resorbable	Early clinical use in alveolar grafting
Bioactive glass coatings	Ion release (Ca^{2+}, PO_4^{3-}); antimicrobial	Enhances osseointegration; resists infection	Clinical trials ongoing
Growth factor films (BMP-2, L-PRF)	Osteoinductive biological coatings	Accelerates healing; stimulates vascularization	Experimental; regulatory challenges

Using bioactive and bioresorbable implants helps eliminate the disadvantages of permanent dental implants, including chronic foreign body reactions and the need for removal interventions. They are most appropriate to use when it involves patients with impaired bones or defective combinations, and then a gradual transfer of the load and increased regeneration is essential. Nonetheless, issues persist in altering degradation by modifying degradation rates to correlate with bone healing chronologies and providing adequate mechanical support at the initial stage of implantation. Acquiring further long-term safety and efficacy would require larger clinical trials. Key hurdles include regulatory complexity for combination products (device plus drug/biologicals) requiring robust and standardized evidence of long-term safety, controlled release profiles, and manufacturing consistency; scalability and quality control for surface functionalization (batch-to-batch reproducibility, sterilization compatibility, and shelf-life); clinical validation gaps, that is, paucity of large, prospective, multi-center trials with harmonized endpoints and cost-effectiveness data; integration challenges with the existing digital workflows and component ecosystems; and reimbursement, procurement, and training constraints that slow adoption. These factors necessitate the coordinated generation of clinical evidence, clear regulatory pathways, and robust manufacturing/QA frameworks to enable the routine use of these technologies.

3.4. Personalized Implants and AI-Driven Design in Dental Implantology

A combination of AI and individualised design strategies has significantly transformed dental implantology, enabling the provision of personalised approaches to treatment that consider each patient's anatomy, biology, and risk factors. Over the five years between 2020 and 2025, AI-enhanced technologies have progressed from the research phase into a clinical application phase, enhancing diagnostic accuracy, implantation, treatment planning, and outcome prediction. Patient-specific implants are now utilising advanced manufacturing methodologies to optimise fit and functionality. The latest AI protocols can now achieve stunning accuracies (> 98%) in robotic tooth counting, defining implant types, and detecting anatomical landmarks (Figure 12). The built-in capabilities enable chair-side real-time diagnostics, which minimize human error and streamline the workflow. For example, neural networks identify nerves and anatomical structures on fixed-scan CBCT with an almost perfect accuracy essential for avoiding surgical complications. AI models incorporate a variety of patient variables, such as bone quality, systemic conditions, and loading regimes, to

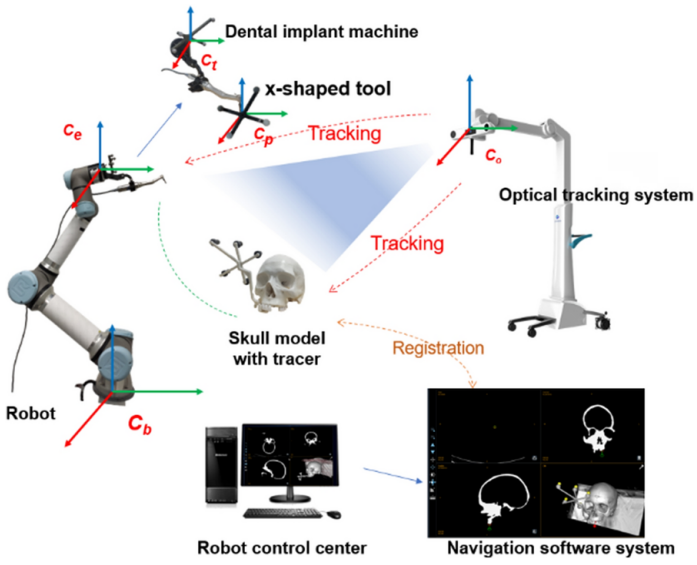

FIGURE 12. An optics-guided robotic system integrates robotic arms, optical tracking, and navigation software to enhance precision in dental implant surgery.[128] (Permission under the

predict implant success rates and the risks of biological complications.[121–127] The AUC values of machine learning classifiers are larger than 0.90 in terms of discriminatory power to predict peri-implantitis, implant failure, or mechanical complications. This prognostic ability allows data-driven individual treatment planning, informed consent, and optimisation of clinical decision-making.

Table 9 summarizes the primary AI technologies currently applied in dental implantology, outlining their clinical applications, associated benefits, and documented performance metrics. The result of blending AI and personalised implant design is the creation of highly customised treatment plans that can enhance surgical safety, improve the success of prosthetic implants, and increase the postoperative durability of implants. The AI workflows are helpful because they help reduce operator variability, thereby speeding up clinical processes and supporting informed decision-making about complex issues. Individual-tailored implants using additive manufacturing processes can better match patient anatomy, enhancing primary stability and biomechanical performance, primarily when used in compromised or unusual bone models.

TABLE 9. AI technologies in dental implantology: applications, clinical benefits, and performance.

Application Area	AI Technology/ Method	Clinical Benefits	Outcome/ Accuracy
Anatomical segmentation	Deep learning neural networks	Precise nerve and bone mapping	> 98% accuracy in nerve segmentation
Implant classification	Machine learning classifiers	Automated implant type recognition	> 98% classification accuracy
Predictive risk modelling	Multivariate AI models	Risk stratification for peri-implantitis/failure	AUC > 0.90 in predictive performance
Generative implant design	AI-driven finite-element optimization	Personalized, optimized implant geometries	Improved biomechanical load distribution
Robotic-assisted Navigation	AI-guided real-time surgical control	Sub-0.5 mm placement accuracy	Pilot clinical use success
Prosthetic design optimization	AI-based occlusal and fit adjustment	Reduced adjustment time; improved aesthetics	Up to 40% reduced lab turnaround time

Expanded opportunities in the future include continuous learning of AI algorithms that improve over time and with the accumulation of clinical data, as well as utilising augmented reality (AR) to create intraoperative visualisation. These smart, closed-loop implants can monitor and adapt in real-time. Regulatory frameworks and broad clinical validation are the most essential aspects that need improvement and development. Specifically, AI solutions often entail non-trivial upfront and recurring costs (such as software licenses, hardware, and integration with imaging/records), which can be prohibitive for small or resource-limited practices. Effective use requires staff training in data acquisition quality (CBCT/intraoral scans), workflow integration, and interpretation of model outputs, along with ongoing calibration and updates. Accessibility is uneven due to variable Internet infrastructure, interoperability with existing systems, and data privacy and consent requirements; reimbursement pathways are still evolving. To promote equitable deployment, the text highlights phased implementation (pilot modules with measurable ROI), vendor support/education, and preference for interoperable, standards-compliant tools that integrate with the current imaging and CAD–CAM pipelines. Over the past five years alone, disruptive shifts toward digitally enhanced workflows in dental implantology have incorporated the latest imaging technology, AI, and the power of additive manufacturing to deliver new levels of precision, efficiency, and individualised patient outcomes. Such workflows span the entire treatment sequence, from diagnosis and surgery planning to guided surgery and restoration with prosthetics.

4. CLINICAL LOADING CONCEPTS IN DENTAL IMPLANTOLOGY

The implant loading protocol, including the timing and method of placing the prosthetic crown or denture into a functional occlusion, has undergone considerable changes. The clinical intervention ensures the most advantageous

osseointegration, reduces complications, and promotes patient satisfaction, which in turn depends on a shorter treatment period. Various loading protocols have been broadly categorised into three: immediate loading (prosthetic restoration is placed within 1 week of implant positioning); early loading (loading that occurs after 1 week to 2 months after implantation); and conventional (or delayed) loading, in which restoration is not placed up to 2 months to allow extended healing before functional loading.[129–132] It is now known with reasonable certainty that survival with immediate and early loading can be equivalent to conventional loading as long as specific stability criteria have been fulfilled according to recent systematic reviews and consensus guidelines. These are an insertion torque of at least 40 N·cm, or typically around this value, to achieve mechanical fixation, and an ISQ of at least 70, as tested by resonance frequency analysis, which indicates that the implant is stable. The 3D and 6D gain measures, which minimise micromotion that may interfere with osseointegration, make these thresholds essential, thus allowing for safe and functional early loading. They significantly reduce the time patients live without teeth, thereby enhancing their overall quality of life, enabling them to eat comfortably, speak clearly, and restore their smile and social confidence more quickly. This restoration, carried out promptly, improves psychological well-being and comfort. Furthermore, since secondary surgeries are usually minimized with immediate or early loading protocols, the treatment does not become cumbersome, with a drastic decrease in patients' overall morbidity. Special attention should be paid to short implants (≤ 8 mm), the immediate loading of which under appropriate stability conditions is associated with cumulative success rates exceeding 98%. Such implants often eliminate the need for sinus augmentation or excessive bone grafting, especially when treating atrophic maxillae, making treatment significantly easier.[133–136] Table 10 presents the definitions, typical survival rates, and key inclusion criteria for the three primary loading protocols in implant dentistry. Notably, the loading scheme is to be made considering the quality of the bone, general patient factors, and anatomy. AI-driven risk assessment and modern digital imaging modalities are commonly incorporated into clinical practice to individualise loading strategies and maximise outcomes at the individual level. These developments have elevated implant loading practices from a conservative, long-term process to an objective, evidence-based methodology that balances the biological wound-healing process and patient-based efficiency and comfort.

TABLE 10. Dental Implant Loading Protocols: Definitions, Survival Rates, and Key Inclusion Criteria.

Loading Protocol	Definition	Typical Survival Rate (%)	Key Inclusion Criteria
Immediate loading	Prosthesis in occlusion ≤ 1 week	98–100	Insertion torque ≥ 40 N cm; ISQ ≥ 70
Early Loading	Restoration between 1 week and 2 months	97–99	Adequate primary stability
Conventional loading	Restoration after >2 months	96–98	No specific stability requirement

Clinicians must pay close attention to the primary stability by measuring torque, ISQ, and patient-specific factors (bone quality, systemic health, and smoking). Protocols applicable to immediate and early loading are implemented successfully and without jeopardising the longevity of implants when the criteria are followed. Improved technology includes AI-based predictive models, CAD–CAM fabricated prostheses, and robotic devices that assist in planning treatment and facilitating a smooth transition from implant positioning to its ultimate restoration, which further positively influences accelerated loading. The current research aims to optimise biomaterials and surface treatments to allow further acceleration and stability of osseointegration, which in turn could expand indications toward immediate loading. Using biosensors on implants to measure loading forces and track healing in real-time promises to play a role in the near-term use of dynamic, patient-specific loading programs. Table 11 summarizes the loading thresholds, timing definitions, and clinical recommendations for implant-supported restorations.

TABLE 11. Loading thresholds and clinical recommendations for different implant loading protocols.

Protocol	Timing Definition	Primary Stability Thresholds	When to Recommend	Typical Notes
Immediate loading	Prosthesis in occlusion within 1 week of implant placement	Insertion torque ≥ 40 N·cm; ISQ ≥ 70	Single units or splinted cases with excellent bone quality, intact socket walls, controlled occlusion, and an experienced operator	Prefer nonfunctional occlusion if borderline; ensure a protective occlusal scheme and patient compliance
Immediate restoration (non-occlusal)	Provisional placed within 1 week, kept out of occlusion	Insertion torque ≥ 30–35 N·cm; ISQ ≥ 65–70	Aesthetic zones where soft tissue support is desired, but functional loading risk is high	Strict soft diet; frequent follow-up and RFA monitoring
Early loading	Restoration in occlusion at 1 week–2 months	Insertion torque ≥ 35–40 N·cm; ISQ ≥ 70 at loading visit	Good bone density and primary stability; sites without graft immaturity	Verify the rising ISQ trend before loading
Conventional (delayed) loading	Restoration after > 2 months	No fixed torque/ISQ, prioritize complete uneventful healing	Compromised bone quality, extensive augmentation, systemic risk factors, or low initial stability	Consider staged increases in function and progressive occlusion
Short implants (≤ 8 mm) under immediate/early loading	As above	Insertion torque ≥ 40 N·cm; ISQ ≥ 70	Atrophic ridges where grafting is to be avoided and stability is confirmed	Favour splinting and carefully controlled occlusion

5. MANAGEMENT OF BIOLOGICAL COMPLICATIONS IN DENTAL IMPLANTS

Although advances in materials and surgery indicate that dental implantology is becoming more efficient, clinical and biological complications, especially peri-implant diseases, including peri-implant mucositis and peri-implantitis, remain a significant issue in the field of dental implantology. Peri-implant mucositis is an inflammatory process that affects the non-sensitised (soft) tissues surrounding an implant, causing the latter to bleed on probing, but with no bone loss, and is reversible when properly addressed and maintained. On the contrary, peri-implantitis is a condition characterised by both inflammation and progressive bone loss around the implant. Peri-implantitis encompasses 10–20% of both patients and implants within a 5–10-year period.[137–140] Prevention and early detection are the first steps for proper management. Proactive measures can be taken to reduce the number of diseased cases by educating patients about oral maintenance, controlling risk factors such as smoking and systemic diseases, and providing professional patient care tailored to the risk profile, which significantly minimises disease incidents. Peri-implant mucositis and early peri-implantitis are typically treated using nonsurgical management as the first line of therapy, aiming for mechanical debridement with plastic or titanium curettes, ultrasonic equipment, and glycine powder air-polishing to safely eliminate biofilm without harming the implant surface. Photodynamic therapy, although potentially helpful in a limited way, is a potential adjunctive therapy that, when combined with an antibiotic regimen and antiseptics, such as chlorhexidine irrigation, can reduce microbial count. Although persistent nonsurgical treatment usually resolves mucositis, surgery is typically required for peri-implantitis in most instances. Surgical management may be performed through surgery of the access flap, allowing for the visualisation and cleaning of the implant surface with mechanical assistance and other adjunctive means, such as lasers and chemical cleaning agents.[141–145] The intention is to replace lost bone during bone regenerative surgery, which involves the use of grafts and membranes. However, roughened or contaminated implant surfaces are altered in the corresponding surgeries, such as implantoplasty.

Nevertheless, even after surgical intervention, one-year recurrence rates of peri-implantitis vary considerably, ranging from approximately 3% in carefully selected cases with complete decontamination and augmentation to 44% in patients with multiple risk factors such as poor

oral hygiene, smoking, and severe baseline bone loss. This substantial variation highlights the multifactorial nature of recurrence and underscores the importance of individualised risk assessment and maintenance protocols. Recurrence in the long term is a predominant clinical dilemma, depending on the features of the implant surface, implant duration, the presence of basic suppuration, and the severity of bone loss at the initial diagnosis. Titanium implant debris and reservoir of microbial organisms might also blur the healing process, which leads to the ongoing inflammation [146–150]

New adjunctive treatments in research include novel bioactive coatings, such as bioactive glass and antimicrobial carbon-based films (e.g., graphene and DLC), to reduce bacterial colonisation and promote re-osseointegration. Innovative solutions, such as locally controlled-release antimicrobials and host modulation therapies, as well as other novel laser treatment options, are currently under clinical trial and are yet to be completed. Peri-implant diseases should be treated using a stepwise management protocol. This involves proper diagnosis and categorisation of the level of illness, educating the patient and reinforcing oral healthcare, providing nonsurgical mechanical debridement as the first line of treatment, repeating these lessons after evaluation, and surgical intervention in cases of need. Longer, individualised peri-implant care is essential to prevent recurrences and maintain the implant's health.[151–154] Table 12 outlines the main management approaches, their indications, key techniques or interventions, and the associated clinical outcomes and limitations. It is a multi-modal approach that is still necessary to adequately address biological issues in dental implants, produce durable implants, and achieve good, long-term clinical outcomes.

TABLE 12. Management Strategies for Peri-Implant Diseases: Indications, Techniques, and Outcomes.

Management Approach	Indications	Key Techniques/ Interventions	Outcomes and Limitations
Nonsurgical therapy	Peri-implant mucositis, early peri-implantitis	Mechanical debridement, air-polishing, and photodynamic therapy	Effective for mucositis; limited for advanced peri-implantitis
Surgical therapy	Advanced peri-implantitis	Access flap, decontamination, regenerative, or respective surgery	Improves clinical parameters; recurrence rates up to 44%
Adjunctive therapies	Supporting nonsurgical/ surgical treatment	Laser therapy, antiseptics, and antimicrobial coatings	Promising but evidence variable; under study
Maintenance and prevention	All implant patients	Regular professional cleaning, risk factor control	Reduces disease incidence; critical for long-term success

The treatment of biological complications surrounding dental implants is increasingly shifting toward evidence-based and integrated pathways, where precise diagnosis, individualised treatments, and long-term maintenance are strictly adhered to. Although the number of treatment methods is now diverse, the frequency of reappearance and development of peri-implant diseases, including mucositis and peri-implantitis, is represented by high clinical rates, which dictate the need to improve on several levels.[155–157] Among the main priorities are innovations in early detection and risk evaluation based on AI methods and salivary markers or crevicular biomarkers, which enable the provision that allow providing timely and customized interventions before the damage is irreparable. Similar works aim to create more effective bioactive and antimicrobial surfaces for implants (coatings containing BG, bioactive peptides, and carbon-based nanofilms) that would enable them to resist bacterial colonisation and achieve re-osseointegration even at damaged sites. There is a focus on new regenerative treatments to replace lost peri-implant bone and enhance long-term strength, including the use of growth factors, stem cell therapy, and biomimetic scaffolds. Improved patient education can be equally vital for achieving better oral hygiene and

compliance with the maintenance program, as patient compliance is a key factor in preventing recurrence.[158–161] Therefore, a multimodal, holistic approach, encompassing prosthodontic, surgical, periodontal, microbiological expertise, and digital diagnostic and reasoning skills, involving adherence to contemporary international clinical guidelines, is the most promising way to manage these complicated sequelae and maintain peri-implant health and implant longevity.

Antimicrobial strategies for next-generation implants encompass several innovative approaches aimed at preventing infection and promoting tissue integration. Peptide coatings, such as GL13K and engineered chimerics, inhibit early pathogenic adhesion and biofilm formation on titanium surfaces while maintaining compatibility with surrounding cells. These coatings often incorporate adhesion motifs to promote effective sealing of soft tissue around the implant. Another approach involves metallic ion-doped surfaces, including zinc-, fluorine-, and bismuth-modified calcium phosphates, as well as photoactivated titanium dioxide and titanium nitride variants. These surfaces offer bactericidal and antibiofilm properties against peri-implant pathogens, and in many cases, enhance bone growth; however, long-term durability still requires validation. Controlled-release interfaces, such as chlorhexidine reservoirs and antimicrobial peptide–graphene oxide hybrids, maintain antimicrobial activity around the abutment–implant and transmucosal regions while exhibiting low cytotoxicity in vitro. Complementing these methods, mesoporous bioactive glass and other ion-releasing coatings elevate the local pH and release calcium and phosphate ions, forming a hydroxyapatite-like layer that discourages bacterial colonization and promotes bone bonding. Incorporating fluoride or zinc into calcium phosphate or glass matrices further contributes to antibacterial effects without compromising osteoconductivity. Together, these multifaceted strategies provide a dual-action preventive approach against peri-implantitis by combining infection control with the promotion of bone integration.

6. FUTURE PERSPECTIVES IN DENTAL IMPLANTOLOGY

The last few years have taken dental implantology to the edge of the next era, whose future orientations will be determined by the convergence of disciplines in materials science, digital technologies, AI, and regenerative medicine. The idea behind next-generation dental implants is to address unresolved clinical problems, individualise their approach to therapy, and adopt biologically mediated processes to create a positive tissue reception environment. Studies are rapidly developing the so-called smart surfaces of implants that can release treatment agents in response to environmental stimuli. For example, coatings that sense local pH or bacterial metabolites can provide an antibiotic, growth factor, or anti-inflammatory agent in a time- and place-specific manner. As demonstrated by preclinical research, no such responsive coatings can prevent biofilm formation and regulate peri-implant bone remodelling better than static surfaces. It is predicted that applying antimicrobial peptides, silver nanoparticles, or growth factors (such as BMP-2) to the coating of implants will enhance infection control and accelerate osseointegration, thereby minimizing the need for systemic medications.

Future implant material development encompasses fully absorbable implants, particularly Mg screws, scaffolds, and combinations with 3D-printed PLA/β-TCP polymers. The purpose of these systems is to create initial stability and wear out over time as bone cells rebuild on their own, thereby eliminating the need for surgery to remove the implant. Clinical translation must optimise degradation rates and mechanical performance to achieve specific healing curves, which, thus far, have had to be speculative. A highly desirable clinical translation goal is currently being achieved through novel surface engineering and the design of composite materials. Clinical decision-making, risk profiling, and real-time intraoperative adjustments are now guided by predictive analytics and machine learning. Patient-specific anatomical and biomechanical information is used in an AI-based generative design loop to iteratively optimize the geometry, surface features, and surgical access of implants. These tools can generate thousands of combinations and select the one that provides optimum primary stability, the lowest stress

concentration, and adjusts to local bone quality. This type of automation yields less operator-induced bias and provides more predictable data outcomes. In future, clinical practice will likely need the integration of on-site 3D printing of patient-specific implants with high-quality standards (ISO 13485). As digital imaging, CAD, and in-clinic prototyping advance, there is hope to provide fully personalised metallic, ceramic, or resorbable implants in a single sitting. The paradigm eliminates the backlog of off-site production and expands access to innovative treatments for complex or emergency cases.

Since peri-implantitis is one of the significant reasons for implant failure, it is one of the topics that are studied extensively as far as the prevention and treatment of the complication is concerned. Bioactive coatings on glasses, antibacterial nanofilms on carbon, and machine learning-based risk stratification are underway to reduce the likelihood of recurrence and re-osseointegration at affected sites. In the future, dental implants may include biosensors that provide real-time, physical feedback on mechanical load, temperature, or biochemical indicators of peri-implant health. These smart implants can trigger premonitory signs of biomechanical overload or infection and even initiate the release of therapeutic compounds, leading to real closed-loop care. Additionally, future convergence with tissue engineering through stem cell seeding and grafting, as well as the delivery of growth factors and immune modification, may lead to the on-demand reconstitution of whole dento-periodontal tissues. The given innovations necessitate revisions to regulatory frameworks and interdisciplinary collaboration among clinicians, materials scientists, engineers, and data scientists. Additional focus on using evidence to support adoption, safety, and long-term monitoring is crucial to realising the full clinical potential of these gains.

7. CONCLUSIONS

Contemporary implant dentistry is transitioning toward predictable personalized care enabled by synergistic advances in implant materials, multifunctional surface engineering, and digitally enhanced workflows. Established systems, such as micro-roughened titanium and high-performance ceramics, demonstrate high mid-term survival. In contrast, β-type titanium alloys, polymer-based frameworks, and bioresorbable constructs broaden indications with biomechanical tailoring and regenerative intent. Coupling CBCT and intraoral scanning with AI-assisted planning, CAD–CAM prosthetics, and additive manufacturing improves surgical precision, prosthetic fit, and the feasibility of stability-guided immediate or early loading in appropriately selected cases. These developments emphasize increased bone-to-implant contact, reduce biofilm susceptibility through surface functionality, and streamline clinical pathways. Key challenges remain and define the near-term agenda. First, peri-implantitis recurrence persists despite improved decontamination and maintenance protocols. This underscores the need for durable antibiofilm strategies, ion-releasing or peptide-based coatings, and robust soft tissue integration around transmucosal components. Second, for bioresorbable and hybrid systems (e.g., Mg alloys, PLA–β-TCP scaffolds), precise control of degradation kinetics and an early-phase mechanical reliability are essential to match healing timelines, mitigate particulate/corrosion by-products, and ensure long-term host compatibility. Priorities include standardized clinical endpoints and longer prospective cohorts for preventive surfaces, traceable metrology for *in vivo* degradation and wear, and integration of AI decision support with outcomes registries to translate design and materials innovation into consistently improved clinical performance.

AUTHOR CONTRIBUTIONS

Conceptualization, A.P., P.P. and V.K.; Methodology, A.P.; Validation, A.P., P.P. and V.K.; Formal Analysis, A.P., P.P. and V.K.; Investigation, A.P., P.P. and V.K.; Resources, A.P. and P.P.; Data Curation, A.P. and P.P.; Writing–Original Draft Preparation, A.P.; Writing–Review & Editing, V.K.; Visualization, P.P. and V. K.; Supervision, V.K.; Project Administration, V.K.

FUNDING

This research received no external funding.

DATA AVAILABILITY STATEMENT

All data that support the findings of this study are included within the article.

CONFLICTS OF INTEREST

The authors declare that they have no competing interests.

ETHICS APPROVAL AND CONSENT TO PARTICIPATE

Not applicable.

CONSENT FOR PUBLICATION

Not applicable.

REFERENCES

1. Alfaraj, T.A., Al-Madani, S., Alqahtani, N.S., et al. Optimizing osseointegration in dental implantology: a cross-disciplinary review of current and emerging strategies. *Cureus*. 2023;15(10):e47943. https://doi.org/10.7759/cureus.47943.
2. Kumar, V., Seth, J., Aeran, M., et al. From surface to success: how implant surfaces shape osseointegration. *IJPI*. 2024;9(2):58–63. https://doi.org/10.18231/j.ijpi.2024.013.
3. Joshi, N.P., Agwani, K.M., Mathur, R., et al. Rooted in bone: the role of osseointegration in dental implantology. *IJISRT*. 2025;10(4):2164–2169. https://doi.org/10.38124/ijisrt/25apr1088.
4. Pandey, C., Rokaya, D., Bhattarai, B.P. Contemporary concepts in osseointegration of dental implants: a review. *BioMed Res Int*. 2022:6170452. https://doi.org/10.1155/2022/6170452.
5. Cooper, L.F., and Shirazi, S. Osseointegration—the biological reality of successful dental implant therapy: a narrative review. *Front Oral Maxillofac Med*. 2022;4:39. https://doi.org/10.21037/fomm-21-77.
6. Sharma, P., Mishra, V., Murab, S. Unlocking osseointegration: surface engineering strategies for enhanced dental implant integration. *ACS Biomat Sci Eng*. 2025;11(1):67–94. https://doi.org/10.1021/acsbiomaterials.4c01178.
7. Beschnidt, S.M., Cacaci, C., Dedeoglu, K., et al. Implant success and survival rates in daily dental practice: 5-year results of a non-interventional study using CAMLOG SCREW-LINE implants with or without platform-switching abutments. *Int J Implant Dent*. 2018;4(1):33. https://doi.org/10.1186/s40729-018-0145-3.
8. Waghmare, G., Waghmare, K., Bagde, S., et al. Materials evolution in dental implantology: a comprehensive review. *J Adv Res Appl Mech*. 2024;123(1):75–100. https://doi.org/10.37934/aram.123.1.75100.
9. Manfredini, M., Poli, P.P., Giboli, L., et al.Clinical factors on dental implant fractures: a systematic review. *Dent J*. 2024;12(7):200. https://doi.org/10.3390/dj12070200.
10. Kupka, J.R., König, J., Al-Nawas, B., et al. How far can we go? A 20-year meta-analysis of dental implant survival rates. *Clin Oral Invest*. 2024;28(10):541. https://doi.org/10.1007/s00784-024-05929-3.
11. Liu, C., Liu, Y., Xie, R., et al. The evolution of robotics: research and application progress of dental implant robotic systems. *Int J Oral Sci*. 2024;16(1):28. https://doi.org/10.1038/s41368-024-00296-x.
12. Hakim, L.K., Yari, A., Nikparto, N., et al. The current applications of nano and biomaterials in drug delivery of dental implant. *BMC Oral Health*. 2024;24(1):126. https://doi.org/10.1186/s12903-024-03911-9.
13. Bahrami, R., Pourhajibagher, M., Nikparto, N., et al. Robot-assisted dental implant surgery procedure: a literature review. *J Dent Sci*. 2024;19(3):1359–1368. https://doi.org/10.1016/j.jds.2024.03.011.
14. Wu, X.Y., Shi, J.Y., Qiao, S.C., et al. Accuracy of robotic surgery for dental implant placement: a systematic review and meta-analysis. *Clin Oral Implants Res*. 2024;35(6):598–608. https://doi.org/10.1111/clr.14255.
15. Maher, N., Mahmood, A., Fareed, M.A., et al. An updated review and recent advancements in carbon-based bioactive coatings for dental implant applications. *J Adv Res*. 2025;72:265–286. https://doi.org/10.1016/j.jare.2024.07.016.
16. Accioni, F., Vázquez, J., Merinero, M., et al. Latest trends in surface modification for dental implantology: innovative developments and analytical applications. *Pharmaceutics*, 2022;14(2):455. https://doi.org/10.3390/pharmaceutics14020455.
17. Kochar, S.P., Reche, A., Paul, P. The etiology and management of dental implant failure: a review. *Cureus*. 2022;14(10):e30455. https://doi.org/10.7759/cureus.30455.
18. Sailer, I., Karasan, D., Todorovic, A., et al. Prosthetic failures in dental implant therapy. *Periodontol 2000*. 2022;88(1):130–144. https://doi.org/10.1111/prd.12416.
19. Papadakis, I., Spanou, A., Kalyvas, D. Success rate and safety of dental implantology in patients treated with antiresorptive medication: a systematic review. *J Oral Implantol*.

2021:47(2):169–180. https://doi.org/10.1563/aaid-joi-D-19-00088.

20. Ebenezer, S., Kumar, V.V., Thor, A. Basics of dental implantology for the oral surgeon. In *Oral and maxillofacial surgery for the clinician*. Bonanthaya, K., Panneerselvam, E., eds. Springer Nature: Singapore, 2021; pp. 385–405. https://doi.org/10.1007/978-981-15-1346-6_18.
21. Matos, G.R.M. Surface roughness of dental implant and osseointegration. *J Maxillofac Oral Surg*. 2021;20(1):1–4. https://doi.org/10.1007/s12663-020-01437-5.
22. Lokwani, B.V., Gupta, D., Agrawal, R.S., et al. The use of concentrated growth factor in dental implantology: a systematic review. *J Indian Prosthodont Soc*. 2020;20(1):3–10. https://doi.org/10.4103/jips.jips_375_19.
23. Zhang, Y., Gulati, K., Li, Z., et al. Dental implant nano-engineering: advances, limitations and future directions. *Nanomaterials*. 2021;11(10):2489. https://doi.org/10.3390/nano11102489.
24. Lang, N.P., Berglundh, T., Giannobile, W.V., et al. *Lindhe's clinical periodontology and implant dentistry*, 7th ed.; John Wiley: Hoboken, NJ, USA; 2021; pp. 3–49.
25. Dutta, S.R., Passi, D., Singh, P., et al. Risks and complications associated with dental implant failure: critical update. *Nat J Maxillofac Surg*. 2020;11(1):14–19. https://doi.org/10.4103/njms.NJMS_75_16.
26. Dutta, S.R., Passi, D., Singh, P., et al. Risks and complications associated with dental implant failure: Critical update. *Nat J Maxillofac Surg*. 2020;11(1):14–19. https://doi.org/10.4103/njms.NJMS_75_16.
27. Pellegrino, G., Bellini, P., Cavallini, P.F., et al. Dynamic navigation in dental implantology: the influence of surgical experience on implant placement accuracy and operating time. An in vitro study. *Int J Environ Res Public Health*. 2020;17(6):2153. https://doi.org/10.3390/ijerph17062153.
28. Nulty, A. A literature review on prosthetically designed guided implant placement and the factors influencing dental implant success. *Br Dent J*. 2024;236(3):169–180. https://doi.org/10.1038/s41415-024-7050-3.
29. Jia, S., Wang, G., Zhao, Y., et al. Accuracy of an autonomous dental implant robotic system versus static guide-assisted implant surgery: a retrospective clinical study. *J Pros Dent*. 2025;133(3):771–779. https://doi.org/10.1016/j.prosdent.2023.04.027.
30. Li, Z., Xie, R., Bai, S., et al. Implant placement with an autonomous dental implant robot: a clinical report. *J Prosth Dent*. 2025;133(2):340–345. https://doi.org/10.1016/j.prosdent.2023.02.014.
31. Panahi, O. Smart robotics for personalized dental implant solutions. *Dental*. 2025;7(1):21. https://doi.org/10.35702/dent.10021.
32. Kang, D.Y., Duong, H.P., Park, J.C. Application of deep learning in dentistry and implantology. *J Implant Appl Sci*. 2020;24(3):148–181. https://doi.org/10.32542/implantology.202015.
33. Do, T.A., Le, H.S., Shen, Y.W., et al. Risk factors related to late failure of dental implant—a systematic review of recent studies. *Int J Environ Res Public Health*. 2020;17(11):3931. https://doi.org/10.3390/ijerph17113931.
34. Mohammad-Rahimi, H., Motamedian, S.R., Pirayesh, Z., et al. Deep learning in periodontology and oral implantology: a scoping review. *J Periodont Res*. 2022;57(5):942–951. https://doi.org/10.1111/jre.13037.
35. Kligman, S., Ren, Z., Chung, C.H., et al. The impact of dental implant surface modifications on osseointegration and biofilm formation. *J Clin Med*. 2021;10(8):1641. https://doi.org/10.3390/jcm10081641.
36. Lee, J.H., Kim, Y.T., Lee, J.B., et al A performance comparison between automated deep learning and dental professionals in classification of dental implant systems from dental imaging: a multi-center study. *Diagnostics*. 2020;10(11):910. https://doi.org/10.3390/diagnostics10110910.
37. Kim, J.C., Lee, M., Yeo, I.S.L. Three interfaces of the dental implant system and their clinical effects on hard and soft tissues. *Mat Horiz*. 2022;9(5):1387–1411. https://doi.org/10.1039/D1MH01621K.
38. Gao, J., Pan, Y., Gao, Y., et al. Research progress on the preparation process and material structure of 3D-printed dental implants and their clinical applications. *Coatings*. 2024;14(7):781. https://doi.org/10.3390/coatings14070781.
39. Hossain, N., Mobarak, M.H., Islam, M.A., et al. Recent development of dental implant materials, synthesis process, and failure – a review. *Results Chem*. 2023;6:101136. https://doi.org/10.1016/j.rechem.2023.101136.
40. Jambhulkar, N., Jaju, S., Raut, A., et al. A review on surface modification of dental implants among various implant materials. *Mat Today Proc*. 2023;72:3209–3215. https://doi.org/10.1016/j.matpr.2022.12.022.
41. Alagatu, A., Dhapade, D., Gajbhiye, M., et al. Review of different material and surface modification techniques for dental implants. *Mat Today Proc*. 2022;60:2245–2249. https://doi.org/10.1016/j.matpr.2022.03.338.

42. Kurup, A., Dhatrak, P., Khasnis, N. Surface modification techniques of titanium and titanium alloys for biomedical dental applications: a review. *Mats Today Proc*. 2021;39:84–90. https://doi.org/10.1016/j.matpr.2020.06.163.
43. Sun, X.D., Liu, T.T., Wang, Q.Q., et al. Surface modification and functionalities for titanium dental implants. *ACS Biomat Sci Eng*. 2023;9(8):4442–4461. https://doi.org/10.1021/acsbiomaterials.3c00183.
44. Herráez-Galindo, C., Rizo-Gorrita, M., Maza-Solano, S., et al. A review on CAD/CAM yttria-stabilized tetragonal zirconia polycrystal (Y-TZP) and polymethyl methacrylate (PMMA) and their biological behavior. *Polymers*. 2022;14(5):906. https://doi.org/10.3390/polym14050906.
45. Bai, Z., Wang, B., Bian, J., et al. Antibacterial and osteogenic activities of thiolated and aminated yttria-stabilized tetragonal zirconia polycrystal with tolerance to low temperature degradation. *Ceramics Int*. 2023;49(23):37817–37828. https://doi.org/10.1016/j.ceramint.2023.09.110.
46. Cho, Y.E., Lim, Y.J., Han, J.S., et al. Effect of yttria content on the translucency and masking ability of yttria-stabilized tetragonal zirconia polycrystal. *Materials*. 2020;13(21):4726. https://doi.org/10.3390/ma13214726.
47. Küçükekenci, A.S., Çakmak, G., Güven, M.E., et al. Implant-supported fixed complete denture frameworks in additively and subtractively manufactured high-performance polymers: fabrication and fit accuracy. *J Dent*. 2025;105838. https://doi.org/10.1016/j.jdent.2025.105838.
48. Alqutaibi, A.Y., Alghauli, M.A., Algabri, R.S., et al. Applications, modifications, and manufacturing of polyetheretherketone (PEEK) in dental implantology: a comprehensive critical review. *Int Mat Rev*. 2025;70(2):103–136. https://doi.org/10.1177/09506608251314251.
49. Zol, S.M., Alauddin, M.S., Said, Z., et al. Description of poly (aryl-ether-ketone) materials (PAEKs), polyetheretherketone (PEEK) and polyetherketoneketone (PEKK) for application as a dental material: a materials science review. *Polymers*. 2023;15(9):2170. https://doi.org/10.3390/polym15092170.
50. McMullan, R., Golbang, A., Salma-Ancane, K., et al. Review of 3D printing of polyaryletherketone/apatite composites for lattice structures for orthopedic implants. *Applied Sci*. 2025;15(4):1804. https://doi.org/10.3390/app15041804.
51. Menini, M., Delucchi, F., Bagnasco, F., et al. Shock absorption capacity of high-performance polymers for dental implant-supported restorations: in vitro study. *Dent J*. 2024;12(4):111. https://doi.org/10.3390/dj12040111.
52. Dong, H., Liu, H., Zhou, N., et al. Surface-modified techniques and emerging functional coating of dental implants. *Coatings*. 2020;10(11):1012. https://doi.org/10.3390/coatings10111012.
53. Nasr Azadani, M., Zahedi, A., Bowoto, O.K., et al. A review of current challenges and prospects of magnesium and its alloy for bone implant applications. *Prog Biomat*. 2022;11(1):1–26. https://doi.org/10.1007/s40204-022-00182-x.
54. Herber, V., Okutan, B., Antonoglou, G., et al. Bioresorbable magnesium-based alloys as novel biomaterials in oral bone regeneration: general review and clinical perspectives. *J Clin Med*. 2021;10(9):1842. https://doi.org/10.3390/jcm10091842.
55. Omigbodun, F.T., Oladapo, B.I., Osa-uwagboe, N. Exploring the frontier of polylactic acid/hydroxyapatite composites in bone regeneration and their revolutionary biomedical applications – a review. *J Reinforced Plast Comp*. 2024;0(0). https://doi.org/10.1177/07316844241278045.
56. Topuz, M. Hydroxyapatite – Al2O3-reinforced poly(lactic acid) hybrid coatings on magnesium: characterization, mechanical and in vitro bioactivity properties. *Surf Interfaces*. 2023;37:102724. https://doi.org/10.1016/j.surfin.2023.102724.
57. Nilawar, S., Uddin, M., Chatterjee, K. Surface engineering of biodegradable implants: emerging trends in bioactive ceramic coatings and mechanical treatments. *Mat Adv*. 2021;2(24):7820–7841. https://doi.org/10.1039/D1MA00733E.
58. Eldokmak, M.M., Essawy, M.M., Abdelkader, S., et al. Bioinspired poly-dopamine/nano-hydroxyapatite: an upgrading biocompatible coat for 3D-printed polylactic acid scaffold for bone regeneration. *Odontology*. 2025;113(1):89–100. https://doi.org/10.1007/s10266-024-00945-x.
59. Zhao, F., Yang, Z., Liu, L., et al. Design and evaluation of a novel sub-scaffold dental implant system based on the osteoinduction of micro-nano bioactive glass. *Biomat Translat*. 2020;1(1):82. https://doi.org/10.3877/cma.j.issn.2096-112X.2020.01.008.
60. Cannillo, V., Salvatori, R., Bergamini, S., et al. Bioactive glasses in periodontal regeneration: existing strategies and future prospects—a literature review. *Materials*. 2022;15(6):2194. https://doi.org/10.3390/ma15062194.
61. Ali, N., Lone, N.F., Siddiquee, A.N., et al. A novel hybrid approach to develop bioresorbable material. *J Orthopaed*. 2022;34:61–66. https://doi.org/10.1016/j.jor.2022.08.012.

62. Nogueira, D.M.B., de Oliveira Rosso, M.P., Buchaim, D.V., et al. Update on the use of 45S5 bioactive glass in the treatment of bone defects in regenerative medicine. *World J Orthoped*. 2024;15(3):204–214. https://doi.org/10.5312/wjo.v15.i3.204.
63. Manesh, M.B., Vatankhah, N., Manesh, F.B. Comparison of microbiota in zirconia and titanium implants: a qualitative systematic review. *Int Dent J*. 2025;75(1):51–58. https://doi.org/10.1016/j.identj.2024.08.001.
64. Zhang, L.C., Chen, L.Y., Wang, L. Surface modification of titanium and titanium alloys: technologies, developments, and future interests. *Adv Eng Mat*. 2020;22(5):1901258. https://doi.org/10.1002/adem.201901258.
65. Losic, D. Advancing of titanium medical implants by surface engineering: recent progress and challenges. *Expert Opinion Drug Deliv*. 2021;18(10):1355–1378. https://doi.org/10.1080/17425247.2021.1928071.
66. Li, M., Cokic, S., Van Meerbeek, B., et al. Novel zirconia ceramics for dental implant materials. *J Mat Sci Technol*. 2025;210:97–108. https://doi.org/10.1016/j.jmst.2024.05.041.
67. Hong, G., Liao, M., Wu, T., et al. Improving osteogenic activity of Y-TZP (Yttria-stabilized tetragonal zirconia polycrystal) surfaces by grafting of silanes with different end groups. *App Surf Sci*. 2021;570:vp. https://doi.org/10.1016/j.apsusc.2021.151144.
68. Fiorin, L., Moris, I.C., Faria, A.C., et al. Effect of different grinding protocols on surface characteristics and fatigue behavior of yttria-stabilized zirconia polycrystalline: an in vitro study. *J Prosth Dent*. 2020;124(4):486.e1–486.e8. https://doi.org/10.1016/j.prosdent.2020.03.016.
69. Dobrzyńska-Mizera, M., Dodda, J.M., Liu, X., et al. Engineering of bioresorbable polymers for tissue engineering and drug delivery applications. *Adv Healthcare Mat*. 2024;13(30):e2401674. https://doi.org/10.1002/adhm.202401674.
70. Narayanan, S., Singh, M., Kandasubramanian, B. Innovative approaches in regenerative medicine for the development of sustainable and bioactive implants. *Biomed Mat Devices*. 2025;1–25. https://doi.org/10.1007/s44174-025-00397-z.
71. Chio, A., Mak, A. The digital workflow in implant dentistry. In *Prac Proc Implant Dent*. Ho, C.C.K. John Wiley: Hoboken, NJ, USA; 2021; pp. 335-349. https://doi.org/10.1002/9781119399186.ch34.
72. Pradies, G., Morón-Conejo, B., Martínez-Rus, F., et al. Current applications of 3D printing in dental implantology: a scoping review mapping the evidence. *Clin Oral Implants Res*. 2024;35(8):1011–1032. https://doi.org/10.1111/clr.14198.
73. Papaspyridakos, P., Chen, Y.W., Alshawaf, B., et al. Digital workflow: in vitro accuracy of 3D printed casts generated from complete-arch digital implant scans. *J Prosth Dent*. 2020;124(5):589–593. https://doi.org/10.1016/j.prosdent.2019.10.029.
74. Altalhi, A.M., Alharbi, F.S., Alhodaithy, M.A., et al. The impact of artificial intelligence on dental implantology: a narrative review. *Cureus*. 2023;15(10):e47941. https://doi.org/10.7759/cureus.47941.
75. Macrì, M., D'Albis, V., D'Albis, G., et al. The role and applications of artificial intelligence in dental implant planning: a systematic review. *Bioengineering*, 2024;11(8):778. https://doi.org/10.3390/bioengineering11080778.
76. Wu, Z., Yu, X., Wang, F., et al. Application of artificial intelligence in dental implant prognosis: a scoping review. *J Dent*. 2024;144:104924. https://doi.org/10.1016/j.jdent.2024.104924.
77. Revilla-León, M., Gómez-Polo, M., Vyas, S., et al. Artificial intelligence applications in implant dentistry: A systematic review. *J Prosth Dent*. 2023;129(2):293–300. https://doi.org/10.1016/j.prosdent.2021.05.008.
78. Alqutaibi, A.Y., Algabri, R.S., Elawady, D., et al. Advancements in artificial intelligence algorithms for dental implant identification: a systematic review with meta-analysis. *J Prosth Dent*. 2025;134(4):1089–1098. https://doi.org/10.1016/j.prosdent.2023.11.027.
79. Tomohisa O, Kamio T, Maeda Y, et al. Application of medical imaging and 3D printing technology in teaching the handling of novel medicine in periodontal surgery. *Cureus*. 2022;14(9):e29271. https://doi.org/10.7759/cureus.29271.
80. Zaheer, M.U., Razzaq, M.H., Aycan, M.F., et al. AI-assisted design and evaluation of SLM-Ti64 implants for enhanced bone regeneration. *Adv Healthcare Mat*. 2025;e03154. https://doi.org/10.1002/adhm.202503154.
81. Joshi, N., Patil, S., hatrak, P. March design and development of porous titanium alloy dental implant: a review. *AIP Conf Proc*. 2025;3227(1):020007. https://doi.org/10.1063/5.0241968.
82. Chen, Z., Liu, Y., Xie, X., et al. Influence of bone density on the accuracy of artificial intelligence-guided implant surgery: an in vitro study. *J Pros Dent*. 2024;131(2):254–261. https://doi.org/10.1016/j.prosdent.2021.07.019.

83. Zaww, K., Abbas, H., Sáenz, J.R.V., et al. AI-driven innovations for dental implant treatment planning: a systematic review. *J Pros Res*. 2025. https://doi.org/10.2186/jpr.JPR_D_24_00338.
84. Verma, A., Singh, S.V., Arya, D., et al. Mechanical failures of dental implants and supported prostheses: a systematic review. *J Oral Biol Craniofac Res*. 2023;13(2):306–314. https://doi.org/10.1016/j.jobcr.2023.02.009.
85. Romanos, G.E., Fischer, G.A., Delgado-Ruiz, R. Titanium wear of dental implants from placement, under loading and maintenance protocols. *Int J Mol Sci*. 2021;22(3):1067. https://doi.org/10.3390/ijms22031067.
86. Kashi, A., and Saha, S. Failure mechanisms of medical implants and their effects on outcomes. In: *Biointegration of medical implant materials*. Sharma, C.P. Woodhead Publishing: Cambridge, UK; 2020; pp. 407–432. https://doi.org/10.1016/B978-0-08-102680-9.00015-9.
87. Gherde, C., Dhatrak, P., Nimbalkar, S., et al. A comprehensive review of factors affecting fatigue life of dental implants. *Mat Today Proc*. 2021;43:1117–1123. https://doi.org/10.1016/j.matpr.2020.08.414.
88. Markarian, R.A., Galles, D.P., França, F.M. Dental implant-abutment fracture resistance and wear induced by single-unit screw-retained CAD components fabricated by four CAM methods after mechanical cycling. *J Pros Dent*. 2022;128(3):450–457. https://doi.org/10.1016/j.prosdent.2020.08.052.
89. Sailer, I., Karasan, D., Todorovic, A., et al. Prosthetic failures in dental implant therapy. *Periodontol 2000*. 2022;88(1):130–144. https://doi.org/10.1111/prd.12416.
90. Chen, L., Tong, Z., Luo, H., et al. Titanium particles in peri-implantitis: distribution, pathogenesis and prospects. *Int J Oral Sci*. 2023;15(1):49. https://doi.org/10.1038/s41368-023-00256-x.
91. Ossowska, A., and Zieliński, A. The mechanisms of degradation of titanium dental implants. *Coatings*. 2020;10(9):836. https://doi.org/10.3390/coatings10090836.
92. Saha, S., and Roy, S. Metallic dental implants wear mechanisms, materials, and manufacturing processes: a literature review. *Materials*. 2022;16(1):161. https://doi.org/10.3390/ma16010161.
93. Souza, J.C., Apaza-Bedoya, K., Benfatti, C.A., et al. A comprehensive review on the corrosion pathways of titanium dental implants and their biological adverse effects. *Metals*. 2020;10(9):1272. https://doi.org/10.3390/met10091272.
94. Rodríguez-Rojas, F., Kovylina, M., Pinilla-Cienfuegos, E., et al. Effect of a DLC film on the sliding-wear behaviour of Ti-6Al-4V: implications for dental implants. *Surf Coat Technol*. 2023;460:129409. https://doi.org/10.1016/j.surfcoat.2023.129409.
95. Gaur, S., Agnihotri, R., Albin, S. Bio-tribocorrosion of titanium dental implants and its toxicological implications: a scoping review. *Sci World J*. 2022:4498613. https://doi.org/10.1155/2022/4498613.
96. Levin, L. Nonsurgical and surgical management of biologic complications around dental implants: peri-implant mucositis and peri-implantitis. *Quintessence Int*. 2020;51(10):810–820. https://doi.org/10.3290/j.qi.a44813.
97. López-Valverde, N., Flores-Fraile, J., Ramírez, J.M., et al. Bioactive surfaces vs. conventional surfaces in titanium dental implants: a comparative systematic review. *J Clin Med*. 2020;9(7):2047. https://doi.org/10.3390/jcm9072047.
98. Eftekhar Ashtiani, R., Alam, M., Tavakolizadeh, S., et al. The role of biomaterials and biocompatible materials in implant-supported dental prosthesis. *Evid Based Comp Altern Med*. 2021:3349433. https://doi.org/10.1155/2021/3349433.
99. Ngo, H.X., Bai, Y., Sha, J., et al. A narrative review of u-HA/PLLA, a bioactive resorbable reconstruction material: applications in oral and maxillofacial surgery. *Materials*. 2021;15(1):150. https://doi.org/10.3390/ma15010150.
100. Sonaye, S.Y., Dal-Fabbro, R., Bottino, M.C., et al. Osseointegration of 3D-printable polyetheretherketone–magnesium phosphate bioactive composites for craniofacial and orthopedic implants. *ACS Biomat Sci Eng*. 2025;11(2):1060–1071. https://doi.org/10.1021/acsbiomaterials.4c01597.
101. Wychowański, P., Starzyńska, A., Adamska, P., et al. Methods of topical administration of drugs and biological active substances for dental implants—a narrative review. *Antibiotics*. 2021;10(8):919. https://doi.org/10.3390/antibiotics10080919.
102. Dua, R., Jones, H., Noble, P.C. Evaluation of bone formation on orthopedic implant surfaces using an ex vivo bone bioreactor system. *Sci Rep*. 2021;11(1):22509. https://doi.org/10.1038/s41598-021-02070-z.
103. Naig, P.J., Kuo, Z.Y., Chung, M.F., et al. Enhancing bone regeneration using blended poly (L-lactide-co-D, L-lactide) and β-tricalcium phosphate nanofibrous periodontal biodegradable membranes. *Polymers*. 2025;17(3):256. https://doi.org/10.3390/polym17030256.

104. Ni, X., Feng, J., Liang, M., et al. Enhancing bone repair with β-TCP-based composite scaffolds: a review of design strategies and biological mechanisms. *Orthoped Res Rev*. 2025;17:313–340. https://doi.org/10.2147/ORR.S525959.

105. Wang, W., Liu, P., Zhang, B., et al. Fused deposition modeling printed PLA/nano β-TCP composite bone tissue engineering scaffolds for promoting osteogenic induction function. *Int J Nanomed*. 2023;18:5815–5830. https://doi.org/10.2147/IJN.S416098.

106. Kucko, S.K., Raeman, S.M., Keenan, T.J. Current advances in hydroxyapatite- and β-tricalcium phosphate-based composites for biomedical applications: a review. *Biomed Mat Devices*. 2023;1(1):49–65. https://doi.org/10.1007/s44174-022-00037-w.

107. Abodunrin, O.D., El Mabrouk, K., Bricha, M. A review on borate bioactive glasses (BBG): effect of doping elements, degradation, and applications. *J Mat Chem B*. 2023;11(5):955–973. https://doi.org/10.1039/D2TB02505A.

108. Chand, P., Malik, M., Prasad, T. Bioactive glass for applications in implants: a review. *Chem Select*. 2024;9(29):e202304337. https://doi.org/10.1002/slct.202304337.

109. Huang, C., Yu, M., Li, H., et al. Research progress of bioactive glass and its application in orthopedics. *Adv Mat Interfaces*. 2021;8(22):2100606. https://doi.org/10.1002/admi.202100606.

110. Al-Harbi, N., Mohammed, H., Al-Hadeethi, Y., et al. Silica-based bioactive glasses and their applications in hard tissue regeneration: a review. *Pharmaceuticals*. 2021;14(2):75. https://doi.org/10.3390/ph14020075.

111. Zhang, X., Zeng, D., Li, N., et al. Functionalized mesoporous bioactive glass scaffolds for enhanced bone tissue regeneration. *Sci Rep*. 2016;6:19361. https://doi.org/10.1038/srep19361.

112. de Lima Barbosa, R., Stellet Lourenço, E., de Azevedo dos Santos, J.V., et al. The effects of platelet-rich fibrin in the behavior of mineralizing cells related to bone tissue regeneration—a scoping review of in vitro evidence. *J Funct Biomat*. 2023;14(10):503. https://doi.org/10.3390/jfb14100503.

113. Blanco, J., García, A., Hermida-Nogueira, L., et al. How to explain the beneficial effects of leukocyte-and platelet-rich fibrin. *Periodontol 2000*. 2025;97(1):74–94. https://doi.org/10.1111/prd.12570.

114. Farshidfar, N., Apaza Alccayhuaman, K.A., Estrin, N.E., et al. Advantages of horizontal centrifugation of platelet-rich fibrin in regenerative medicine and dentistry. *Periodontol 2000*. 2025. https://doi.org/10.1111/prd.12625. Epub ahead of print. PMID: 40130760.

115. Tarallo, F., Mancini, L., Pitzurra, L., et al. Use of platelet-rich fibrin in the treatment of grade 2 furcation defects: systematic review and meta-analysis. *J Clin Med*. 2020;9(7):2104. https://doi.org/10.3390/jcm9072104.

116. Hwan Jung, M., Hun Lee, J., Wadhwa, P., et al. Bone regeneration in peri-implant defect using autogenous tooth biomaterial enriched with platelet-rich fibrin in animal model. *App Sci*. 2020;10(6):1939. https://doi.org/10.3390/app10061939.

117. On, S.W., Park, S.Y., Yi, S.M., et al. Current status of recombinant human bone morphogenetic protein-2 (rh-BMP-2) in maxillofacial surgery: should it be continued? *Bioengineering*. 2023;10(9):1005. https://doi.org/10.3390/bioengineering10091005.

118. Aghaloo, T., Valentini, P., Yardley, R., et al. Application of biologics in maxillary sinus augmentation surgery: a narrative review. *Clin Implant Dent Related Res*. 2025;27(3):e70004. https://doi.org/10.1111/cid.70004.

119. Soares, C.S., Babo, P.S., Faria, S., et al. Standardized platelet-rich fibrin (PRF) from canine and feline origin: an analysis on its secretome pattern and architectural structure. *Cytokine*. 2021;148:155695. https://doi.org/10.1016/j.cyto.2021.155695.

120. Nemcakova, I., Litvinec, A., Mandys, V., et al. Coating Ti-6Al-4V implants with nanocrystalline diamond functionalized with BMP-7 promotes extracellular matrix mineralization in vitro and faster osseointegration in vivo. *Sci Rep*. 2022;12(1):5264. https://doi.org/10.1038/s41598-022-09183-z.

121. Afrashtehfar, K.I., Abuzayeda, M.A., Murray, C.A. Artificial intelligence in reconstructive implant dentistry—current perspectives. *Prosthesis*. 2024;6(4):767–769. https://doi.org/10.3390/prosthesis6040054.

122. Memon, A.R., Li, J., Egger, J., et al. A review on patient-specific facial and cranial implant design using artificial intelligence (AI) techniques. *Expert Rev Med Devices*. 2021;18(10):985–994. https://doi.org/10.1080/17434440.2021.1969914.

123. Hu, C., Li, F., Wang, S., et al. The role of artificial intelligence in enhancing personalized learning pathways and clinical training in dental education. *Cogent Edu*. 2025;12(1):2490425. https://doi.org/10.1080/2331186X.2025.2490425.

124. Pitchika, V., Büttner, M., Schwendicke, F. Artificial intelligence and personalized diagnostics in periodontology: a narrative review. *Periodontol 2000*. 2024;95(1):220–231. https://doi.org/10.1111/prd.12586.

125. Kumar, N.V., Chakradhar, D., Abhilash, P.M. Advancing bioimplant manufacturing through artificial intelligence. In: *Bioimplants manufacturing*. 1st ed.; M, P.A., Gajrani, K.K., eds. CRC Press: Boca Raton, USA; 2024; pp. 284–312. https://doi.org/10.1201/9781003509943-13.

126. Najeeb, M., and Islam, S. Artificial intelligence (AI) in restorative dentistry: current trends and future prospects. *BMC Oral Health*. 2025;25(1):592. https://doi.org/10.1186/s12903-025-05989-1.

127. Elgarba, B.M., Fontenele, R.C., Tarce, M., et al. Artificial intelligence serving pre-surgical digital implant planning: a scoping review. *J Dent*. 2024;143:104862. https://doi.org/10.1016/j.jdent.2024.104862.

128. Yan, B., Zhang, W., Cai, L., et al. Optics-guided robotic system for dental implant surgery. *Chin J Mech Eng*. 2022;35(1):55. https://doi.org/10.1186/s10033-022-00732-1.

129. Huang, Y.C., Huang, Y.C., Ding, S.J. Primary stability of implant placement and loading related to dental implant materials and designs: a literature review. *J Dent Sci*. 2023;18(4):1467–1476. https://doi.org/10.1016/j.jds.2023.06.010.

130. Aiquel, L.L., Pitta, J., Antonoglou, G.N., et al. Does the timing of implant placement and loading influence biological outcomes of implant-supported multiple-unit fixed dental prosthesis—a systematic review with meta-analyses. *Clin Oral Implants Res*. 2021;32(Suppl 21):5–27. https://doi.org/10.1111/clr.13860.

131. D'Amico, C., Bocchieri, S., Sambataro, S., et al. Occlusal load considerations in implant-supported fixed restorations. *Prosthesis*. 2020;2(4):252–265. https://doi.org/10.3390/prosthesis2040023.

132. Zhao, G., Zhou, Y., Shi, S., et al. Long-term clinical outcomes of immediate loading versus non-immediate loading in single-implant restorations: a systematic review and meta-analysis. *Int J Oral Maxillofac Surg*. 2022;51(10):1345–1354. https://doi.org/10.1016/j.ijom.2022.03.057.

133. Francisco, H., Marques, D., Pinto, C., et al. Is the timing of implant placement and loading influencing esthetic outcomes in single-tooth implants?—a systematic review. *Clin Oral Implant Res*. 2021;32(Suppl 21):28–55. https://doi.org/10.1111/clr.13811.

134. Pardo-Zamora, G., Ortiz-Ruíz, A.J., Camacho-Alonso, F., et al. Short dental implants (≤ 8.5 mm) versus standard dental implants (≥10 mm): a one-year post-loading prospective observational study. *Int J Environ Res Public Health*. 2021;18(11):5683. https://doi.org/10.3390/ijerph18115683.

135. Yang, Q., Guan, X., Wang, B., et al. Implant survival rate and marginal bone loss with the all-on-4 immediate-loading strategy: a clinical retrospective study with 1 to 4 years of follow-up. *J Prost Dent*. 2023;130(6):849–857. https://doi.org/10.1016/j.prosdent.2021.12.020.

136. Valera-Jiménez, J.F., Burgueño-Barris, G., Gómez-González, S., et al. Finite element analysis of narrow dental implants. *Dent Mat*. 2020;36(7):927–935. https://doi.org/10.1016/j.dental.2020.04.013.

137. Atieh, M.A., Almutairi, Z., Amir-Rad, F., et al. A retrospective analysis of biological complications of dental implants. *Int J Dent*. 2022;2022:1545748. https://doi.org/10.1155/2022/1545748.

138. Chochlidakis, K., Ercoli, C., Einarsdottir, E., et al. Implant survival and biologic complications of implant fixed complete dental prostheses: an up to 5-year retrospective study. *J Prost Dent*. 2022;128(3):375–381. https://doi.org/10.1016/j.prosdent.2020.12.011.

139. Monje, A., and Nart, J. Management and sequelae of dental implant removal. *Periodontol 2000*. 2022;88(1):182–200. https://doi.org/10.1111/prd.12418.

140. Thoma, D.S., Gil, A., Hämmerle, C.H., et al. Management and prevention of soft tissue complications in implant dentistry. *Periodontol 2000*. 2022;88(1):116–129. https://doi.org/10.1111/prd.12415.

141. Kotsakis, G.A., and Romanos, G.E. Biological mechanisms underlying complications related to implant site preparation. *Periodontol 2000*. 2022;88(1):52–63. https://doi.org/10.1111/prd.12410.

142. Adler, L., Buhlin, K., Jansson, L. Survival and complications: a 9-to 15-year retrospective follow-up of dental implant therapy. *J Oral Rehab*. 2020;47(1):67–77. https://doi.org/10.1111/joor.12866.

143. Tsigarida, A., Chochlidakis, K., Fraser, D., et al. Peri-implant diseases and biologic complications at implant-supported fixed dental prostheses in partially edentulous patients. *J Prosthodont*. 2020;29(5):429–435. https://doi.org/10.1111/jopr.13165.

144. Silva, R.C., Agrelli, A., Andrade, A.N., et al. Titanium dental implants: an overview of applied nanobiotechnology to improve biocompatibility and prevent infections. *Materials*. 2022;15(9):3150. https://doi.org/10.3390/ma15093150.

145. Wychowański, P., Starzyńska, A., Adamska, P., et al. Methods of topical administration of drugs and biological active substances for dental implants—a narrative review. *Antibiotics*. 2021;10(8):919. https://doi.org/10.3390/antibiotics10080919.

146. Karlsson, K., Derks, J., Wennström, J.L., et al. Occurrence and clustering of complications in implant dentistry. *Clin Oral Implants Res*. 2020;31(10):1002–1009. https://doi.org/10.1111/clr.13647.

147. Roccuzzo, A., Imber, J.C., Marruganti, C., et al. Clinical outcomes of dental implants in patients with and without history of periodontitis: a 20-year prospective study. *J Clin Periodontol*. 2022;49(12):1346–1356. https://doi.org/10.1111/jcpe.13716.

148. D'Ambrosio, F., Amato, A., Chiacchio, A., et al. Do systemic diseases and medications influence dental implant osseointegration and dental implant health? An umbrella review. *Dent J*. 2023;11(6):146. https://doi.org/10.3390/dj11060146.

149. Urban, I., Sanz-Sánchez, I., Monje, A., et al. Complications and treatment errors in peri-implant hard tissue management. *Periodontol 2000*. 2023;92(1):278–298. https://doi.org/10.1111/prd.12472.

150. Cortes-Breton Brinkmann, J., García-Gil, I., Pedregal, P., et al. Long-term clinical behavior and complications of intentionally tilted dental implants compared with straight implants supporting fixed restorations: a systematic review and meta-analysis. *Biology*. 2021;10(6):509. https://doi.org/10.3390/biology10060509.

151. Lampkin, A., Bensoussan, J., Curtis, D., et al. Effect of self-reported clinician experience level on perceptions of the relative rankings of risk factors for biological complications with dental implant therapy. *J Prosth Dent*. 2025;133(1):209–214. https://doi.org/10.1016/j.prosdent.2023.03.019.

152. Schwarz, F., and Ramanauskaite, A. It is all about peri-implant tissue health. *Periodontol 2000*. 2022;88(1):9–12. https://doi.org/10.1111/prd.12407.

153. Dioguardi, M., Spirito, F., Quarta, C., et al. Guided dental implant surgery: systematic review. *J Clin Med*. 2023;12(4):1490. https://doi.org/10.3390/jcm12041490.

154. Schierz, O., and Reissmann, D.R. Dental patient-reported outcomes—the promise of dental implants. *J Evid Dent Pract*. 2021;21(1):101541. https://doi.org/10.1016/j.jebdp.2021.101541.

155. Wang, I.C., Barootchi, S., Tavelli, L., et al. The peri-implant phenotype and implant esthetic complications. Contemporary overview. *J Esthet Restor Dent*. 2021;33(1):212–223. https://doi.org/10.1111/jerd.12709.

156. Cervino, G., Meto, A., Fiorillo, L., et al. Surface treatment of the dental implant with hyaluronic acid: an overview of recent data. *Int J Environ Res Public Health*. 2021;18(9):4670. https://doi.org/10.3390/ijerph18094670.

157. Comino-Garayoa, R., Cortés-Bretón Brinkmann, J., Peláez, J., et al. Allergies to titanium dental implants: what do we really know about them? A scoping review. *Biology*. 2020;9(11):404. https://doi.org/10.3390/biology9110404.

158. Cortellini, P., Stalpers, G., Mollo, A., et al. Periodontal regeneration versus extraction and dental implant or prosthetic replacement of teeth severely compromised by attachment loss to the apex: a randomized controlled clinical trial reporting 10-year outcomes, survival analysis and mean cumulative cost of recurrence. *J Clin Periodontol*. 2020;47(6):768–776. https://doi.org/10.1111/jcpe.13289.

159. Barrak, F.N., Li, S., Muntane, A.M., et al. Particle release from implantoplasty of dental implants and impact on cells. *Int J Implant Dent*. 2020;6(1):50. https://doi.org/10.1186/s40729-020-00247-1.

160. Agliardi, E.L., Panigatti, S., Romeo, D., et al. Clinical outcomes and biological and mechanical complications of immediate fixed prostheses supported by zygomatic implants: a retrospective analysis from a prospective clinical study with up to 11 years of follow-up. *Clin Implant Dent Related Res*. 2021;23(4):612–624. https://doi.org/10.1111/cid.13017.

161. Omori, Y., Lang, N.P., Botticelli, D., et al. Biological and mechanical complications of angulated abutments connected to fixed dental prostheses: a systematic review with meta-analysis. *J Oral Rehab*. 2020;47(1):101–111. https://doi.org/10.1111/joor.12877.

Received February 7, 2025, accepted July 25, 2025, publication date for online-first December 21, 2025.

Original Research Article

Disruptive Technological Innovation Through Ambulatory Blood Pressure Monitoring and Telemedicine for Patients with Cardiovascular Risk

Pedro Galván[1,2,*], José Ortellado[2], Santiago Servín[2], María Teresa Barán[2] and Enrique Hilario[3]

[1] German-Paraguayan University, Paraguay.
[2] Ministry of Public Health and Welfare, Asunción, Paraguay.
[3] Medical School, Basque Country University, Bilbao, Spain.

[*] Corresponding Author Email: pedro.galvan@upa.edu.py

ABSTRACT

Objective: To study the feasibility of using telematics as an innovative method for diagnosing patients with arterial hypertension, using blood pressure curves recorded at regular intervals over 24 hours, obtained by means of an Ambulatory Blood-Pressure Monitoring (ABPM) device and a telemedicine platform.

Methods: Between August 2023 and December 2024, a multicenter descriptive observational feasibility study was conducted based on the 24-hour remote assessment of blood pressure readings—every 30 minutes during the day and every 60 minutes at night—in hypertensive patients who attended public hospitals. The diagnosis of blood pressure curves obtained remotely with ABPM was carried out through a telemedicine platform. Subsequently, a team of cardiologists evaluated the results to determine their feasibility for the diagnosis and management of high blood pressure in remote patients. Blood pressure curves and diagnostic results were sent via a telemedicine platform.

Results: The remote study of 64 patients with high cardiovascular risk was conducted in 10 hospitals nationwide. Most patients were between 50 and 54 years old, followed by the 40 to 44 and 65 to 69 age groups. The mean age was 54.0 years, and 53.4% were male.

Among the patients, 50.0% had hypertension, 40.0% had uncontrolled hypertension, and 10.0% had normal blood pressure. An average of 40% adherence to treatment was determined among patients diagnosed with hypertension.

Conclusions: Our results suggest that it is feasible to use this disruptive technological innovation for the development of a remote, resilient capacity for the diagnosis of patients with high cardiovascular risk through ABPM and a telemedicine platform in public hospitals without cardiology services in Paraguay. In any case, a larger sample size will be required to validate and generalize the study results.

Keywords—*Tele-ABPM, Hypertension, Cardiovascular risk, Telemedicine, Telediagnosis, Digital technology, Paraguay.*

INTRODUCTION

Arterial hypertension is a very prevalent pathology worldwide (approximately 40%)[1] and represents a relevant public health problem, according to the World Health Organization (WHO). According to the latest 2021 update of the WHO Global Health Observer, the prevalence of hypertension in the Paraguayan population in the age group of 30 to 79 years was 61.6% among men and 50.9% among women.[2]

Hypertension is one of the most important risk factors for chronic cardiovascular, cerebrovascular, and renal diseases. In general, most hypertensive patients are undiagnosed, and only one-fifth of hypertensive patients have adequate blood pressure values. The gold standard for determining blood pressure is the blood pressure monitor, or sphygmomanometer, which uses an inflatable cuff connected to a pressure gauge and the aid of a stethoscope. Measurements may be affected by the positioning and arrangement of the inflatable cuff, as well as the calibration of the device, which needs to be performed periodically.

Ambulatory blood pressure monitoring (ABPM) is recommended for patients with elevated blood pressure, those with unstable blood pressure, or those suffering from the white coat phenomenon or masked hypertension.[3] The ABPM device is an essential element for the diagnosis and monitoring of hypertension in patients with fluctuating blood pressures. For this, the use of validated (calibrated) devices and good practice techniques is required to ensure strict diagnostic control and monitoring over a period of 24 hours. It allows measurement of a patient's blood pressure by observing its variations in relation to different times and activities of the day. However, the use of the ABPM method in clinical practice is limited by factors such as the cost of the device, accessibility, and basic training of both physicians and patients,[3] especially in middle-income countries such as Paraguay. In addition, ABPM provides data on many important parameters to define the profile and variability of hypertension, in order to classify the patient into a group of phenotypes, which cannot be obtained with any other form of blood pressure measurement.[4] For all these reasons, ABPM is considered the gold standard for diagnosing hypertension and evaluating the usefulness of antihypertensive therapy, according to the guidelines of the National Institute for Health and Clinical Excellence (NICE) in the United Kingdom.[5]

This study aims to improve the diagnostic capacity and follow-up of treatment for arterial hypertension in patients from public hospitals without cardiology services in Paraguay, to mitigate cardiovascular events in hypertensive patients by facilitating accessibility and universal coverage through the technological innovation proposed in this study. The specific challenges of our study involve anticipating cardiovascular events and carrying out appropriate interventions to avoid them, in order to impact universal coverage of patients with cardiovascular risk, reduce risk through adequate treatment, and minimize healthcare costs in a low-resource country. Thus, we consider that the ABPM method with telemedicine tools is particularly relevant in Paraguay for the initiation, follow-up, and control of antihypertensive therapy at the national level due to the high prevalence of arterial hypertension in the population. However, this is the first time that this type of study (joint ABPM and telemedicine) is carried out in Paraguay. This study intends to resolve existing problems in a low-income country and seek universal ABPM service coverage with a high standard level.

It should be noted that the technological innovation proposed in this study is not intended to replace diagnosis in a family medicine or cardiology service, but rather to improve accessibility to ABPM technology and, in this way, facilitate early diagnosis and appropriate treatment, avoiding unnecessary transfers of patients with high cardiovascular risk. This makes it possible to reduce overcrowding in specialized centers and optimize the use of the always-limited resources available in public hospitals. Another aspect to highlight is that, in order to implement the Tele-ABPM service, the telemedicine technician is considered a non-medical professional responsible for placing the ABPM device on the patient and then, after 24 hours, removing it to transfer all the recordings of the blood pressure curves to the telemedicine platform; following a protocol developed by cardiologists from the Cardiovascular Prevention Service of the Ministry of Public Health and Social Welfare (MSPBS).

In this context, the Paraguayan German University (UPA), in collaboration with the Directorate of Telemedicine and the National Cardiovascular Prevention Program (PNPC) of the MSPBS, carried out this study to evaluate the feasibility of using telematics as an innovative, disruptive method for the diagnosis, follow-up, and control of patients with arterial hypertension. We used blood pressure curves recorded by ABPM and a telemedicine platform in public hospitals without cardiology services in Paraguay.

MATERIALS AND METHODS

A descriptive research design was used to investigate the feasibility of a remote ABPM diagnostic service using a telemedicine platform. The multicenter, cross-sectional descriptive study was carried out between August 2023 and March 2024 in 10 regional public hospitals countrywide without cardiology services in the health regions of the MSPBS. The reporting of this study conforms to the Strengthening the Reporting of Observational Studies in Epidemiology (STROBE) Statement: guidelines for reporting observational cross-sectional studies. The completed checklist, as a supplementary file, can be found as Annex 1, according to Enhancing the QUAlity and Transparency Of health Research.

The diagnosis and remote monitoring of patients with arterial hypertension were performed using the following technological components, following the specific data collection protocol for each component to avoid potential sources of bias:

- The device for ambulatory blood pressure monitoring (ABPM) was used to record all information on blood pressure curves at regular intervals for 24 hours—every 30 minutes during the day and every 60 minutes at night—in hypertensive patients who attended the 10 public regional hospitals of the MSPBS. The ABPM and the management of the recordings of the pressure curves were carried out with an exclusive computer where the digital recordings were downloaded in the device's proprietary format and then processed with proprietary software and stored in the database through a web application. The measuring devices (ABPM) used in the study were validated according to the protocol of the European Society of Hypertension.[6] The ABPM devices used were from a single manufacturer (Eccosur, model MP260, manufacturing year 2022, www.eccosur.com). The measurements of the blood pressure have a precision of ± 5 mmHg for systolic (60–230 mmHg) and diastolic (40–130 mmHg) pressure with a 95% confidence interval.
- The telemedicine system, based on information and communication technology (ICT) tools, was used to send digital records of the blood pressure curves obtained by the ABPM device in the 10 regional hospitals of the Tele-ABPM network. The patient's clinical data was attached to the recording of the blood pressure curves through an electronic chart that the telemedicine technician then sends encrypted (SSL type) to the telemedicine platform hosted in the cloud. The digital technology used for the transmission of the images is called store & forward, in which, once the blood pressure curves have been obtained, the patient's electronic record module (web application) is executed for the patient's clinical data and blood pressure curves collection. The communication of the results of diagnosis, monitoring, and control from the remote cardiologists to the doctors responsible for the patient's treatment was carried out through the same telemedicine platform.

The strategy for the diagnosis, monitoring, and control of patients with arterial hypertension was carried out in the following sequence, see Figure 1:

- All patients who met the inclusion criteria underwent ABPM by telemedicine technicians (remote) according to the protocol for recording blood pressure curves established by cardiologists in the 10 hospitals of the Tele-ABPM network, which were also regional referral hospitals for ABPM.
- The cardiologists of the telemedicine diagnosis, monitoring, and control service downloaded the blood pressure curve records from the platform along with the patient's clinical data and carried out the corresponding diagnosis, monitoring, and control in a predefined and standardized format.

• The remote cardiologist's diagnosis, monitoring, and control report was then sent to the attending physician of the hospital where the patient was being treated via the telemedicine platform. Depending on the severity of the pathology, the patient was referred to a specialized cardiology hospital or to its outpatient clinic to receive antihypertensive treatment.

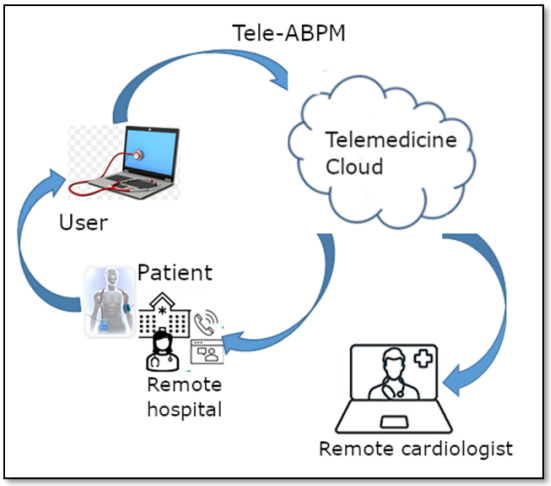

FIGURE 1. Implementation steps for the data transmission process of Tele-ABPM.

Inclusion Criteria

Patients with suspected or confirmed elevated blood pressure, especially those with unstable blood pressure or suffering from the white coat phenomenon or masked hypertension, were included. Hospitals without cardiology services were selected to recruit patients.

Exclusion Criteria

Patients with signs and symptoms that were not compatible with high blood pressure.

Population

Patients with arterial hypertension of varying severity, with a medical request for diagnosis by ABPM, were included. Patient recruitment was carried out through outpatient consultations and emergency services in the 10 regional hospitals of the MSPBS Tele-ABPM network, using a prospective sequential sampling strategy to reach the study size.

Statistical Analysis

According to the study population, design, factor of interest, and results, descriptive statistics (figures) were used to present the data of the studied population. For quantitative and qualitative variables, statistical methods such as frequency distribution, trends, dispersion, averages, and comparisons, among others, were used to analyze the outcomes. To avoid or control confounding and missing data, a consistency check was performed according to a data collection protocol. Interactions of data subgroups and sensitivity analyses were conducted using an analysis protocol defined by the cardiologists of the Cardiovascular Prevention Institute of the MSPBS.

Ethical and Confidentiality Issues

Prior to the study, all patients were informed about its purpose and informed consent was obtained. To ensure the confidentiality of the information, as well as its integrity and consistency, security mechanisms were used in the telemedicine platform, including controlled access to the system (username and password), prioritized queries by type of user, encrypted databases, encrypted communication such as secure sockets layer (SSL), encryption keys, and encryption protocols that provide secure communication. The research protocol was approved by the scientific and ethical committees of the Institute for Research in Health Sciences of the National University of Asunción; the ethics committee approval number is P38/2020.

Satisfaction Survey

To measure the usefulness and satisfaction with the technological innovation implemented in this study, a semi-structured online satisfaction survey was administered to users. A scale from 1 to 5 was used, with 1 being very poor and 5 being excellent. The 5 cardiologists reporting ABPM (100%), the 10 telemedicine technicians (100%)—including radiology technicians, nurses, and nursing assistants who worked as telemedicine technicians—and all patients diagnosed by this innovative remote service were surveyed.

RESULTS

Sixty-four patients with high cardiovascular risk were diagnosed in 10 hospitals nationwide. Most patients were between 50 and 54 years old, followed by the age groups 40 to 44 and 65 to 69 years, as shown in Figure 2. The average age was 54 years; 53.4% were male. The most frequent findings were hypertension (50%), uncontrolled hypertension (40%), and normal blood pressure (10%). An average of 40% adherence to antihypertensive treatment among patients diagnosed with hypertension was determined by the National Cardiovascular Prevention Program according to their established treatment protocol.

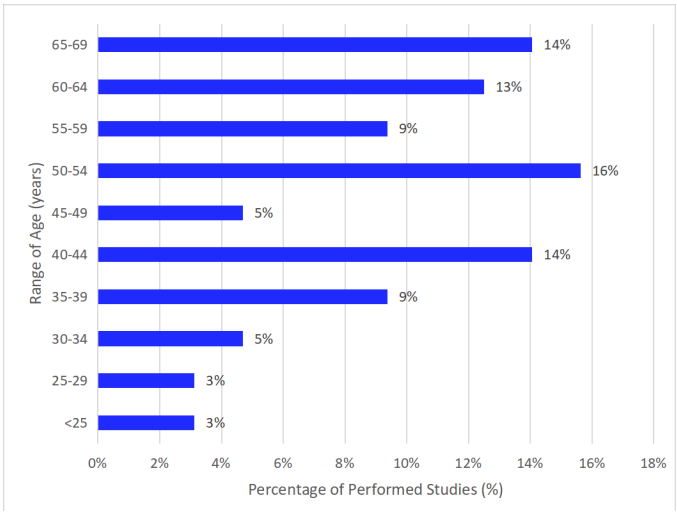

FIGURE 2. Age range of patients diagnosed by ABPM (n = 64).

The hemodynamic parameters determined and assessed by ABPM over 24 hours in the present study for mean systolic arterial pressure were as follows (Figure 3): 20.3% hypertension and 79.7% normal blood pressure. For mean diastolic blood pressure, 32.8% had hypertension and 67.2% had normal blood pressure.

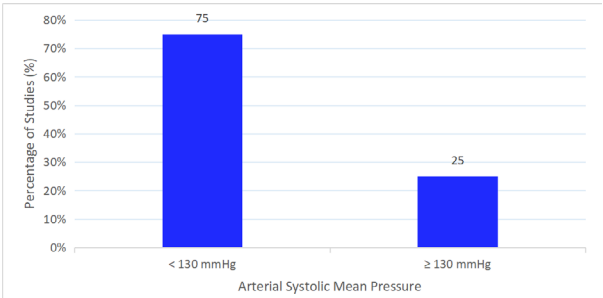

FIGURE 3. Mean systolic (24 hours) arterial pressure diagnosed by ABPM (n = 64).

For the mean diurnal systolic arterial pressure (Figure 4), 23.4% had hypertension and 76.6% had normal blood pressure. For the mean diurnal diastolic arterial pressure, 28.1% had hypertension and 71.9% had normal blood pressure.

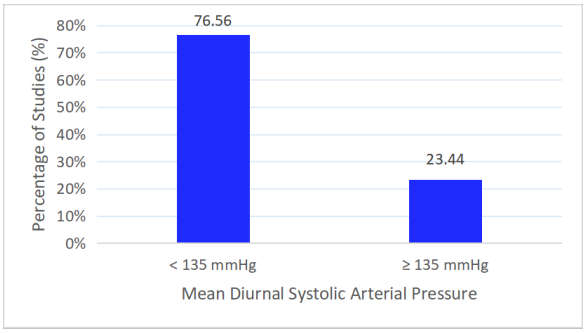

FIGURE 4. Mean diurnal systolic arterial pressure diagnosed by ABPM (n = 64).

For the mean nocturnal systolic arterial pressure (Figure 5), 35.9% had hypertension and 64.1% had normal blood pressure. For the mean nocturnal diastolic blood pressure, 60.9% had hypertension and 39.1% had normal blood pressure.

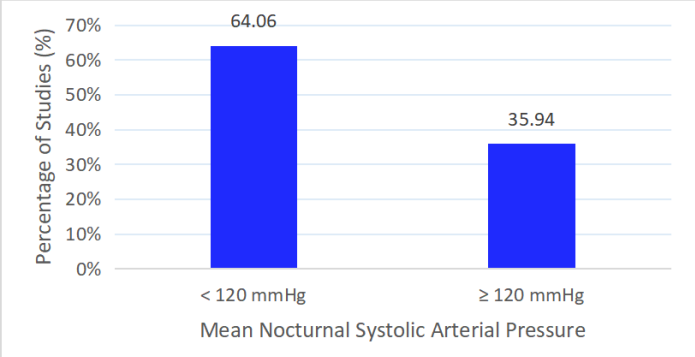

FIGURE 5. Mean nocturnal systolic arterial pressure diagnosed by ABPM (n = 64).

The heart rate range (Figure 6) was 47.0% between 65–74 bpm and 28.0% between 75–84 bpm. The percentage of systolic burden was 35.9% pathological and 64.1% non-pathological. The percentage of diastolic burden was 39.1% pathological and 60.9% non-pathological.

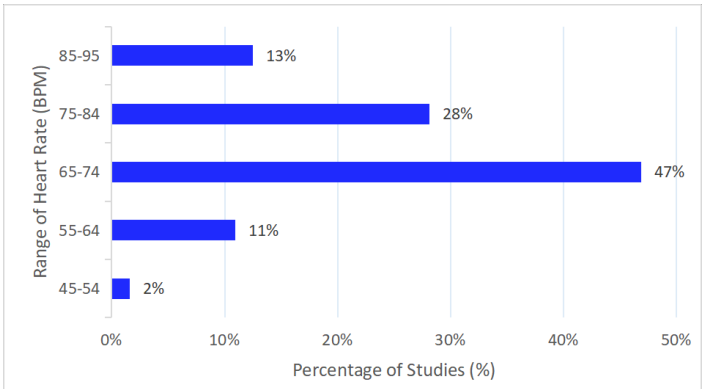

FIGURE 6. Heart rate range diagnosed by ABPM (*n* = 64).

Pulse pressure (Figure 7) was 27.0% pathological and 73.0% non-pathological. Among the main reasons for performing ambulatory blood pressure monitoring were arterial hypertension (40.6%), chest pain (17.2%), white coat hypertension (4.7%), dyspnea (3.1%), masked hypertension (1.6%), and uncontrolled hypertension (1.6%).

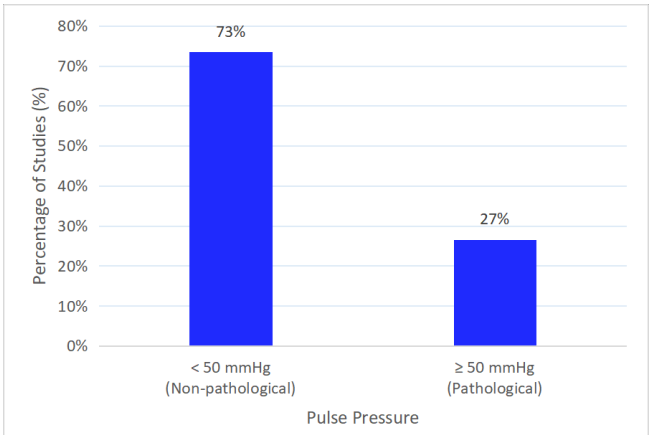

FIGURE 7. Pulse pressure of patients diagnosed by ABPM (*n* = 64).

Satisfaction with the Remote Diagnostic Service

The degree of satisfaction expressed by patients using the Tele-ABPM service regarding the care received from remote specialists was rated as "excellent" by 94.6%. Additionally, all reporting physicians and telemedicine technicians stated that they "agreed" (62.5%) or "strongly agreed" (37.5%)—the highest rating—with the ease of use and quality of care offered by the Tele-ABPM system. Among the most frequent complaints reported by patients were sweating of the arm with the bracelet (40.0%) and difficulty falling asleep due to the inflation of the bracelet (40.0%). For the reporting technicians and physicians, the most common difficulties were internet service instability (13.0%), disconnection of the ABPM bracelet tubing during measurements (7.0%), and limitations in using computer tools (3.0%). Missing data were identified in 7.0% of all patients, mainly due to disconnection of the ABPM bracelet during the measurement process, particularly overnight.

DISCUSSION

Taking into account the high prevalence of arterial hypertension in the country[2] and the need for a system that is accessible and universally available within the public services of the MSPBS for the diagnosis, monitoring, and control of high-risk hypertensive patients, the ABPM method was used in the present study because it is the most widely recommended[5,7] for detecting, recording, and analyzing variations in blood pressure, pulse pressure, heart rate, and the dipper phenomenon.[5,8,9] The dipper phenomenon refers to the variations observed when evaluating the percentage ratio between the average blood pressure during sleep and the average blood pressure during wakefulness. A patient is considered a dipper, or having a nocturnal drop in blood pressure, when there is a decrease greater than or equal to 10% in systolic and/or diastolic blood pressure during sleep compared to wakefulness.

In this study, 58 patients with high cardiovascular risk were identified using the ABPM device, which is recommended by several national and international institutions[4–6,10,11] for confirming diagnosis, monitoring hypertension, and evaluating the effectiveness of pharmacological treatment. The diagnostic model developed and applied in this feasibility study combined the ABPM device with telemedicine tools, representing an innovative and disruptive approach for the country's public health. This approach offers technology considered the gold standard for diagnosing arterial hypertension, making it feasibly accessible to the population and universally covered across health regions through the MSPBS telemedicine platform.[12] One of the major advantages of this technological innovation is its potential to anticipate serious cardiovascular

events and enable timely interventions to prevent them. Based on the results obtained, health authorities adopted a proactive stance to control arterial hypertension in the studied population by providing free antihypertensive medication within the service areas of the Tele-ABPM units implemented in the 10 regional hospitals. This strategy was utilized by the Cardiovascular Prevention Institute of the Ministry of Health to improve treatment adherence among hypertensive patients.

The hemodynamic parameters determined and assessed in this study through ABPM are consistent with findings from similar research and hold diagnostic significance according to scientific literature. Specifically, the pulse pressure differential (the difference between systolic and diastolic pressure) is considered an indirect predictor of adverse cardiovascular and cerebrovascular outcomes,[5,13–16] which are attributed to arterial stiffness. In this context, other studies have found that untreated hypertensive patients exhibiting the dipper phenomenon have higher arterial stiffness compared to non-dipper patients, with stiffness values inversely related to nocturnal decreases in blood pressure.[5,17,18] Additionally, research has identified pulse pressure variability, dipper status, and systolic and diastolic blood pressure as independent predictors of arterial stiffness.[5,19]

Patients rated the accessibility of this diagnostic method within their communities very positively. Regarding the usability of the ABPM system, the main complaints were sweating under the bracelet and the annoying noise caused by the periodic inflation of the device's cuff.[20–22] For telemedicine technicians and physicians, the primary advantages included the ease of use of the Tele-ABPM web application. The most frequently reported challenges were internet service instability, disconnection of the ABPM cuff during measurements, and limitations in using computer tools. The satisfaction survey results from this study aim to provide valuable feedback from both patients and technical users to enhance the Tele-ABPM system's usability and align with findings from similar studies.[20–22]

As with any patient diagnostic system, Tele-ABPM has both advantages and disadvantages. Among the advantages, three stand out: 1) Ambulatory blood pressure monitoring (ABPM) is recommended for patients with elevated or unstable blood pressure, including those experiencing the white coat phenomenon or masked hypertension; 2) The ABPM device is essential for diagnosing and monitoring hypertension in patients with fluctuating blood pressures; 3) It enables measurement of blood pressure variations throughout different times and daily activities. Regarding disadvantages, four points are notable: 1) Clinical use of ABPM is limited by factors such as device cost, accessibility, and the need for basic training for both physicians and patients; 2) Serious risks from ambulatory blood pressure monitoring are rare; 3) Minor side effects reported include pain or discomfort (9%), skin irritation (8%), noise from the device (8%), and inconvenience at work (3%); 4) A minority of patients report sleep disturbances, although the vast majority eventually adapt to the monitor.

The results of this pilot study are very promising, as they enable cross-referencing of hemodynamic parameters to assess the indirect predictive capacity of factors such as dipper status, pulse pressure variability, and others for adverse cardiovascular and cerebrovascular outcomes. Consequently, it can be concluded that this innovative combination of the ABPM device with telemedicine has the potential to mitigate the limited availability of adequately equipped cardiology centers and specialized staff to meet demand. However, data saturation (sample size) was not reached in this study, and a larger sample size will be necessary to validate and generalize these findings. The results are consistent with similar research.[22,23] This is especially important for public hospitals without cardiology services, as it offers a viable alternative to optimize the use of scarce human and technological resources, while promoting equity and universal access to advanced diagnostic technologies in low-income countries such as Paraguay. These findings suggest that it is possible to overcome the socioeconomic barriers that currently limit the widespread use of such technologies in resource-constrained settings.[23–27] Additionally, this innovative approach provides important benefits to patients, including early diagnosis and timely treatment,

which helps avoid unnecessary transfers of patients at high cardiovascular and cerebrovascular risk.[25] It is expected that an increase in the number of diagnosed and subsequently treated patients will translate into clinical benefits and overall population health improvements.[26] However, the real impact of this intervention on patient health outcomes will be assessed in a planned future study focused on clinical endpoints. Moreover, this approach reduces out-of-pocket expenses for patients by minimizing transfers, easing overcrowding in specialized centers, and optimizing the limited resources available within public hospitals.

Among the main limitations of this study are the limited number of ABPM devices available in district hospitals and health centers, as well as the scarcity of research focused on improving the scientific evidence regarding the classification of hypertensive patients into phenotypic groups within the country, which is essential for enhancing cardiovascular and cerebrovascular prevention programs and enabling early intervention to prevent adverse events. The observed 40% adherence rate to antihypertensive treatment among patients is concerning and indicates a need for additional support mechanisms to improve adherence, especially in remote settings. Our findings suggest that the primary factor contributing to low adherence is the geographical distance between patients and treatment centers, which, according to the Ministry of Health's Cardiovascular Prevention Institute strategy, could be addressed by expanding Tele-ABPM services closer to rural and underserved communities.

CONCLUSIONS

In this preliminary study, we aimed to improve the diagnosis, monitoring, and control of patients with high cardiovascular risk across 10 public hospitals in Paraguay without cardiology services by evaluating the feasibility of an innovative telematics approach using Ambulatory Blood Pressure Monitoring (ABPM) devices integrated with a telemedicine platform. Our results revealed a high prevalence of hypertension (50%), uncontrolled hypertension (40%), and normal blood pressure (10%) among the studied population, with an average adherence to antihypertensive treatment of only 40%. Despite these challenges, the findings are encouraging as they suggest potential improvements in both patient outcomes and public health system efficiency through better resource optimization. Importantly, patient satisfaction with the Tele-ABPM service and care from remote specialists was rated as excellent, underscoring the promise of this technological innovation to enhance accessibility and management of hypertension in resource-limited settings.

This tool also holds significant potential for monitoring the progress of hypertensive patients undergoing antihypertensive treatment in remote communities with limited access to specialized healthcare professionals, particularly in middle- and low-income countries. Additionally, it could be valuable in higher-income countries, where healthcare resources might be reallocated to other pressing health programs. Nevertheless, to validate and generalize these promising findings, studies with larger sample sizes will be necessary.

ANNEX

EQUATOR, https://www.equator-network.org/reporting-guidelines/strobe/. Retrieved July 5, 2024.

AUTHOR CONTRIBUTIONS

Conceptualization, P.G. and E.H.; Methodology, P.G. and E.H; Software, S.S.; Validation, P.G., J.O., S.S., and E.H.; Formal Analysis, P.G., J.O., and E.H.; Investigation, P.G. and E.H.; Resources, S.S. and M.B.; Data Curation, S.S.; Writing–Original Draft Preparation, P.G.; Writing–Review & Editing, E.H.; Visualization, S.S.; Supervision, M.B.; Project Administration, P.G.; Funding Acquisition, J.J.

ACKNOWLEDGMENTS

We would like to thank Joshua Harper for editing and all the institutions that have supported the development of the disruptive remote diagnosis system, in particular the Directorate-General of the Cabinet (DGG), the Directorate of Information Technologies (DGTIC), the General

Directorate for the Development of Health Services and Networks (DGSRS), the General Directorate of Human Resources (DGRRHH) of the Ministry of Public Health and Social Welfare (MSPBS) of the Republic of Paraguay for the institutional support received for the implementation of this system.

CONFLICTS OF INTEREST

The authors declare no conflict of interest.

FUNDING

The author(s) received no financial support for the research, authorship, and/or publication of this article.

ETHICS APPROVAL AND CONSENT TO PARTICIPATE

The research protocol was approved by the scientific and ethical committees of the Institute for Research in Health Sciences at the National University of Asunción, in accordance with the ethical principles of the Declaration of Helsinki. The ethics committee approval number is P38/2020.

INFORMED CONSENT/PATIENT CONSENT

Before the study, all patients were informed about its purpose, and informed consent was obtained. To ensure the confidentiality, integrity, and consistency of the information, security mechanisms were implemented in the telemedicine platform.

TRIAL REGISTRATION NUMBER/DATE

The research protocol was approved by the scientific and ethical committees of the Institute for Research in Health Sciences at the National University of Asunción (Approval No.: P38/2020).

DATA AVAILABILITY STATEMENT

The data that support the findings of this study are available on request from the corresponding author, Dr. Pedro Galván.

CONSENT FOR PUBLICATION

Before the study, all patients were informed about its purpose, and informed consent was obtained. To ensure the confidentiality, integrity, and consistency of the information, security mechanisms were implemented in the telemedicine platform.

FURTHER DISCLOSURE

Not applicable.

REFERENCES

1. World Health Organization. Global Health Observatory (GHO) data. Raised blood pressure. Available online: https://www.who.int/data/gho/data/themes/topics/topic-details/GHO/ncd-risk-factors.
2. World Health Organization. Global Health Observatory (GHO) data. Raised blood pressure. Available online: https://www.who.int/data/gho/data/indicators/indicator-details/GHO/prevalence-of-hypertension-among-adults-aged-30-79-years.
3. Kario,K., Hoshide,S., Chia, Y.C., et al. Guidance on ambulatory blood pressure monitoring: A statement from the HOPE Asia Network. *J Clin Hypertens (Greenwich)*. 2021;23(3):411–21. https://doi.org/10.1111/jch.14128.
4. Hodgkinson, J., Mant, J., Martin, U., et al. Relative effectiveness of clinic and home blood pressure monitoring compared with ambulatory blood pressure monitoring in diagnosis of hypertension: systematic review. *BMJ (Clinical research ed.)*. 2011;342:d3621. https://doi.org/10.1136/bmj.d3621.
5. O'Brien, E., Parati, G., Stergiou, G., et al. European Society of Hypertension position paper on ambulatory blood pressure monitoring. *J Hypertens*. 2013;31(9):1731–68. https://doi.org/10.1097/HJH.0b013e328363e964.
6. 2018 ESC/ESH Guidelines for the management of arterial hypertension. European Society of Hypertension; 2018. Available online: https://www.eshonline.org/guidelines/arterial-hypertension/.
7. Hamada, T., Murata, T., Narita, K., et al. The clinical significance of abnormal diurnal blood pressure variation in healthy late middle-aged and older adults. *Blood Press*. 2008;17(3):134–40. https://doi.org/10.1080/08037050802162839.
8. Turner,J.R., Viera, A.J., Shimbo, D. Ambulatory Blood Pressure Monitoring in Clinical Practice: A Review. *Am J Med*. 2015;128:14-20. https://doi.org/10.1016/j.amjmed.2014.07.021.

9. Redon, J. The Importance of 24-Hour Ambulatory Blood Pressure Monitoring in Patients at Risk of Cardiovascular Events. *High Blood Press Cardiovasc Prev*. 2013;20:13-8. https://doi.org/10.1007/s40292-013-0006-3.
10. Hermida, R.C., Smolensky, M.H., Ayala, D.E., et al. Ambulatory Blood Pressure Monitoring (ABPM) as the reference standard for diagnosis of hypertension and assessment of vascular risk in adults. *Chronobiol Int*. 2015;32(10):1329–42. https://doi.org/10.3109/07420528.2015.1113804.
11. JCS Joint Working Group. Guidelines for the Clinical Use of 24 Hour Ambulatory Blood Pressure Monitoring (ABPM) (JCS 2010). *Circ J*. 2012;76:508-19. https://doi.org/10.1253/circj.cj-88-0020.
12. Galván, P., Velázquez, M., Benítez, G., et al. Impact on public health of the telediagnosis system implemented in Paraguay. *Rev Panam Salud Pública*. 2017;41:e74. https://doi.org/10.26633/RPSP.2017.74.
13. Weber, M.A., Neutel, J.M., Smith, D.H., et al. Diagnosis of mild hypertension by ambulatory blood pressure monitoring. *Circulation*. 1994;90(5):2291–2298. https://doi.org/10.1161/01.cir.90.5.2291.
14. The sixth report of the Joint National Committee on prevention, detection, evaluation, and treatment of high blood pressure. Arch Intern Med. 1997 Nov 24;157(21):2413-46. doi: 10.1001/archinte.157.21.2413. Erratum in: Arch Intern Med 1998 Mar 23;158(6):573. PMID: 9385294.
15. Gorostidi, M., Sobrino, J., Segura, *J., Sierra*, C., et al. Ambulatory blood pressure monitoring in hypertensive patients with high cardiovascular risk: a cross-sectional analysis of 20,000-patient database in Spain. J Hypertens. 2007;25:977–84. https://doi.org/10.1097/HJH.0b013e32809874a2.
16. Thijis, L., Hansen, T., Kikuya, M., et al. The International Database of Ambulatory blood pressure in relation to Cardiovascular Outcome (IDACO). *Blood Press Monit*. 2007;12(4):255–62. https://doi.org/10.1097/mbp.0b013e3280f813bc.
17. Qin, T., Jiang, H., Jiao, Y., et al. Ambulatory arterial stiffness index correlates with ambulatory pulse pressure but not dipping status in patients with grade 1/grade 2 essential hypertension. *J Int Med Res*. 2014;42(6):1323–34. https://doi.org/10.1177/0300060514548288.
18. Schillaci, G., Parati, G., Pirro, M., et al.. Ambulatory Arterial Stiffness Index Is Not a Specific Marker of Reduced Arterial Compliance. *Hypertension*. 2007;49:986–91. https://doi.org/10.1161/HYPERTENSIONAHA.106.082248.
19. Lee, H.T., Lim, Y.H., Kim, B.K., et al. The Relationship between Ambulatory Arterial Stiffness Index and Blood Pressure Variability in Hypertensive Patients. *Korean Circ J*. 2011;41:235–40. https://doi.org/10.4070/kcj.2011.41.5.235.
20. García, M., Caraballo, C., Hincapié, A., et al. Behavior of hemodynamic parameters evaluated by 24-hour ambulatory blood pressure monitoring. *Colomb J Cardiol*. 2016;23(6):487–94. https://doi.org/10.1016/j.rccar.2016.04.003.
21. Giraldo, M.L., Ibero, G.P., García, H.I. Comparison of serial blood pressure measurement and ambulatory monitoring for the diagnosis of essential hypertension in a Colombian population. *Rev Col Cardiol*. 2013;20(6):342–51. https://doi.org/10.1016/S0120-5633(13)70081-0.
22. Galván, P., Velázquez, M., Rivas, R., et al. Health diagnosis improvement in remote community health centers through telemedicine. *Medicine Access @ Point of Care*. 2018;2. https://doi.org/10.1177/239920261775310.
23. Westbrook, J.I., Braithwaite, J., Gibson, K., et al. Use of information and communication technologies to support effective work practice innovation in the health sector: a multi-site study. *BMC Health Serv Res*. 2009;9:201. https://doi.org/10.1186/1472-6963-9-201.
24. Systematic review of literature on telemedicine. *Rev Panam Salud Pública*. 2001;10(4):257–8. https://doi.org/10.1590/S1020-49892001001000006.
25. Galván, P., Velázquez, M., Rivas, R., et al. Health diagnosis improvement in remote community health centers through telemedicine. *Med Access Point Care*. 2018;2:1–4. https://doi.org/10.1177/2399202617753101.
26. Parati, G., Stergiou, G., O`Brein, E., et al. European Society of Hypertension practice Guidelines for ambulatory blood pressure monitoring. *J Hypertens*. 2014;32:1359–66. https://doi.org/10.1097/HJH.0000000000000221.
27. Gijón-Conde, T., Gorosti, M., Banegas, J.R., et al. Position statement on ambulatory blood pressure monitoring (ABPM) by the Spanish Society of Hypertension (2019). *Hipertens Riesgo Vasc*. 2019;36(4):199–212. https://doi.org/10.1016/j.hipert.2019.05.002.